QUANTITATIVE ANALYSIS OF CHEMICAL AND BIOLOGICAL KINETICS FOR THE ACID MINE DRAINAGE PROBLEM

MEND Project 1.51.1

This work was done on behalf of MEND and sponsored by
Environment Canada

June 1994

QUANTITATIVE ANALYSIS OF CHEMICAL AND BIOLOGICAL KINETICS FOR THE ACID MINE DRAINAGE PROBLEM

by

M. Otwinowski
Synergetic Technology
139, 31-Avenue N.W.
Calgary, Alberta T2M 2P1

REPORT PREPARED FOR
MINE ENVIRONMENT NEUTRAL DRAINAGE PROGRAM
AND
BRITISH COLUMBIA ACID MINE DRAINAGE TASK FORCE

CONTENTS

Acknowledgements

The guidance by Benoit Godin who provided several ideas and continued support for this project is gratefully acknowledged. This project benefited greatly from discussions and information provided by M. Blanchette, C.J. Bland, R.F. Chaiken, P. Clark, K. Ferguson, P. Grabinski, H.R. Krouse, B. Krusche, E.J. Laishlay, H. Lizama, G.W. Luther III, R. McCandless, M.A. McKibben, K.A. Morin, R.V. Nicholson, C. Pelletier, W.A. Price, I. Suzuki, G.A. Tremblay, G. Weres, W.W. White III and R.M. Yoon. This project was jointly funded by Mine Neutral Environment Program (CANMET) and Environment Canada.

Summary

This report describes the results of a research project which has been initiated with the purpose to provide a quantitative analysis of the interrelated elementary chemical and biological processes which are responsible for pyrite oxidation and acid rock drainage (ARD). The highly nonlinear nature of the kinetic equations describing coupled chemical and microbial reactions involved in pyrite oxidation raised serious questions about the predictability of the environmental impact of acid rock drainage.

The main objective of this project was to determine whether the coupled chemical reactions involved in a multistage oxidation of pyrite lead to irregular or chaotic in time changes of products of the chemical and microbial reactions responsible for acid rock drainage. The main conclusion of the model analysis described in this report is the absence of such an irregular temporal behaviour. The set of nonlinear kinetic equations for the chemical reactions involved in pyrite oxidation does not produce a chaotic behaviour or other types of chemical oscillations. The nonlinear nature of the elementary nonequilibrium processes is responsible for the presence of the quasi-equilibrium values of the concentrations of ferrous and ferric iron. This property is a key to understanding the complexity of acidic drainage and should be helpful in designing efficient ways of minimizing acidic drainage. The presence of the quasi-equilibrium states increases our chances to formulate predictive ARD models. This study does not exclude, however, physico-chemical oscillations when processes of water and oxygen transport are included in a future model. (The analysis of transport processes was outside the scope of the present project designed as a low-budget preliminary analysis of the nonlinear chemical and biological kinetics.)

Several experimental results are reevaluated and, in some cases, values of rate constants different than those previously published in the literature are determined. A kinetic model in the form of coupled nonlinear ordinary differential equations is constructed for the coupled chemical reactions responsible for acid rock drainage. The equations describe the time dependence of the concentrations of the hydronium ions, ferrous and ferric iron, sulphate and oxygen dissolved in water.

In our analysis a clear distinction is made between the chemical and bacterial reactions which require the presence of dissolved oxygen and the chemical and bacterial processes which do not require oxygen.

At pH values greater than four, the process of pyrite oxidation is mainly due to the pyrite oxidation by oxygen dissolved in water:

$$FeS_2(s) + 7/2\ O_2 + H_2O = Fe^{2+} + 2SO_4^{2-} + 2H^+ . \qquad (R1)$$

Ferrous iron is released to the water solution where it is oxidized to ferric iron:

$$Fe^{2+} + 1/4\ O_2 + H^+ = Fe^{3+} + 1/2\ H_2O . \qquad (R2)$$

At pH values less than four the ferric iron reacts with pyrite

$$FeS_2(s) + 14Fe^{3+} + 8H_2O = 15Fe^{2+} + 2SO_4^{2-} + 16H^+ . \qquad (R3)$$

At high pH values the ferric iron reacts further with oxygen and water, and forms ferric hydroxide which precipitates:

$$Fe^{3+} + 3H_2O = Fe(OH)_3(s) + 3H^+. \qquad (R4)$$

Reactions (R1), (R3) and (R4) produce acid which, if not neutralized, mobilizes the metal ions contained in the waste rock. High pH values can be maintained by neutralizing minerals which often are present in the waste rock, or by minerals (like calcite) added to the waste rock. The process of neutralization by calcite is described by two reactions

$$CaCO_3 + 2\ H^+ + SO_4^{2-} + 2H_2O = CaSO_4 \cdot 2\ H_2O + H_2CO_3^{\circ} , \qquad (R5.1)$$

$$CaCO_3 + H^+ + SO_4^{2-} + H_2O = CaSO_4 \cdot 2\ H_2O + HCO_3^- . \qquad (R5.2)$$

The relative rates of the reactions (R5.1) and (R5.2) depend on pH values and are responsible for the efficiency of the neutralization process. The rate of oxidation of ferrous iron increases with increasing pH values and the neutralizing potential of the reactions (R5.1) and (R5.2) decreases when pH increases. This leads to a stoichiometric incompatibility between acid-generating and acid-neutralizing reactions. Minimizing the stoichiometric incompatibility during the neutralization process should reduce the amount of sludge generated and lower the cost of neutralization. Since the analysis of the neutralization process is limited to equilibrium conditions for the neutralizing species (pH is a control parameter), further analysis is required.

At pH less than four, ferric hydroxide is soluble and the reaction of pyrite oxidation by ferric iron contributes to acidic drainage. The source of ferric iron may be reaction (R2) (oxidation of ferrous iron) or the ferric hydroxide formed higher in the pile and washed down to a region where pH is low. The reaction of pyrite oxidation by ferrous iron may also be initiated if an insufficient amount of neutralizing minerals is used.

The kinetic model is analyzed for different regimes corresponding to possible different situations at various sites. The rates of pyrite oxidation and oxygen depletion are analyzed at different temperatures between 273 K and 333 K, and at concentrations of dissolved oxygen corresponding to the concentration of oxygen in the gaseous phase ranging from 21% to 2%. The ratio between the active surface area, S and the water volume, V, varies between 0.1 m^2/l and 100 m^2/l. The nonlinear nature of the elementary chemical processes involved is responsible for a dramatic increase in iron concentration by increasing acidity. The competition between increasing temperature and decreasing concentration of oxygen

dissolved in water is analyzed in detail. The increasing temperature, while accompanied by a lower concentration of dissolved oxygen, leads to the oxidation rates increasing about ten times per a 20 K increase in temperature. Computer simulations for the concentrations of hydronium ions, ferrous iron, ferric iron and sulphate generated during time intervals ranging from a few hours to several months have been performed for different values of the chemical and physical parameters which control the process of acidic drainage. In some cases the nonlinear kinetic equations have been solved analytically and several useful closed-form mathematical formulae have been obtained.

At low pH values and at temperatures about 303 K, Thiobacillus ferrooxidans at concentrations on order of one gram of wet cells per litre, can accelerate the process of pyrite dissolution by about a thousand times. Kinetic equations for the bacterial processes of pyrite oxidation by dissolved oxygen and by ferric iron are proposed for the first time. Bacterial processes accelerate each of the reactions (R1), (R2) and (R4) in a different way. The reaction (R1) is accelerated about three hundred times. The reaction (R2) becomes about a million times faster. The reaction (R4) is accelerated by bacteria about three times.

The reactions of the bacterial oxidation of ferrous iron to ferric iron and the pyrite oxidation by ferric iron provide a nonlinear negative feedback mechanism which is responsible for a smaller than desired effect of slowing-down pyrite oxidation by reducing oxygen concentration. When oxygen partial pressure decreases from 0.21 atm to 0.04 atm (i.e. by 75%), the rate of pyrite oxidation by Thiobacillus ferrooxidans decreases by only 30%. This negative feedback mechanism is also responsible for a chemistatic bacterial action and prolonged bacterial activity in an acidic environment.

Several problems which merit further experimental and modelling studies are identified.

Quantitative results presented in this study should be confronted with field data and, after calibration, the kinetic model presented here can be used as a part of a comprehensive physical waste rock model and an underwater disposal model.

SOMMAIRE

Dans ce rapport, on décrit les résultats d'un projet de recherche entrepris en vue d'analyser quantitativement les processus chimiques et biologiques élémentaires interreliés qui sont responsables de l'oxydation de la pyrite et du drainage rocheux acide (DRA). Vu la nature hautement non linéaire des équations décrivant la cinétique des réactions chimiques et microbiennes couplées qui interviennent dans l'oxydation de la pyrite, il y a lieu de se poser de graves questions sur la prévisibilité de l'impact du drainage rocheux acide sur l'environnement.

Ce projet avait comme principal objectif de déterminer si les réactions chimiques couplées intervenant dans l'oxydation à plusieurs étapes de la pyrite sont accompagnées de changements, irréguliers ou chaotiques dans le temps, dans les produits des réactions chimiques et microbiennes responsables du drainage rocheux acide. L'absence d'un tel comportement irrégulier dans le temps constitue la principale conclusion de l'analyse de modélisation décrite dans ce rapport. Le système d'équations décrivant la cinétique non linéaire des réactions chimiques intervenant dans l'oxydation de la pyrite ne révèle ni comportement chaotique ni autres types de fluctuations de nature chimique. La nature non linéaire des processus élémentaires non à l'équilibre est à l'origine des concentrations d'ions ferreux et ferriques à quasi-équilibre. Cette propriété est essentielle pour comprendre la complexité du drainage acide et devrait être utile dans la mise au point de méthodes permettant de le réduire le plus possible. L'existence d'états de quasi-équilibre améliore nos chances d'élaborer des modèles permettant de prévoir le DRA. Toutefois, dans cette étude on n'exclut pas les fluctuations physico-chimiques qui seront observées après inclusion, dans un modèle futur, des processus de transport de l'eau et de l'oxygène. (L'analyse des processus de transport débordait le cadre du présent projet qui a été conçu comme une analyse préliminaire, à faible budget, de la cinétique chimique et biologique non linéaire.)

On a réévalué plusieurs résultats expérimentaux et, dans certains cas, on a obtenu des constantes de vitesse différentes de celles qui avaient été publiées dans la littérature. On a élaboré un modèle cinétique se présentant sous forme d' équations différentielles ordinaires non linéaires couplées, afin de décrire les réactions chimiques couplées responsables du

drainage rocheux acide. Les équations décrivent la dépendance sur le temps de la concentration des ions hydronium, du fer ferreux et du fer ferrique, du sulfate et de l'oxygène dissous dans l'eau.

Dans notre analyse, nous faisons une distinction bien nette entre les réactions chimiques et bactériennes qui exigent et qui n'exigent pas la présence d'oxygène dissous. À un pH supérieur à 4, c'est l'oxygène dissous dans l'eau qui est surtout responsable de l'oxydation de la pyrite:

$$FeS_2(s) + 7/2\ O_2 + H_2O = Fe^{+2} + 2\ SO_4^{-2} + 2H^+ \qquad (R1)$$

Le fer ferreux passe en solution dans l'eau et est oxydé en fer ferrique:

$$Fe^{+2} + 1/4\ O_2 + H^+ = Fe^{+3} + 1/2\ H_2O \qquad (R2)$$

A un pH inférieur à 4, le fer ferrique réagit avec la pyrite:

$$FeS_2(s) + 14\ Fe^{+3} + 8\ H_2O = 15\ Fe^{+2} + 2\ SO_4^{-2} + 16\ H^+ \qquad (R3)$$

À un pH élevé, le fer ferrique réagit encore avec l'eau et l'oxygène pour donner de l'hydroxyde ferrique qui précipite:

$$Fe^{+3} + 3H_2O = Fe(OH)_3(s) + 3\ H^+ \qquad (R4)$$

Les réactions (R1), (R3) et (R4) produisent de l'acide qui, s'il n'est pas neutralisé, dissout les ions contenus dans les stériles. Un pH élevé peut être maintenu par la présence de minéraux neutralisants, que l'on trouve souvent dans les stériles, ou par l'addition de minéraux comme la calcite. Les deux réactions suivantes décrivent le processus de neutralisation par la calcite:

$$CaCO_3 + 2\ H^+ + SO_4^{-2} + 2\ H_2O = CaSO_4{\cdot}2H_2O + H_2CO_3^{\circ} \qquad (R5.1)$$

$$CaCO_3 + H^+ + SO_4^{-2} + H_2O = CaSO_4{\cdot}2H_2O + HCO_3^- \qquad (R5.2)$$

Les vitesses relatives des réactions (R5.1) et (R5.2) dépendent du pH et déterminent l'efficacité du processus de neutralisation. Comme la vitesse d'oxydation du fer ferreux augmente au fur et à mesure qu'augmente le pH et que le potentiel de neutralisation des réactions (R5.1) et (R5.2) diminue au fur et à mesure qu'augmente le pH, il y a incompatibilité stoechiométrique entre les réactions libérant un acide et les réactions de neutralisation. La réduction au minimum de l'incompatibilité stoechiométrique durant le processus de neutralisation devrait entraîner une baisse de la quantité de boue produite et réduire le coût de la neutralisation. Comme le processus de neutralisation ne peut se faire que dans des conditions d'équilibre pour l'espèce neutralisante (le pH est le paramètre de régulation), il faut procéder à une analyse plus approfondie.

À un pH inférieur à 4, l'hydroxyde ferrique est soluble et la réaction d'oxydation de la pyrite par le fer ferrique contribue au drainage acide. Le fer ferrique peut être produit par la réaction (R2) (l'oxydation du fer ferreux) ou provenir de l'hydroxyde ferrique formé plus haut dans la halde et entraîné vers une zone où le pH est plus faible. Il peut aussi y avoir oxydation de la pyrite par le fer ferreux, si la quantité de minéraux de neutralisation ajoutés est insuffisante.

On a analysé le modèle cinétique à différents régimes correspondant à différentes situations possibles à divers sites. On détermine la vitesse d'oxydation de la pyrite et la vitesse de désoxygénation à différentes températures comprises entre 273 K et 333 K et à des concentrations d'oxygène dissous correspondant à des concentrations d'oxygène gazeux comprises entre 21 % et 2 %. Le rapport entre l'aire de la surface active, S, et le volume de l'eau, V, varie entre 0,1 m^2/L et 100 m^2/L. C'est la nature non linéaire des processus chimiques élémentaires qui est à l'origine de la hausse dramatique de la concentration de fer en fonction de l'acidité. On examine en détail la compétition entre l'augmentation de la température et la diminution de la concentration d'oxygène dissous dans l'eau. La hausse de température, bien qu'elle soit accompagnée d'une baisse de la concentration d'oxygène dissous, entraîne une augmentation de la vitesse d'oxydation par un facteur d'environ 10 pour chaque accroissement de température de 20 K. On a procédé à des simulations par ordinateur des concentrations d'ions hydronium, de fer ferreux, de fer ferrique et de sulfate produits au cours de périodes allant de quelques heures à plusieurs mois, pour différentes

valeurs des paramètres chimiques et physiques régissant le drainage acide. Dans certains cas, les équations décrivant la cinétique non linéaire ont été résolues par analyse et plusieurs formules mathématiques utiles de forme fermée ont été obtenues.

À un faible pH et à une température d'environ 303 K, *Thiobacillus ferrooxidans* en concentration de l'ordre de 1 gramme de cellules humides par litre peut accélérer le processus de dissolution de la pyrite par un facteur d'environ 1000. On propose pour la première fois des équations décrivant la cinétique de l'oxydation bactérienne de la pyrite par l'oxygène dissous et par le fer ferrique. Les processus bactériens accélèrent différemment les réactions (R1), (R2) et (R4), l'augmentation de vitesse étant d'environ 300, d'environ 1 000 000 et d'environ 3 respectivement.

Les réactions d'oxydation bactérienne du fer ferreux en fer ferrique et l'oxydation de la pyrite par le fer ferrique constituent un mécanisme de rétroaction négative non linéaire responsable d'un ralentissement, plus faible que le ralentissement escompté, de l'oxydation de la pyrite par diminution de la concentration d'oxygène. Une diminution de la pression partielle d'oxygène de 0,21 atmosphère à 0,04 atmosphère (c.-à-d. une baisse de 75 %) se traduit par une réduction de seulement 30 % de la vitesse d'oxydation de la pyrite par *Thiobacillus ferrooxidans*. Ce mécanisme de rétroaction négative est également à l'origine de l'action bactérienne chémistatique et de l'activité bactérienne prolongée en milieu acide.

On souligne plusieurs problèmes sur lesquels il y aurait lieu d'effectuer d'autres travaux expérimentaux et d'autres études de modélisation.

Les résultats quantitatifs obtenus au cours de cette étude devraient être vérifiés par des données obtenues sur le terrain; ainsi, après étalonnage, le modèle cinétique présenté dans ce rapport peut être utilisé dans le cadre d'un modèle simulant l'ensemble des aspects physiques des stériles et d'un modèle d'élimination subaquatique.

1. INTRODUCTION

Acid Mine Drainage (AMD) results when oxygen and water react with the sulphide minerals contained in natural rock, underground workings, open pit mine walls, mine waste rock piles or mine tailings to produce acidic seepage or leachate. Biological processes also play an important role in acidic drainage. The net result of the chemical and biological reactions involved is the production of low pH water. Low pH water has the potential to mobilize heavy metals which may migrate into and contaminate adjacent soils and waters [BrC], [ChB], [Co], [Fe]. Characterization of waste materials and prediction of their long term environmental impact is not a simple task. Apart from chemical processes AMD depends also on physical, biological and mineralogical factors.

In newly formed piles of chemically active porous medium, for example, one often observes three phases of physico-chemical kinetics [BrC]: the first phase of increasing activity, the second relatively steady phase and the third phase of decreasing activity. The duration of individual phases varies depending on chemical and physical factors involved and, in some cases [Ar], [KoB], [ScD], [Ot1], [Ot2], may be predicted by comprehensive nonlinear models describing chemical kinetics and transport of mass and energy.

The main objective of this project was to analyze the possible natural limitations on the predictive power of AMD models imposed by the nonlinear nature of the chemical and biological processes involved. Networks of chemical reactions described by coupled nonlinear equations often produce irregular or chaotic temporal variations of products. When this happens, special techniques have to be used by collecting the laboratory and field data and additional complexity is introduced to predictive models. The purpose of this study is to provide a quantitative description of the interrelated nonlinear processes responsible for AMD and to determine the time dependence of reaction products as a function of the initial concentrations of reactants and temperature.

This report reviews and critically analyzes several experimental and theoretical results on various chemical, physical and biological aspects of pyrite oxidation. Based on available experimental data, a model in the form of a set of kinetic differential equations is formulated and solved. Unfortunately, experimental results reported by various laboratories are often different and in some cases a subjective choice of entry data for the model had to be made.

For this reason the mathematical analysis is performed together with a critical review and additional analysis of the experimental results published in available literature.

Information about chemical and biological processes provided by this study can be later used in a comprehensive model including mass and energy transport (via diffusion, percolation, thermal conductivity and convection). Previous waste rock models did not consider coupled elementary reactions to describe the oxidation of pyrite under aerobic and anaerobic conditions and did not describe properly the process of pyrite oxidation in regions where oxygen concentration is low and temperature is high.

The report starts with an introductory survey and interpretation of experimental results, which lays the ground for the quantitative model. In Chapter II, we analyze separately the following coupled processes:

- pyrite oxidation by water and oxygen dissolved in water and the release of Fe^{2+} (ferrous) ions and acid (reaction (R1))
- oxidation of ferrous ions to ferric (Fe^{3+}) ions by oxygen (reaction (R2))
- anaerobic oxidation of pyrite by ferric ions and water (reaction (R3))
- precipitation of ferric hydroxide, which eliminates ferric ions from the stream (reaction (R4))
- the neutralization process (reaction (R5))

These processes are analyzed both for abiotic conditions and in the presence of bacterial oxidation responsible for much higher oxidation rates.

Experimental data on the kinetics of elementary chemical reactions and bacterial processes are reviewed. Only the experiments which provide quantitative data suitable for our mathematical analysis are discussed and Chapter II does not pretend to be a complete review of research work on pyrite oxidation. A reader who does not want to spend time on reading the literature review may limit his attention to pages 5, 6, 7 and 28 where stoichiometric equations (R1)-(R4) for chemical oxidation of pyrite and reactions (B1)-(B3) for bacterial oxidation are discussed. On page 39 stoichiometric relations (R5.1) and (R5.2) for the neutralization reactions are presented. These reactions are used in the kinetic model analyzed in Chapters III and IV. In paragraph 2.4 (p. 41) the solubility of oxygen in water is discussed.

A kinetic model for abiotic chemical reactions is constructed and analyzed in Chapter III. We consider the temporal behaviour of concentrations of the chemical species separately for pH values greater than four and less than four. This distinction is necessary because of the dramatic changes in the nature of pyrite oxidation due to precipitation of ferric hydroxide at pH values above four. Section III.0 demonstrates that the kinetic equations used in our model reproduce experimental results for individual chemical reactions. The kinetic model for abiotic reactions without neutralization is given by equations (D1) on page 57 (for pH between 4 and 7) and equations (D2) on page 68 (for pH less than 4). The neutralization process is included in equations (D3) (p. 80) in an equilibrium way by stabilizing pH values. The main results of the analysis presented in Chapter III are: (i) the absence of chaotic behaviour or temporal oscillations of the concentrations of final and transient products (Fig. 3.1.1), and (ii) there is stoichiometric incompatibility between acid-generating and acid-neutralizing reactions (see p. 91). The intermediate asymptotic behaviour of the concentrations of ferric and ferrous ions is referred to as quasi-equilibrium states (eqs. (3.1.5) and (3.2.1), and figures 3.1.5, 3.2.4 and 3.2.5)). The presence of quasi-equilibrium states, if confirmed by field studies, increases chances for formulating reliable predictive AMD models. Pyrite oxidation rates increase dramatically with temperature - for temperatures between 273K and 323K the rate of pyrite oxidation accelerates about ten times per 20K. Other conclusions of Chapter III are listed on pages 45 and 46.

Chapter IV is devoted to bacterial processes. Both aerobic and anaerobic reactions which are accelerated by bacteria are considered in the mathematical model defined by eqs. (DB) on page 100. Anaerobic bacterial oxidation is used in the kinetic model despite a long-time controversy about the anaerobic bacterial oxidation of pyrite. We use recent results of experiments which, in our opinion, are methodologically correct and provide reliable quantitative data. The main conclusion of Chapter IV is the existence of a nonlinear feedback mechanism which is responsible for maintaining significant levels of bacterial activity and sustained bacterial oxidation rates at low oxygen concentrations (figures 4.1.1 and 4.2.1). Another feedback mechanism is responsible for maintaining pH values optimal for bacterial activity. Both feedback mechanisms should be given serious consideration by designing practical ways of reducing and controlling AMD. Other results and conclusions of Chapter IV are summarized on pages 96-98.

In Chapter V, some problems which merit further experimental and modelling work

are discussed.

The model discussed in this report uses laboratory data on pure pyrite. In the next step, the results presented in this report should be confronted with available experimental data on acidic drainage from large samples of pyritic rocks [Res], [Ge], [WhJ] should be used to calibrate the model. Transport processes which control the supply of water and oxygen are ultimately responsible for both the rate of acid generation and its release to the environment.

II. ELEMENTARY CHEMICAL PROCESSES INVOLVED IN ACID MINE DRAINAGE

The rates of chemical processes leading to acid formation are affected by physical, biological and mineralogical factors. Physical parameters include the porosity and permeability of a rock mass, the ratio of particle size/surface area, meteorological factors, etc.. Bacterial activity is often a dominant factor determining the overall rate of acid formation. Important mineralogical factors are: type and quantity of sulphide minerals (pyrite, pyrrhotite, marcasite and non-ferrous sulphides), texture and morphology, degree of rock fracture, content of acid consuming minerals. These factors affect both the chemical rates of acid formation and neutralization.

Interplay between the different elementary processes can be represented by a simplified diagram:

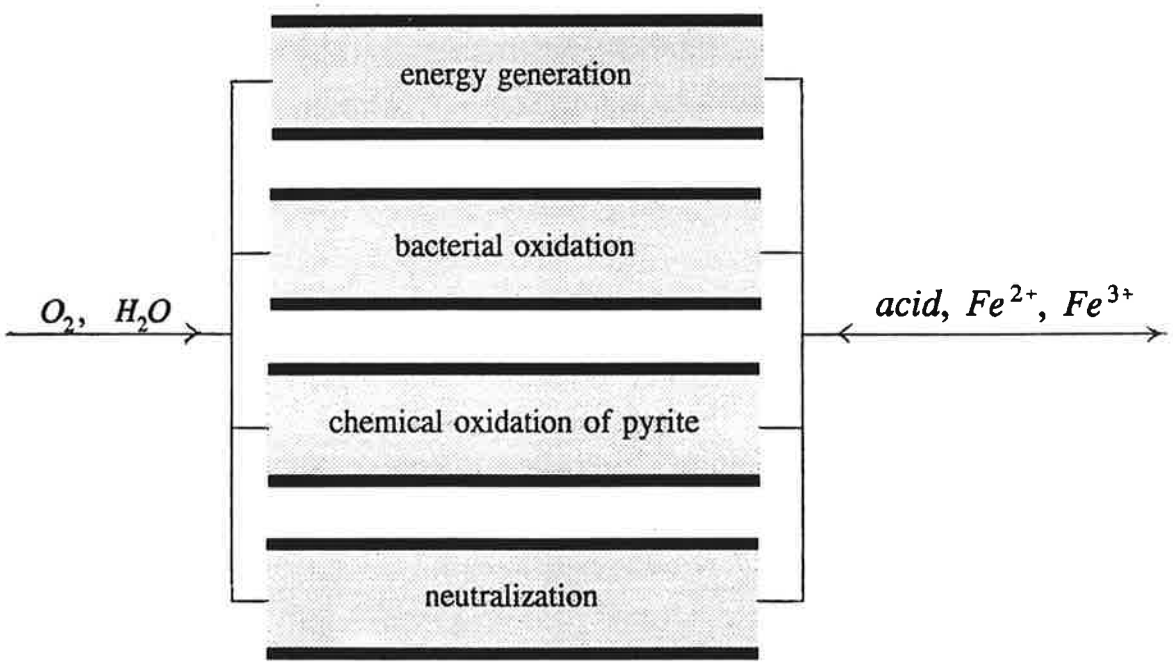

Fig. 2.1. Interrelated processes contributing to ARD

The overall kinetics of acid formation results from the *interrelation* of elementary processes and can be described by a set of coupled differential equations. Each of these equations describes the kinetics of one variable of the model in relation to all other variables.

II.1. Chemical oxidation of pyrite

The overall stoichiometry of pyrite oxidation may be described by the following reactions:

$$FeS_2 + 7/2\ O_2 + H_2O = Fe^{2+} + 2\ SO_4^{2-} + 2H^+ , \qquad (S1)$$

$$FeS_2(s) + 15/4\ O_2\ (aq) + 7/2\ H_2O = Fe(OH)_3(s) + 4H^+ + 2SO_4^{2-} \qquad (S2)$$

summarizing several elementary chemical reactions which take place at low pH values (reaction (S1)) or high pH values (reaction (S2).

In order to describe the oxidation kinetics, the intermediate steps in this reaction must be considered. The following reactions characterizing the oxidation of pyrite have been proposed [StM], [SiS], [TaW]:

$$FeS_2(s) + 7/2\ O_2 + H_2O = Fe^{2+} + 2SO_4^{2-} + 2H^+ , \qquad (R1)$$

$$Fe^{2+} + 1/4\ O_2 + H^+ = Fe^{3+} + 1/2\ H_2O , \qquad (R2)$$

$$FeS_2(s) + 14Fe^{3+} + 8H_2O = 15Fe^{2+} + 2SO_4^{2-} + 16H^+ , \qquad (R3)$$

$$Fe^{3+} + 3H_2O = Fe(OH)_3(s) + 3H^+. \qquad (R4)$$

The model bears hallmarks of electron-transfer processes in biochemical systems and is, in fact, derived from the bacteriological work of Temple and Delchamps [BaO]. The model consists of four reactions:

(R1) The oxidation of pyrite by molecular oxygen to Fe^{2+} and sulphate. The oxidation of iron sulphide (pyrite) to sulphate (eq. (R1)) releases dissolved ferrous ions and acidity into the water.

(R2) Subsequently, the dissolved ferrous ions undergo oxidation to ferric ions (eq. (R2)). This is a slow reaction and viewed as the rate-limiting step determining the overall rate of

pyrite oxidation.

(R3) Sulphide is oxidized again by ferric ion and acidity is released along with additional ferrous ions which may re-enter the reaction cycle via reaction (R2). This is regarded as a fast step.

(R4) Ferric ions hydrolyse to form insoluble ferric hydroxide (eq. (R3)), releasing more acidity to the stream. This reaction takes place only at high pH values which can be attained when the mineral composition of the waste rock is such that self-buffering processes take place or when neutralizing minerals are added.

Reactions (R2) and (R3) provide a feedback loop presented below after Singer and Stumm (p. 471 of ref. [StM]).

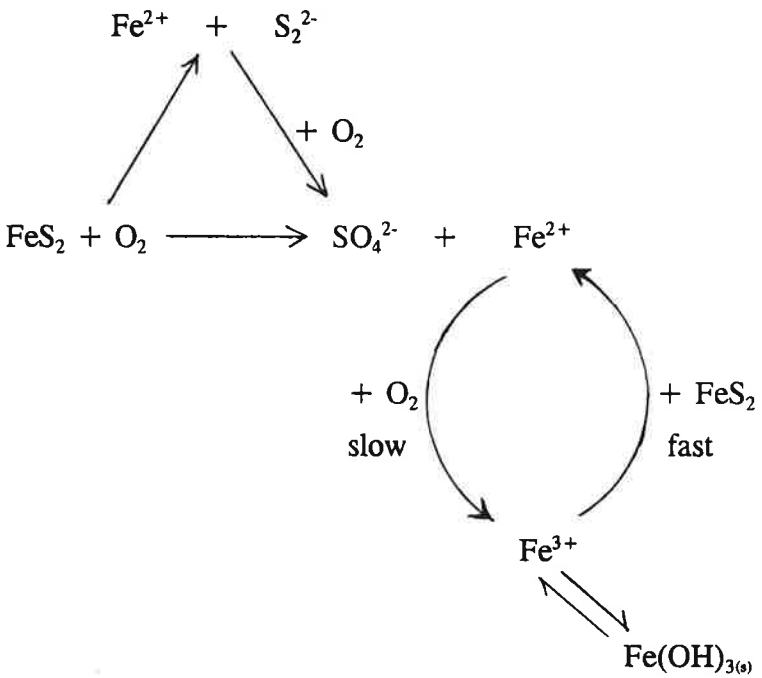

The nature of this feedback is very similar to the autocatalytic mechanism leading to oscillating behaviour, as described in a series of papers by Prigogine and others [PrL], [NiP], [OtL1]. The number of reacting species during acid formation is greater than two. This leads to strong nonlinearities in the kinetic equations and one may suspect that under

some conditions various types of oscillations including chaotic oscillations may be exhibited by the system [FiN], [Ty], [NiP].

If one was to construct kinetic equations for the stoichiometric relations (R1) - (R4) by following (often postulated) the simple rules of chemical reactions in homogeneous solutions, the set of kinetic reactions would have the form (compare [WhJ]:

$$d[Fe^{2+}]/dt = k_1[O_2]^{7/2} - k_2[Fe^{2+}][O_2]^{1/4}[H^+] + 15k_3[Fe^{3+}]^{14} - q_1[Fe^{2+}][SO_4^{2-}]^2[H^+]^2 + q_2[Fe^{3+}] - q_3[Fe^{2+}]^{15}[SO_4^{2-}]^2[H+]^{16},$$

$$d[Fe^{3+}]/dt = k_2[Fe^{2+}][O_2]^{1/4}[H^+] - 14\,k_3[Fe^{3+}]^{14} - k_4[Fe^{3+}] + q_2[Fe^{3+}] + 14q_3[Fe^{2+}]^{15}[SO_4^{2-}]^2[H^+]^{16} + q_4[Fe(OH)_3][H^+]^3 ,$$

$$d[SO_4^{2-}]/dt = 2k_1[O_2]^{7/2} + 2k_3[Fe^{3+}] - 2q_1[Fe^{2+}][SO_4^{2-}]^2[H^+]^2 - 2q_3[Fe^{2+}]^{15}[SO_4^{2-}]^2[H^+]^{16} ,$$

(IC)

$$d[[H^+]/dt = 2k_1[O_2]^{7/2} - k_2[Fe^{2+}][O_2]^{1/4}[H^+] - 16\,k_3[Fe^{3+}]^{14} + 3k_4[Fe^{3+}] - 2q_1[Fe^{2+}][SO_4^{2-}]^2[H^+]^2 + q_2[Fe^{3+}] - 16q_3[Fe^{2+}]^{15}[SO_4^{2}]^2[H+]^{16} + 3q_4[Fe(OH)_3][H^+]^3 ,$$

$$d[O_2]/dt = -(7/2)k_1[O_2]^{7/2} - (1/2)\,k_2[Fe^{2+}][O_2]^{1/4}[H^+] + (7/2)q_1[Fe^{2+}][SO_4^{2-}]^2[H^+]^2 + 1/4q_2[Fe^{3+}] ,$$

$$d[H_2O]/dt = -k_1[O_2]^{7/2} + (1/2)k_2[O_2]^{1/4}[H^+] - 8k_3[Fe^{3+}]^{14} + q_1[Fe^{2+}][SO_4^{2-}][H^+]^2 - q_2[Fe^{3+}] + 8q_3[Fe^{2+}]^{15}[SO_4^{2-}]^2[H^+]^{16} + 3q_4[Fe(OH)_3][H^+]^3 .$$

In the above set of nonlinear kinetic equations (IC), coefficients k_1, k_2, k_3 , k_4 are rate constants for equations (R1)-(R4) for reactions with products on the right hand side, and q_1, q_2, q_3, q_4 are rate constants for the reverse reactions with products on the left hand side of

equations (R1)-(R4). Square brackets denote concentration of species in moles per litre and powers of concentrations define the order of reactions with respect to the species involved. $[O_2]$ denotes concentration of oxygen dissolved in water. (In Section II.4 we will also discuss $[O_2]$ as a function of oxygen concentration in the gas phase (denoted by $[O_2]_{gas}$) surrounding the aqueous solution.

Equations (IC) (from "incorrect") are not realistic, however. Simple stoichiometric rules in the case of pyrite oxidation cannot be applied for several physico-chemical reasons.

1. Reaction (R1)-(R4) are complex multistep reactions. Only one or two electrons are transferred per elementary reaction and usually one elementary reaction is rate limiting and dominates the order of a complex reaction with respect to individual reactants.
2. Reactions (R1) and (R3) are heterogeneous surface reactions between dissolved species and a solid surface of pyrite crystals.
3. There are arguments about the electrochemical nature of the chemical process described by stoichiometric relations (R1) and (R3) for which Eh values are also significant[Yo].
4. Ferric and ferrous ions have a tendency to form water complexes which may limit the probability of reaction (R3) - one should then expect that the order with respect to ferrous iron, Fe^{2+} should be lower than 1.
5. Even in perfect homogeneous solutions staeric relations make it impossible for a large number of species to interact chemically at the same moment - this comment applies in particular to reaction (R3) whose stoichiometry suggests the largest number of species involved.

All of the above arguments lead to the conclusion that the nonlinearities corresponding to the multi-molecular nature of reactions, should not be derived from stoichiometric relations and probabilistic principles disregarding the size of the reacting species (even if the multi-species reactions were very fast). In principle, one could theoretically derive the orders of chemical reactions by using methods of molecular dynamics based on computer simulations. Such an approach does not seem efficient, however, given the practical nature of the acid mine drainage problem. Fortunately there are several sets of independent experimental data which allow the construction of a reasonable kinetic model for the chemical, biological and physical processes responsible for acidic drainage.

In subsequent paragraphs we analyze in detail various experiments and on that basis

we derive kinetic equations which recognize the significance of various individual chemical reactions and at the same time provide quantitative information which cannot be derived from stoichiometric relations (R1) - (R4). In analyzing individual reactions it is important to keep in mind that experimental data are obtained for some control parameters. These parameters are easily and economically measurable during large scale field tests at different sites and can be controlled by using prevention methods or by the natural transport processes in waste rock piles - such as mass and energy transport.

In our analysis we have used several results obtained before 1982 , and summarized in three review articles by Lowson [Lo] and Nordstrom [No], as well as more recent data published in a series of articles in geochemical journals after 1982.

II.1.1. *Oxidation of pyrite by dissolved oxygen*

The reaction of pyrite with aqueous solutions containing dissolved oxygen is described by the overall reaction

$$FeS_2(s) + 7/2\ O_2 + H_2O \rightarrow Fe^{2+} + 2SO_4^{2-} + 2H^+ \qquad (R1)$$

As mentioned before, eq. (R1) should be considered as giving only some qualitative information on the recognized process of direct pyrite oxidation by dissolved oxygen. Relation (R1) is not the only possible reaction stoichiometry for the oxidation of pyrite by dissolved oxygen in acidic solutions. Two other scenarios have been considered in the literature:

$$FeS_2 + 3/2O_2 \rightleftarrows Fe^{2+} + S_2O_3^{2-} \qquad (2.1)$$

and

$$FeS_2 + 7/4O_2 + H^+ \rightleftarrows Fe^{2+} + 1/2\ S_4O_6^{2-} + 1/2H_2O \qquad (2.2)$$

Reaction (R1) indicates that 12.5% of the oxygen in the sulphate ions originates from water molecules and 87.5% originates from the dissolved oxygen molecules. Reactions (2.1) and (2.2) indicate that all oxygen originates from dissolved oxygen molecules.

We have selected scenario (R1) because it is supported by isotopic trace analysis [EvK], [TaW1], [TaW2], [ReB], [PrT], [WaK], [Jo], [KrG] which indicates that part of oxygen in sulphate is derived from water molecules. In addition, there is no evidence for the presence of $S_2O_3^{2-}$ or $S_4O_6^{2-}$ species as stable products [Gol], [Ni].

We also consider reactions (R1), (R2) and (R3) as unidirectional. This is motivated by practical reasons. There are no experimental data for rates of reverse reactions. In this and other paragraphs the rate constants should be interpreted as cumulative rate constants whose values account for slow reverse reactions. The argument that very small rate constants for reverse reactions do not affect the qualitative behaviour of a chemical system, is not always correct, however. There are situations when slow reverse reactions significantly modify the kinetics of a nonlinear chemical network [OtL1].

Even when a chemical system is far from equilibrium, it is possible for transient species to exhibit oscillatory behaviour or evolve to weakly time dependent quasi-equilibrium states [NiP], [Ty]. Often chemical oscillations occur for very narrow ranges of kinetic parameters. Accurate values of rate constant should be determined before a mathematical analysis initiated.

(a) order with respect to oxygen

It is important to identify reactants and products whose rate of change can be used to define a rate of pyrite oxidation unambiguously. In a series of experiments McKibben and Barnes [McK], were able to measure the oxidation of pyrite by measuring concentrations of ferrous ions in the absence of ferric iron. The rate dependence on dissolved oxygen concentration was determined in a series of runs conducted at two different ambient oxygen pressures, 1.0 and 0.21 atm. The results are shown in Fig. 2.2, where the logarithm of rate of increase of ferrous iron concentration is plotted against the logarithm of initial oxygen concentration.

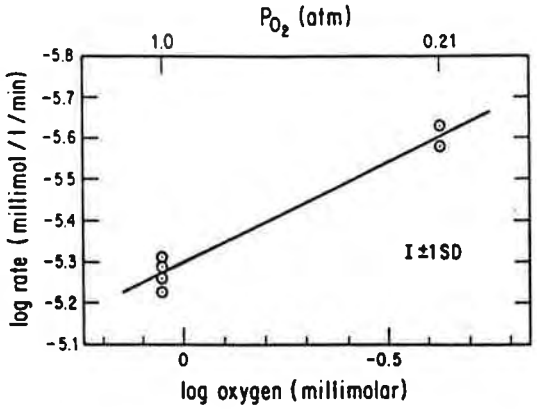

Fig. 2.2. The effect of oxygen molarity on the volumetric rate of oxidation of pyrite by dissolved oxygen at pH 1.89, 30°C, $[O_2]_{gas}$ 1.0 and 0.21 atm. (From McKibben and Barnes [McK])

Linear regression of the data in Fig.2.1 yields a slope of 0.49 indicating that the rate is proportional to the square root of oxygen concentration in water:

$$d[Fe^{2+}]/dt \sim [O_2]^{1/2} \qquad (2.3)$$

A very similar result has been published by Nicholson et al. [NiG] who also confirmed the rate of oxidation to be nonlinear with respect to the concentration of oxygen. (Nicholson et al. [NiG] also provide profound arguments about variable rate order). According to the existing interpretation [McK], [NiG] an apparent 1/2 order rate dependence on dissolved oxygen is a result of adsorption of O_2 on the pyrite surface followed by reduction to H_2O_2 by water and oxidation of pyrite by the H_2O_2. This interpretation is consistent with the results of isotope studies which show that part of oxygen in sulphate is derived from water molecules.

In reaction (R1) 87.5% of the sulphate oxygen is derived from molecular oxygen and 12.5% from water molecules. Thus the rate of reaction (R1) can be limited by oxygen partial pressure.

Usually the concentration of dissolved oxygen is described by Henry's law

$$[O_2] \sim K[O_2]_{gas} \tag{2.4}$$

which indicates that the concentration of dissolved oxygen is a linear function of oxygen concentration in the gas phase of the surroundings. At 298 K and in contact with air of atmospheric conditions

$$\max [O_2] = 8.3 \text{ mg/l} \tag{2.5}$$

In large piles of waste rock, far from the pile boundaries, the concentration of dissolved oxygen can be very low. Both theoretical estimates and field data [BeR], [PaR] indicate that the oxygen concentration $[O_2]_{gas}$ may be below 1% inside a pile. In this way the rates of diffusive and convective transport of oxygen inside a waste rock pile play a significant role as one of the main rate limiting factors in the process of pyrite oxidation.

In our further numerical studies we will treat $[O_2]_{gas}$ as a model parameter . Detailed analysis of convective and diffusive transport as a function of pile porosity and temperature distribution goes beyond the scope of this study and should be performed in a future project.

(b) pH dependence

Many chemical reactions are sensitive to pH values. Results presented by McKibben and Barnes [McK] indicate, however, that in reaction (R1) the rate of abiotic pyrite oxidation by dissolved oxygen is effectively independent of pH over the range of pH between 2 and 4. Linear regression of experimental data for the logarithm of the rate of oxidation of pyrite versus the logarithm of proton concentration [McK] yields a slope of 0.09 which is negligible. In a later study Moses et al. [MoN] concluded that reaction (R1) is pH independent up to pH=7.

(c) rate constant

McKibben and Barnes [McK] give the value of the rate constant determined at temperature T_o=30°C as

$$k_1(T_o)=2.83 \times 10^{-9} M^{1/2} cm^{-1/2} s^{-1}. \tag{2.6}$$

One can find in the literature other values of the rate constant for reaction (R1) [Lo]. Those values were not measured directly but were always determined as a proportionality

coefficient between the rates of change of product and substrate concentrations at a constant temperature after assuming the order of reaction. The value (2.6) does not reproduce, however, fundamental experimental results presented by McKibben and Barnes [McK]. We had to reanalyze the experimental data and a correct value is given in Chapter III.

(d) activation energy

Rate constants are temperature dependent and usually can be represented as a product of the pre-exponential factor $A_1 = k_1(T=\infty)$ and an exponential factor depending on activation energy. Because in most experiments the rate constants were determined at a certain temperature T_o, we use the formula

$$k_1(T) = k_1(T_o) \exp [E_1(T-T_o)/(RTT_o)] \qquad (2.7)$$

where $k_1(T_o) = A_1 \exp(-E_1/RT_o)$ and E_1 is the activation energy, R is the gas constant and T is temperature Kelvins. The activation energy was determined in a series of experiments. The values obtained by various researchers range from 39 kJ/mol to 88 kJ/mol [Lo]. Values above 90kJ/mol have been reported for temperatures above 100°C.

Temperatures observed in waste rock piles do not exceed 90°C and for our model we will use the values

$$E_1 = 57 \pm 7.5 \text{ kJ/mol for pH} < 4 \text{ and } E_1 = 88 \text{ kJ/mol for pH} > 4 \qquad (2.8)$$

determined by McKibben and Barnes [McK] and Nicholson et al. [NiG] at temperatures between 20°C and 40°C. Other values quoted by Lowson [Lo] have been obtained from an analysis of experimental data in which the authors assumed rather than determined the orders of reaction and obtained pre-exponential factors which varied with temperature. We favour the value obtained by McKibben and Barnes because they did not make such assumption and their pre-exponential factor does not show a temperature variation.

It is important that a future waste rock model uses a correct value of the activation energy. The higher the value of activation energy the faster the acceleration of the oxidation process when temperature increases.

(e) pre-exponential factor

For a value of activation energy equal to 56.9 kJ/mol we obtain the pre-exponential factor

$$A_1 = 1.1 \times 10^{-8} M^{1/2} cm^{-1/2} s^{-1} \qquad (2.9)$$

For the process of pyrite oxidation the value of the pre-exponential factor measured in any experiment cannot be considered as a universal material constant. The pre-exponential factor depends strongly on the surface area/mass ratio for a pyrite sample and may be different for rocks of different morphology. Experimental data collected by Nicholson et al. [NiG2] for tailings over a period of 4 years indicate that after some time - as a result of coating by ferric hydroxide - one observes a crossover from a linear dependence on surface area/mass ratio to a linear dependence on volume/mass ratio. This tendency is accompanied by a decrease in the chemical activity of the rock samples. These experimental facts may be interpreted as an indication that the fractal dimensions of a pore structure may be an important factor contributing to the chemical activity of waste rock. In general it is difficult to use basic physico-chemical principles to derive numerical values of pre-exponential factors for different fractal dimensions. A possible way to account for variability in reactivity of minerals containing pyrite is to include a factor S/V which measures the active surface area, S per volume, V of water. In our model we use values observed in some experiments. One must remember, however, that rocks have different morphology at different sites and the pre-exponential factor should be measured for every site in order to provide reliable entry data for a predictive waste rock model [Lap].

As the result of the above discussion we can write

$$d[Fe^{2+}]_{(R1)}/dt = (S/V)\, k_1(T_o) \exp[E_1(T-T_o)/(RTT_o)]\, [O_2]^{1/2} \qquad (2.10)$$

The symbol $[Fe^{2+}]_{(R1)}$ is used to indicate the contribution from reaction (R1). (The total rate of change of ferrous iron concentration is a sum of contributions from all elementary reactions (R1)-(R4)).

In an analogous way we can write

$$d[O_2]_{(R1)}/dt = -(7S/2V)\, k_1\, (T_o) \exp\, [E_1(T-T_o)/(RTT_o)]\, [O_2]^{1/2} , \qquad (2.11)$$

$$d[SO_4^{2-}]_{(R1)}/dt = (2S/V)\, k_1\, (T_o) \exp\, [E_1(T-T_o)/(RTT_o)]\, [O_2]^{1/2} , \qquad (2.12)$$

$$d[H^+]_{(R1)}/dt = (2S/V)\, k_1(T_o) \exp\, [E_1(T-T_o)/(RTT_o)]\, [O_2]^{1/2} , \qquad (2.13)$$

$$d[H_2O]_{(R1)}/dt = - (S/V)\ k_1(T_o)\ \exp\ [E_1(T-T_o)/(RTT_o)]\ [O_2]^{1/2} \quad . \qquad (2.14)$$

In equations (2.11) - (2.14) the concentration of FeS_2 does not appear explicitly. This is due to the fact that the pyrite solubility in water is very low and that reactions leading to the release of ferric and ferrous ions take place mostly on solid surface. The effective active surface area is described by the parameter S/V. Parameter S is constant for times short in comparison with the decay time for the pyrite crystal. Usually the decay process is described by various versions of the shrinking core model. In the shrinking core model the parameter S decreases in time [NiG2]. Nicholson et al. [NiG2] performed their analysis for tailings. Unfortunately, we do not have any similar data for waste rock. The values of S/V are site specific and depend on several mineralogical factors.

II.1.2. *Oxidation of ferrous iron*

The oxidation of ferrous iron to ferric iron by molecular oxygen:

$$Fe^{2+} + 1/4\ O_2 + H^+ = Fe^{3+} + 1/2\ H_2O \qquad (R2)$$

is a well documented step occurring in acid rock drainage. Singer and Stumm [SiS] suggested that this can become and is known to limit the rate of pyrite oxidation at low pH, because it is slower than reaction (R3). This step is important for the reaction (R3) because it regenerates the ferric irons which are reduced during reaction (R3). Moses and Herman [MsH] investigated the microscopic features of the oxidation of aqueous Fe^{2+} at circumneutral pH and 23°C. They suggested that Fe^{2+} and dissolved oxygen react in a termolecular transition state complex. The reaction produces as an intermediate species the superoxide radical (O_2^-) and hydrogen peroxide. Fe^{2+} and H_2O_2 react in a termolecular reaction or in a two-step bimolecular reaction which depends on [OH^-] concentration.

(a1) reaction order with respect to dissolved oxygen

The order of the reaction with respect to dissolved oxygen was determined by Stumm and Singer [SiS]. They found it to be equal to one and independent of pH for low pH values, and independent of ferric iron concentration. Moses and Herman [MsH] demonstrated later that the order with respect to oxygen is independent of pH also for higher pH values up to pH=7.

(a2) reaction order with respect to ferrous iron concentration

At low pH values, the stoichiometric reaction (R2) has two different paths whose relative rates depend on the ferrous ion concentration [SaG]. At concentrations below 0.05 mol of Fe^{2+}/l the oxidation is first order with respect to ferrous iron. Above 0.1 mol of Fe^{2+} per litre the reaction is second order. Thus, in general, the rate equation for ferrous iron oxidation will contain terms proportional to [Fe^{2+}] and [Fe^{2+}]^2. The increase in the order of the reaction as a function of concentration can be explained by the fact that ferrous ions form complexes with water molecules and at higher concentrations the reaction takes place when two such complexes are in contact (which is unlikely to happen at low concentrations of ferrous ions). Detailed analysis of this fact is presented by Astanina and Rudenko [AsR].

The presence of more than one microscopic pathway for the reaction (R2) has to be assumed in any experimental study conducted with the purpose of determining the values of rate constants and activation energies at concentrations between 0.05 and 0.1. In many existing reports this assumption has not been made and this fact accounts for large discrepancies between values obtained in those papers [DaS]. In field studies iron concentrations up to 18g/l have been reported [Ge] and it is important that a kinetic model for acidic drainage has both linear and quadratic terms in $[Fe^{2+}]$.

(b) pH dependence and reaction order with respect to hydroxyl

Additional complication is introduced by the dependence of reaction (R2) on the concentration of $[OH^-]$ of hydroxyl groups. At pH values below 3.5, the reaction proceeds at a rate independent of pH. At pH values between 3.5 and 5 the reaction becomes first order with respect to $[OH^-]$. As the pH is raised above 5 to neutral, the reaction rate increases and the order changes to second order with respect to hydroxyl. Increasing the pH into the alkaline region causes precipitation of ferrous hydroxide.

While the neutralization process reduces acidity, it also accelerates the rate of the abiotic reaction (R2) which at pH=7 is five orders of magnitude faster than at pH=4 (see Fig. 2.3). This problem seems to be of great practical importance and one should carefully analyze benefits of the neutralization process in comparison with other methods of reducing acidic drainage. Proper blending of neutralizing minerals seems to be crucial for the effectivness of neutralization process.

(c) activation energy

The value of activation energy shows a tendency of increasing with pH. For pH less than 3.5 and temperatures below 100°C relevant for acidic drainage, Mathews and Robins [MaR1] obtained

$$E_{21}=74\text{kJ/mol} \quad , \quad \text{pH}<3.5 \qquad (2.15)$$

At higher values of pH, a higher value

$$E_{23}=96\text{kJ/mol} \quad , \quad \text{pH}>5 \qquad (2.16)$$

has been reported [StL].

Because of the lack of experimental data for activation energy at pH between 3.5 and 5 we

will use the value

$$E_{22}=85\text{kJ/mol} \quad , \quad 3.5<\text{pH}<5 \tag{2.17}$$

which is assumed to be simply an arithmetic average of E_{21} and E_{23}.

(d) pre-exponential factor

Pre-exponential factor is again site specific. Various field investigations of Fe^{2+} in natural mine drainage waters show higher rates than under laboratory conditions [SiS]. This is due to a catalytic effect of various substances present in natural mine drainage waters. the catalytic effects of copper, manganese, aluminium, charcoal, clay particles have been reported. As a result, values of pre-exponential factors differ often by two or three orders of magnitude [SiS].

The most dramatic effect on the rate of reaction (R2) is bacterial oxidation which may accelerate the reaction by a factor graterer than 10^6. Microbial oxidation is discussed in Section II.3.

The rate equation has the form:

$$d[Fe^{3+}]/dt_{(R2)} = k_{21}(pH)\,[O_{2gas}][Fe^{2+}] + k_{22}\,(pH)\,[O_{2gas}][OH^-][Fe^{2+}] + \\ + \; k_{23}(pH)\,[O_{2gas}][Fe^{2+}][OH^-]^2 \tag{2.18}$$

with the rate constants

$$k_{21}(pH) = 4.0 \times 10^{-6}\ M^{-1}\ atm^{-1}\ s^{-1} \qquad \text{for pH}<3.5,\ T_o=303\ K, \tag{2.19}$$

$$k_{21}(pH) = 1.66 \times 10^{-9}\ atm^{-1}\ s^{-1} \qquad \text{for pH}<5,\ T_o=298\ K, \tag{2.20}$$

$$k_{23}(pH) = 1.33\times10^{13}\ M^{-2}\ atm^{-1}\ s^{-1} \qquad \text{for pH}>5,\ T_o=298\ K \tag{2.21}$$

given in ref. [Lo] and [SiS]. pH dependence of rate constants indicates both different values of activation energy for different pH values (eqs. (15-17)) and different functional dependence as indicated in eqs. (19)-(21) and illustrated in Fig.2.3. Eq. (18) can also be expressed in terms of hydronium ion concentration [We], as discussed in Chapter III.

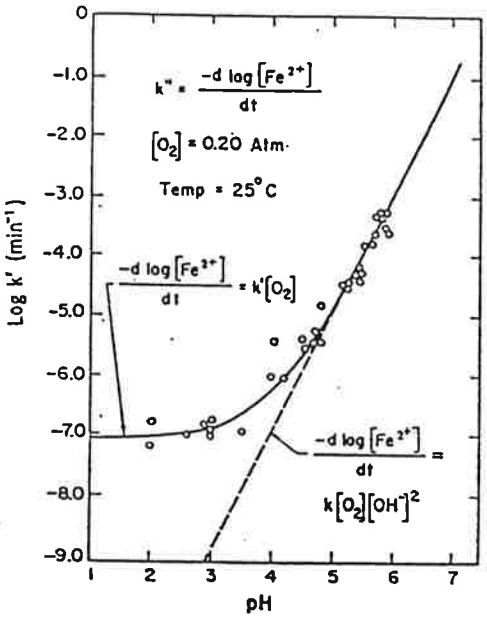

Fig.2.3 Oxidation rate of ferrous iron as a function of pH in abiotic conditions. (From Singer and Stumm [SiS]).

II.1.3. *Oxidation of pyrite by ferric iron*

In reaction (R3) :

$$FeS_2(s) + 14Fe^{3+} + 8H_2O = 15Fe^{2+} + 2SO_4^{2-} + 16H^+ \qquad (R3)$$

all oxygen in sulphate is derived from water molecules. Reaction of pyrite with ferric iron has been analyzed in a series of papers. When pH falls below 4, the solubility of ferric iron increases. At low pH values ferric iron is the major oxidant of pyrite, while the slow process of oxidation of ferrous iron to ferric iron remains the rate limiting factor in the absence of bacteria. As mentioned before, the form of the stoichiometric relations (R1)-(R4) may be misleading if they were used to establish orders of the reaction with respect to the reacting species. At first glance there is a temptation to model the kinetics by using 14th order representation with respect to ferric ions and eighth order with respect to water. As we mentioned earlier such an approach is not correct. Reaction (R3) is a multistep reaction with an essential step taking place on the pyrite surface according to Fig. 2.4 .

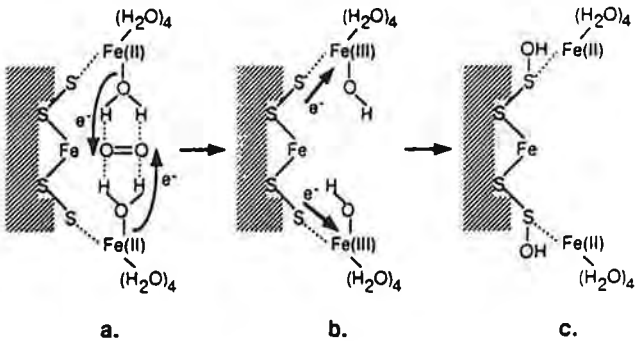

Fig. 2.4. The schematic sequence of reaction steps for the oxidation of pyrite by ferric iron. (from Moses and Herman [MoH].

The reaction takes place on the pyrite surface when ferric ions interact with FeS_2 sites on the crystal surface. As shown in Fig. 2.4 we have a local electrically unbalanced situation. The right-hand side of equation (R3) describes a quasi-equilibrium charge distribution which is reached after a series of microscopic event which occur with different elementary rates. The

molecular scenario does not require a large number of ferric ions to be in direct contact with each other and with pyrite sites, and the order of the reaction with respect to ferric iron is lower than 14. So far there are no elementary microscopic quantitative models which would describe the complex process of charge transfer between the species involved in reaction (R3). The electrochemical nature of this process manifests itself strongly at high temperatures (due to the increased mobility of reactants) and has been investigated by Mayer [Ma] . As pointed out by several researchers (see [WiR]), a specific electrochemical mechanism involving ferric ion and pyrite at the solution/solid interface is a likely rate determining step.

Fortunately there are several experimental results which allow the formulation of a realistic mathematical description of the reaction kinetics. For our model we will use the data obtained by McKibben and Barnes [McK]. The rate of reduction of ferric ion can be used in laboratory tests as a measure of the extent of oxidation of the sulphide mineral, since 14 moles of ferric iron are reduced during the decomposition of one mole of FeS_2, releasing one additional mole of iron to the solution. Because the process involves the ferric-ferrous redox couple, the redox potential, E_h of the solution as given by the Nernst equation (Morgan and Stumm [StM], Nordstrom et al. [NoJ]).

$$E_h = E_o + (RT/F) \ln [a(Fe^{3+})/a(Fe^{2+})] \qquad (2.22)$$

can be used to measure the kinetics of the reaction. In the Nernst equation $a(Fe^{2+})$ and $a(Fe^{3+})$ denote activities of the species in the brackets.

The reaction rates are the same for aerobic and anaerobic conditions. This indicates that in a waste rock pile, rates of pyrite oxidation may be large even in regions where oxygen concentration is low but concentration of ferric iron is high as the result of oxidation of ferrous iron higher in the pile. The transport of water with dissolved ferric ions should be considered as an important factor responsible for acidic drainage.

(a1) order with respect to ferric ion concentration

As the reaction takes place on the pyrite surface one has to distinguish between the physical process of adsorption of ferric iron and the chemical process of pyrite oxidation. Both processes contribute to the observed change in concentration of ferric ions in water. The adsorption process is relatively fast at the beginning and slows down after a large number of ferric ions are adsorbed on the pyrite surface. This initial phase lasts less than an hour and is short on the time scale of acid rock drainage which can be on the order of several years. For

this reason one should use results of measurements performed after the initial fast phase in which the concentration of ferric ions drops dramatically. McKibben and Barnes [McK] determined that the oxidation of pyrite by ferric ions is the reaction of 0.59 order with respect to ferric ions concentration [Fe^{3+}]. Their experimental data are reproduced in Fig. 2.5.

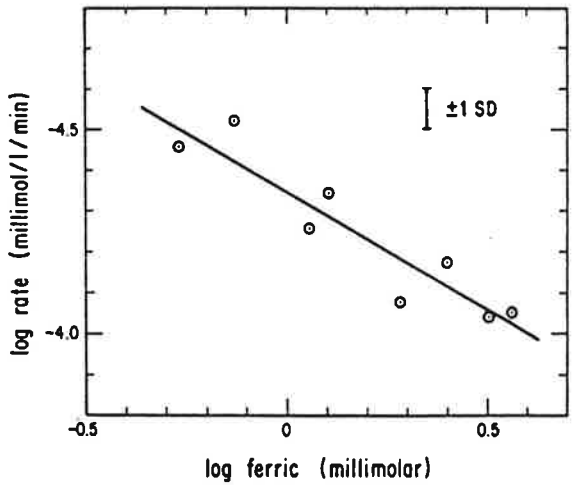

Fig.2.5. The effect of the initial ferric molarity on the initial volumetric oxidation of pyrite by ferric iron at pH 1.89 and T=30°C. Linear regression of the data yields a slope 0.58±0.09. (From McKibben and Barnes [McK])

There are several sets of experimental data in the literature (see for example references [WiR], [MaR2]) which show an order with respect to ferric iron different than 0.59 as reported by McKibben and Barnes. In those studies experimental data are improperly interpreted because of methodological errors. The main error in those papers is the assumption about an integer order of the reaction with respect to ferric iron. This assumption leads to an unacceptable concentration-dependence of rate constants.

(a2) order with respect to ferrous iron concentration

Experimental data [McK] show no detectable effect of ferrous iron concentration on the rate of oxidation by ferric iron.

(b) order with respect to proton concentration

Experimental data [McK] show an inverse square-root dependence of the rate on proton concentration (i.e. reaction rate is proportional to $[H^+]^{-1/2}$ which decreases with increasing proton concentration. Similar value has been obtained by Mathews and Robins [MaR3]. There is no explanation of this fact in literature. We can only speculate that the reaction (R3) is reversible, with a reverse reaction showing a positive order with respect to protons. In the reaction (R3) the adsorbed ferric iron is reduced to ferrous iron by an electron transfer from one of the pyrite sites. (This mechanism is consistent with the semiconductive properties of pyrite).

(c) activation energy

Mathews and Robins [MaR2] and Wiersma and Rimstidt [WiR] obtained activation energy values of 85 kJ/mol and 92 kJ/mole respectively. These values have been obtained over a temperature range 30-70°C and can be used as characteristic values for acid rock drainage. In our model we use the value

$$E_3 = 90 \text{ kJ/mol} \tag{2.23}$$

(d) pre-exponential factor

The pre-exponential factor describes in this case both the characteristic rates of chemical processes taking place on pyrite surface, and the chemical activity, a_3 as a function of the pyrite reactive surface area to volume of solution ratio (Singer and Stumm [SiS])

$$a_3 = k_3 S/V \tag{2.24}$$

(S - pyrite surface area, V - solution volume). Several authors suggested that the reactive surface area is significantly different than the total surface area. Oxidation has been observed to take place on reactive sites with excess surface energy, such as grain boundaries, defects, solid and fluid inclusion pits, cleavages and fractures. A reliable waste rock model must take into consideration the decrease in surface area over time. Usually this is done by using a shrinking core model. The shrinking core model does not take into consideration changes of physico-chemical properties of the rock surface during the oxidation process. The rate constants obtained during most experiments have been measured over time intervals from a few minutes to a few hours and it is possible that they are not representative of long-term acidic drainage. Determining a long-time dependence of the pre-exponential factor should provide important entry data for a waste rock model.

From the relation

$$d[Fe^{3+}]_{(R3)}/dt = S/V\ k_3(T)\ [Fe^{3+}][H^+]^{-0.5} \quad , \qquad (2.25)$$

obtained by McKibben and Barnes [McK], and the stoichiometric relation (R3), we obtain other kinetic equations for water, sulphate, ferrous iron and proton concentrations.

For pyrite concentration in units of moles of pyrite cm^{-2}, McKibben and Barnes obtained the rate constant

$$k_3\ (T_o) = 3.03 \times 10^{-12}\ M\ cm^{-2}\ s^{-1} \qquad \text{at } T_o = 303\ K\ . \qquad (2.26)$$

We could not reproduce experimental data of Mc Kibben and Barnes when we used the above value of k_3. A different value of the rate constant k_3 is determined in Chapter III.

II.1.4. *Precipitation of ferric hydroxide*

The reaction

$$Fe^{3+} + 3H_2O \rightleftarrows Fe(OH)_3(s) + 3H^+ \qquad (R4)$$

is reversible and its direction depends on the pH value. Fig.2.6 presents the diagram of activity of Fe^{3+} (denoted by (Fe^{3+})) as a function of pH:

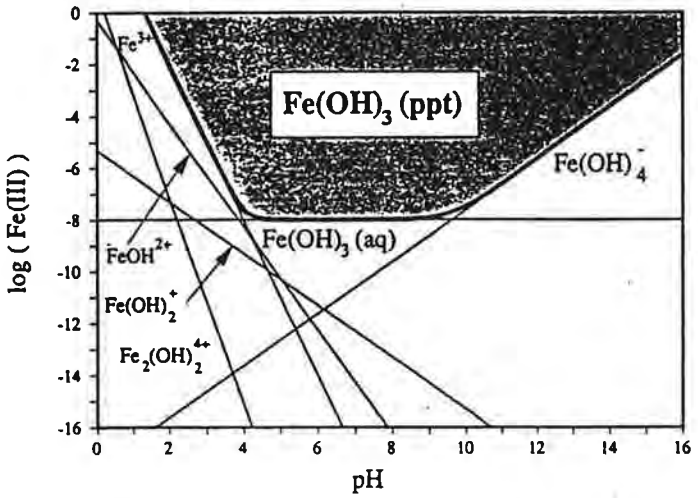

Fig. 2.6. Activity-pH diagram for Fe(III) species in equilibrium with $Fe(OH)_3$(ppt) at 298 K. (From Kelsall and Williams [KeW1].

The equilibrium between ferric iron and ferric hydroxide in silica is given by [KeW1]:

$$\log\{(Fe(OH)_3)/(Fe^{3+})\} = -11.95 + 3\ pH. \qquad (2.27)$$

The solubility equation has the form

$$\log\ (Fe(OH)_3) = -7.98 \qquad (2.28)$$

Processes of precipitation and dissolution of ferric hydroxide play an important role in acidic

drainage by providing a sink (at high pH values) and a source (at low pH values) of ferric ions for reaction (R3). Nicholson et al. [NiG] have found that at circumneutral pH, ferric hydroxide forms a passive protective film on pyrite, which results in lower rates of oxidation by dissolved oxygen. This also means that if we can control and maintain high pH values in waste rock, then we can eliminate pyrite oxidation by ferric iron (reaction (R3) and we can also slow down the oxidation by dissolved oxygen (reaction (R1).

On the other hand, the rate of ferrous iron oxidation in reaction (R2) increases with pH. In this way the neutralization process leads to the formation of reservoir of ferric iron in the solid form, which, if dissolved, may cause accelerated pyrite oxidation. This means that if an insufficient amount of the neutralizing minerals is mixed with waste rock to control acidic drainage, pH may decrease below 4 and pyrite oxidation may become faster than it would have been had neutralization not been attempted. This danger exists in particular when ferric hydroxide accumulates during a dry period and than redissolution occurs during a wet period, when acidic conditions with $pH < 4$ are initiated. Dissolution rates of neutralizing minerals affect the neutralization process. The dissolution rates of calcite, dolomite and magnesite are significantly different and additional kinetic studies are required to determine optimum amounts of neutralizing minerals.

II.2. Bacterial oxidation

Sulphide minerals undergo accelerated oxidation in the presence of bacteria to form sulphuric acid. For pH below 4, reaction (R2) is thought to be the rate-limiting step for reaction (R3), the principal inorganic oxidation mechanism [StM], [SiS]. Bacteria such as Thiobacillus ferrooxidans increase the rate of oxidation of ferrous to ferric iron (reaction (R2)) by several orders of magnitude in acidic environments [In], [An], [BaO], [BoB], [Br], [CaW], [CrT], [Eh], [Ka],[KuM],[LaB][LeK], [LiS], [Lu], [Ol], [Sa], [SuL], [SuT], [UhH], [WiU] . Following several studies, we will incorporate the process of bacterial oxidation by describing it in our model as three stoichiometric reactions

$$FeS_2(s) + 7/2\ O_2 + H_2O \xrightarrow{\text{bacteria}} Fe^{2+} + 2SO_4^{2-} + 2H^+ \ , \qquad (B1)$$

$$Fe^{2+} + 1/4\ O_2 + H^+ \xrightarrow{\text{bacteria}} Fe^{3+} + 1/2\ H_2O \ , \qquad (B2)$$

$$FeS_2(s) + 14Fe^{3+} + 8H_2O \xrightarrow{\text{bacteria}} 15Fe^{2+} + 2SO_4^{2-} + 16H^+ \qquad (B3)$$

which have the same form as the abiotic chemical reactions (R1) , (R2) and (R3). The details of bacterial oxidation of pyrite are different than for abiotic chemical reactions (R1), (R2) and (R3), and remain unknown to some extent. Reaction (B3), in particular, is probably quite different than reaction (R3) . It has been suggested [LiS4] that elemental sulphur is an important intermediate product of the bacterial oxidation of pyrite, while during the abiotic reaction (R3) elemental sulphur has not been detected at any stage of the reaction. Anaerobic oxidation of pyrite T. ferrooxidans has been documented only recently [SuL], [Pr], [Gu], contrary to an earlier belief that pyrite oxidation by T. ferrooxidans under anaerobic conditions is negligibly slow.

The microbial catalysts lower the activation energy of the reactions and greatly accelerate reaction rates. The microbial influence on pyrite oxidation as given by reaction (B2) is usually referred to as an indirect action, as distinguished from a direct action mechanism in which T. ferrooxidans or other microbes attach themselves to the pyrite surface and directly attack the surface, enzymatically oxidizing sulphide to sulphate, in a way similar to reaction (R1).

II.2.1. *Aerobic bacterial oxidation of pyrite*

Bacterial aerobic oxidation of pyrite involves dissolved oxygen and oxygen derived from water molecules. Because products in a bacterial process are the same as in the reaction (R1) we use the same stoichiometric relation

$$FeS_2(s) + 7/2\ O_2 + H_2O \xrightarrow{\text{bacteria}} Fe^{2+} + 2SO_4^{2-} + 2H^+ \qquad (B1)$$

as for the abiotic reaction (R1).

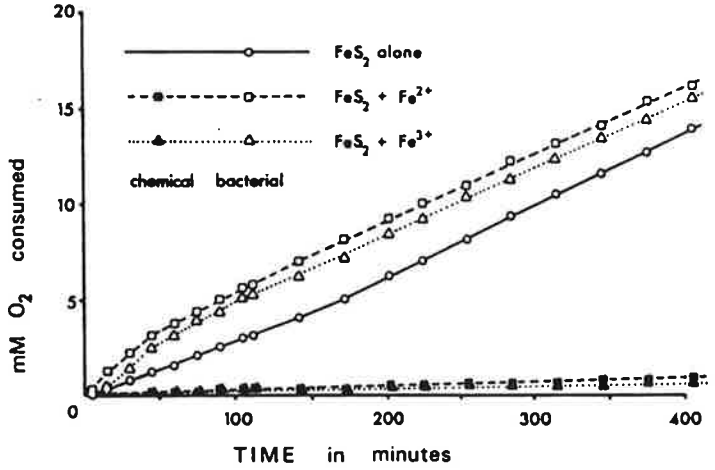

Fig.2.7. Oxygen consumption in the oxidation of washed pyrite with and without Fe^{2+} or Fe^{3+} by T. ferrooxidans. Concentration of T. ferrooxidans, 1 mg of wet cells per ml; Fe^{2+}, 6.25 mM; Fe^{3+}, 13.5 mM. (From Lizama and Suzuki [LiS4].

From Fig.2.7 and other experimental data it is evident that the bacterial oxidation rates are much greater then abiotic chemical oxidation rates. Bacterial activity reaches its maximum at a temperature T_m which is typically between 298K and 338K.

When pyrite and water are in excess we use the formula

$$d[O_2]_{(B1)}/dt = - S/V\ B(T)\ B(pH)\ k_{1b}\ (T_m,[cell])[O_2]^{1/2} \qquad (2.29)$$

Equation for ferrous iron production can be obtained from the stoichiometric formula and has the form

$$d[Fe^{2+}]_{(B1)}/dt = (2S/7V)\ B(T)\ B(pH)\ k_{1b}(T_m,[cell])[O_2]^{1/2} \qquad (2.30)$$

Eqs. (2.28) and (2.29) describe rates oxygen consumption and ferrous iron production as the functions of dissolved oxygen concentration, $[O_2]$ and cell concentration, [cell] at different values of pH and temperature. The coeeficients B(T) and B(pH) are equal to one for $T=T_m$ and pH for which T. ferrooxidans exhibit the maximum activity.

The value of k_{1b} is obtained by analyzing experimental data obtained by Lizama and Suzuki [LiS4]:

$$k_{1b}(T_m,[cell]) = 8.49 \times 10^{-6}\ M^{1/2}lm^{-2}\ s^{-1}$$

for 1 mg of cells per 1 ml. at $T_m=303$ K and pH=2.3 (2.31)

The value (2.31) is obtained in paragraph 4.0.3 by analyzing data presented in Fig.2.7 and data on the reactions (B2) and (B3).

(a1) order with respect to oxygen

There are no quantitative experimental data for the dependence on oxygen concentration and the 1/2 order reaction with respect to oxygen is postulated (the same as for the reaction (R1)).

(a2) dependence on cell concentration

For the reaction (B1) we do not know of any systematic experimental data on the rate dependence on cell concentration. We use a value [cell]=1g/l for which experimental data exist. For large bacteria concentrations in unwashed pyrite some inhibition effects have been observed. We expect to extend our analysis when experimental data on reactions (B1) and (B3) for other cell concentrations become available.

(b) *temperature and pH dependence*

The rate coefficient K_{1b} defined as

$$K_{1b} = k_{1b}(T_m,[cell])\ B(T)\ B(pH). \qquad (2.32)$$

depends on temperature and pH. The form of the coefficients B(T) and B(pH) is assumed to be the same for all bacterial reactions and is discussed in paragraph II.2.2.

II.2.2. Aerobic bacterial oxidation of ferrous iron

Reaction

$$Fe^{2+} + 1/4\ O_2 + H^+ \xrightarrow{\text{bacteria}} Fe^{3+} + 1/2\ H_2O \qquad (B2)$$

is much faster than the analogous abiotic reaction (R2). The mechanism of the biochemical oxidation of ferrous iron has been summarized by Ingledew [In]; see also [LuV], [LuS]). The process involves an Fe^{2+} - oxidoreductase as the initial electron acceptor. To date the nature of the intermediate electron acceptor is not known. However, there are candidates which include rusticyanin, a redox peptide with a molecular weight of 16 000, and a cytochrome c with a molecular weight of about 12 000. The other electron transport components involved in iron oxidation are membrane-bound cytochrome c and cytochrome oxidase. In the first part of the process ferrous iron is oxidized with the release of electrons:

$$2Fe^{2+} \rightarrow 2Fe^{3+} + 2e^- \qquad (2.33)$$

The second part of the reaction takes place on the inside of the cytoplasmic membrane and within the cytoplasm:

$$2e^- + 2H^+ + 1/2\ O_2 \rightarrow H_2O. \qquad (2.34)$$

This means that the membrane properties play an important role by gating the charge transfer in the process of bacterial oxidation.

The rapid elimination of the H^+ as shown in equation (2.34) maintains a neutral pH within the cytoplasm, which is required to establish the H^+ electrochemical gradient, the driving force for producing biological energy. In this way the acidic environment provides energy for bacterial growth and at the same time a neutral pH is maintained inside the bacteria. Lundgren et al.[LuV] estimate that about $3x10^6$ atoms of Fe^{2+} are oxidized per cell per second.

(a1) order with respect to concentration of ferrous iron and with respect to concentration of bacteria

Detailed quantitative studies have been recently performed by Suzuki et al. [SuL] who have determined the rate of Fe^{2+} oxidation by measuring the rate of oxygen consumption at 25°C and pH=2.3

Fig.2.8 shows the effect of Fe^{2+} concentration on oxidizing activity of various concentrations of cells.

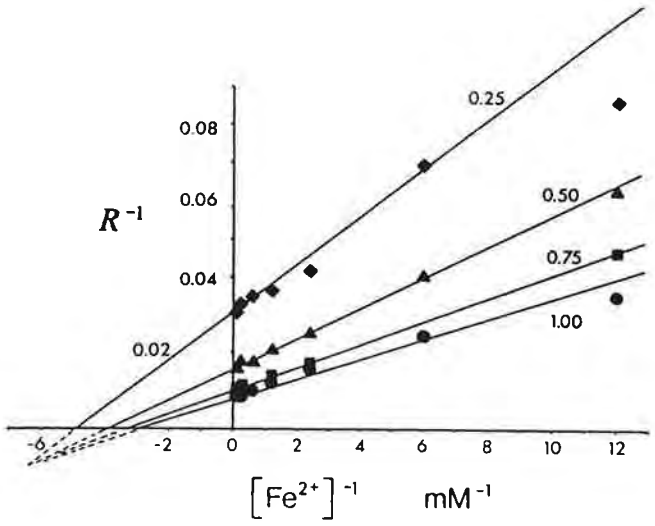

Fig.2.8. Effect of Fe^{2+} concentration on the Fe^{2+}-oxidizing activity of various concentrations of T. ferroxidans (0.25, 0.50, 0.75 and 1.00 mg of wet cells per 1.2 ml). The O_2 consumption rate, R determined in nanomoles of O_2 per min at 25°C; values of R^{-1} are given on vertical axis. (From [SuL]).

The empirical formula proposed by Suzuki et al. [SuL] has the form of Michaelis-Menten relation:

$$d[O_2]_{(B2)}/dt \propto k_{2b}(T_m,[cell]) \propto C_{2b}[cell]\ \{k_{2m}(1+[cell]/k_{2c}) + [Fe^{2+}]\}^{-1}, \qquad (2.35)$$

$$k_{2m} = 110\text{mM } Fe^{2+},\ k_{2c} = 0.33 \text{ mg of cells/ml at } T=298K \text{ and } pH=2.3. \qquad (2.36)$$

Eq. (2.35) describes the effect of competitive inhibition by increasing concentration of cells and Fe^{2+}. Other proportionality constants are discussed below.

(a2) order with respect to dissolved oxygen

We could not find any systematic results on bacterial activity for different values of oxygen concentration. We assume that the bacterial oxidation rate depends linearly on oxygen concentration (i.e. in the same way as the abiotic reaction (R2).

(b) rate constants for bacterial oxidation

For dissolved oxygen concentration Suzuki et al. [SuL] report the rate constant C_{2b} between 1.46 and 2.38 μmol O_2/s per mg of cells per ml for oxygen concentration at atmospheric partial pressure. We will perform our analysis for a particular strain, SM-4 of Tiobacillus ferrooxidans for which Suzuki et al. obtained

$$C_{2b} = (2\pm 0.3)\ \mu M\ O_2/s \text{ per mg of cells per ml at } T=298K \text{ and } pH=2.3 \quad (2.37)$$

(c) pH dependence

We did not find in literature any detailed quantitative study of the pH effect on rates of bacterial oxidation. Typically Thiobacillus ferrooxidans show maximum of activity at pH between 2 and 4. Often it is assumed that Michaelis-Menten factor

$$f_M = (1 + 10^{b1-pH} + 10^{pH-b2})^{-1} \text{ where } b_1 < b_2 \quad (2.38)$$

can be used to describe a pH dependence of bacterial oxidation . Formula (2.38) has been derived for enzymatic reactions [BaO], [Se]. Apart from enzymatic reactions, bacterial oxidation involves also other processes which modify kinetics of enzymatic reactions.

Expression (2.38) has its maximum for $pH=b_m=(b_1+b_2)/2$ and goes to zero for pH less than b_1 and greater than b_2. For $b_1=2.2$ and $b_2=2.4$ it describes quite well the known property that T. ferroxidans are chemically active for low pH values with a maximum at $pH=b_m=2.3$. By introducing the requirement that at the maximum $B(pH=bm)=1$ we obtain

$$B(pH) = (1+10^{b1-bm} + 10^{bm-b2})\,(1 + 10^{b1-pH} + 10^{pH-b2})^{-1}. \quad (2.39)$$

As an alternative one could also use B(pH) in the form

$$B'(pH) = [B(pH)]^n \quad . \qquad (2.40)$$

The last formula introduces an adjustable parameter n which provides some flexibility for describing the quantitative features of pH dependence when more detailed experimental data become available. The problem of detailed pH dependence of bacterial activity merits further experimental work. It is also important to know that Thiobacillus ferrooxidans show a large degree of adaptability and, if grown at very low pH values, they may oxidize pyrite at significant rates at pH values below 2 [Su].

(d) temperature dependence

Bacterial oxidation shows a strong nonlinear temperature dependence as shown in Figs. 2.9.

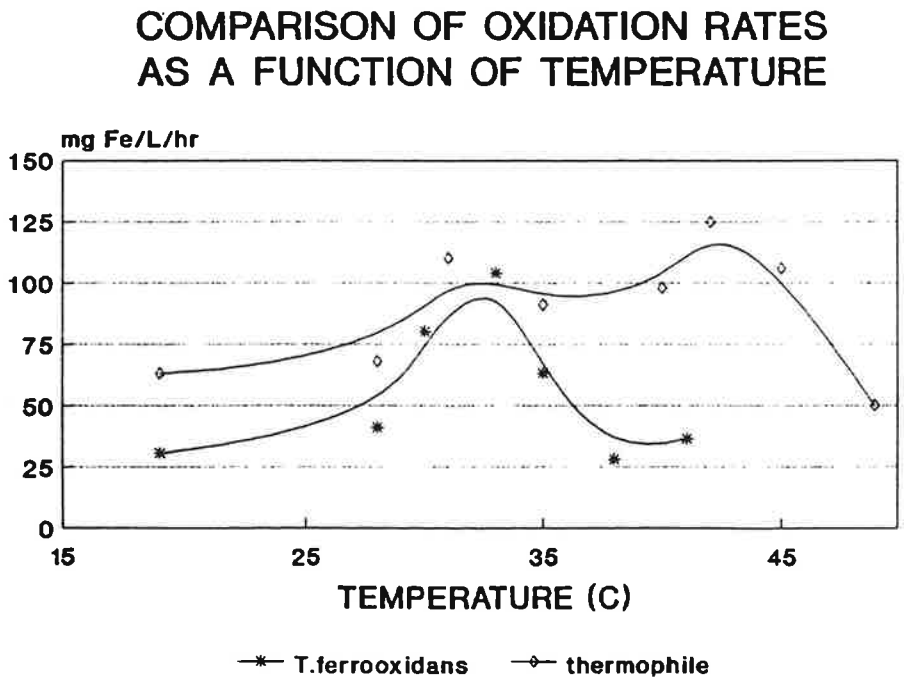

Fig.2.9. Oxidation rates for T. ferrooxidans and a Thermophilic culture (not analyzed in this report) for a range of temperatures. (From Spencer et al. [SpB])

Different strains of Thiobacillus ferrooxidans show sharp maxima of activity at temperatures between 30°C and 40°C. We use the formula

$$B(T) = \exp [- c(T-T_m)^{1.4}] \{1 - th [-d(T-T_m)^3] \} . \qquad (2.41)$$

B(T) has a maximum at $T=T_m$. The factor $(1 - th(-d(T-T_m)^3)$ accounts for the observed asymmetry of temperature dependence and for the sharp decrease in bacterial activity for temperatures higher than T_m . A good agreement with experimental data is obtained for $c=0.05/K^2$ and $d=0.005/K^3$ - see paragraph 4.0.0 for further discussion.

There are studies which use the Arrhenius expression to describe temperature dependence of bacterial activity (Bailay and Ollin [BaO] and [Se]). The main deficiency of the Arrhenius formula in application to bacterial processes is its inability to account for the observed maxima in bacterial activity. It assumes that the bacterial activity is proportional to enzymatic activity for which the Arrhenius expression can be applied. It does not take into account, however, the fact that bacterial activity depends also on membrane permeability and other cell properties which cannot be described by the Arrhenius expression. The membrane permeability often changes faster than exponentially with temperature (see Otwinowski and Paul [OtP], for example) and for this reason we use Gaussian and hyperbolic functions.

$$d[O_2]_{(B2)}/dt = -(1/4)k_{2b}(T_m,[cell]) B(T) B(pH) [O_2][Fe^{2+}] \qquad (2.42)$$

The efficiency of the bacterial oxidation process depends on the bacterial chemical activity and the population growth. So far we did not model the population growth. For practical reasons, controlling bacterial population is an important aspect of acid drainage. A model for population growth under different physico-chemical conditions may be an important tool for both predicting and preventing acid rock drainage.

II.2.3. Anaerobic pyrite oxidation by Thiobacillus ferrooxidans

Details of the biochemical processes responsible for the increased rates of pyrite oxidation by ferric iron remain unknown. For this reason the relation

$$FeS_2(s) + 14Fe^{3+} + 8H_2O \xrightarrow{\text{bacteria}} 15Fe^{2+} + 2SO_4^{2-} + 16H^+ \qquad (B3)$$

should be considered as one of the possible scenarios. As suggested by Lizama and Suzuki [LiS4] a possible reaction may be

$$FeS_2 + 2Fe^{3+} \rightarrow 3Fe^{2+} + 2S^\circ . \qquad (2.43)$$

In the next step sulphur may be oxidized to sulphate according to the reaction:

$$S^\circ + 6Fe^{3+} + 4H_2O \rightarrow H_2SO_4 + 6Fe^{2+} + 6H^+ \qquad (2.44)$$

So far there is no evidence for the presence of elemental sulphur in the process of pyrite oxidation by ferric iron. A more detailed study is required in order to prove this concept. Even if reactions (2.43) and (2.44) are correct, we still may expect that the reaction (B3) provides a correct description of anaerobic bacterial oxidation of pyrite. Unfortunately there is very little quantitative data which can be used for the modelling of this process. The only quantitative data which we have found so far, had been obtained by Lizama and Suzuki [LiS4] and are presented in Fig. 2.10.

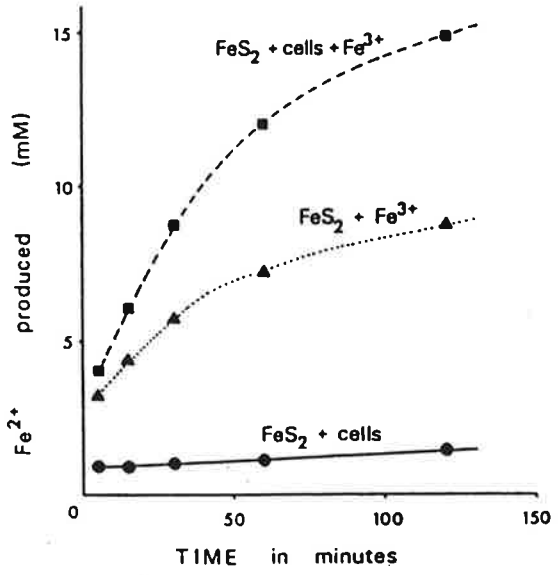

Fig.2.10. Rates of anaerobic Fe^{2+} production from pyrite plus Fe^{3+} by T. ferroxidans. Initial concentrations: T. ferroxidans, 1 mg of wet cells per ml; initial concentration of Fe^{3+}, 13.5 mM. (From ref. [LiS4])

Fig. 2.10 shows that the Fe^{2+} production from Fe^{3+} and pyrite is faster in the presence of bacterial cells.

The order of reaction (B3) with respect to ferric iron, dependence on bacteria concentration and ferrous iron have not yet been analyzed. We use the formula

$$d[Fe^{2+}]_{(B3)}/dt = (15S/14V)\ k_{3b}\ (T_m,[cell])B(T)\ B(pH)\ [Fe^{3+}]^{3/5}[H^+]^{-1/2} \qquad (2.45)$$

(which will be justified later in mathematical analysis in Chapter IV). The value of $k_{3b}(T_m,[cell])$ is estimated as

$$k_{3b}(T_m,[cell]) = 2.18 \times 10^{-4}\ M^{0.9}\ lm^{-2}\ s^{-1} \quad \text{at 1mg of cells/1ml} \qquad (2.46)$$

We also use the same coefficients B(T) and B(pH) as for the other two bacterial reactions.

The rate of anaerobic pyrite oxidation by bacteria is significantly greater than the rates observed for anaerobic oxidation of pyrite by ferric iron in the absence of bacteria. At low pH values and high concentrations of ferric iron the anaerobic bacterial oxidation is a very significant process responsible for acidic drainage. Recently it has been demonstrated that T. ferroxidans may grow under anaerobic conditions. The rates of bacterial growth increase with concentration of carbon dioxide [Se], [Su], [Pr]. This indicates that controlling the levels of carbon dioxide inside waste rock piles may be almost as important as controlling the levels of oxygen. It also indicates that the bacterial oxidation of pyrite may be observed deep inside waste rock piles where oxygen levels are low. We do not know, however, of any field tests which would analyze this possibility. In laboratory tests nutrients containing phosphorus and nitrogen are used. We do not have, however, quantitative data on the effect of phosphorus and nitrogen concentration on the bacterial oxidation rates. This aspect may merit further experimental and modelling studies whose findings may be particularly significant for ARD from apatite bearing rocks.

II.3. Neutralization

Leaching systems are generally self-buffering, i.e. some reactions occurring within the leaching environment are acid-consuming. In many cases rocks containing FeS_2 contain also calcite and other minerals which may neutralize acidic water. For calcite, for example, the neutralization of water involves the reaction:

$$2H^+ + CaCO_3(s) = Ca^{2+} + H_2CO_3 \qquad (2.47)$$

which is often also written as

$$CaCO_3 + 2\ H^+ + SO_4^{2-} + H_2O = CaSO_4 \cdot 2\ H_2O + CO_2 \qquad (2.48)$$

Incorporating the neutralization process into the model will give quantitative information about the efficiency of controlling AMD by mixing neutralizing material with waste material. The neutralization process may take place in two ways:

(i) By adding a neutralizing mineral, like calcite, to the acidic seepage. This process does not affect the rates of pyrite oxidation which proceeds at pH values unaffected by the neutralizing agent. The rate equation describing the neutralization process is then decoupled from other kinetic equations.

(ii) By mixing calcite with the waste rock. This causes pyrite oxidation to occur under high pH values. In this way the pyrite oxidation rate is affected by the presence of a neutralizing agent.

If one could demonstrate that pyrite oxidation is slowed down by the mixing of neutralizing minerals with waste rock, one should favour (ii) over (i) because the amount of effluent sludge would be smaller. In case (ii) the rate equation for the neutralization process is strongly coupled to the rest of the kinetic equations.

In the ideal situation we deal with a self-buffering system which can be described by the set of kinetic equations based on reactions (R1) and (R2):

$$FeS_2(s) + 7/2\ O_2 + H_2O = Fe^{2+} + 2SO_4^{2-} + 2H^+ \qquad (R1)$$

$$Fe^{2+} + 1/4\ O_2 + H^+ = Fe^{3+} + 1/2\ H_2O \qquad (R2)$$

Reaction (R3) is eliminated because ferric iron precipitates as ferric hydroxide (as described by reaction (R4)). For pH above 2.5 and iron concentrations reaching levels of 20 g/l, the rate of formation of ferric hydroxide becomes practically equal to that of the formation of ferric iron.

Eq. (2.48) does not provide all the information about the neutralization process. It turns out that the neutralization process takes place according to two different scenarios depending on the pH. For pH less than 6.3, the scheme

$$CaCO_3 + 2\,H^+ + SO_4^{2-} + 2H_2O = CaSO_4 \cdot 2\,H_2O + H_2CO_3^{\circ} \qquad (R5.1)$$

prevails.

For pH greater than 6.3 the dominant reaction is

$$CaCO_3 + H^+ + SO_4^{2-} + H_2O = CaSO_4 \cdot 2\,H_2O + HCO_3^- \qquad (R5.2)$$

Thus we see that the efficiency of the neutralization process is different, depending on pH values. The reaction (R5.1) neutralizes two hydronium ions per one calcite molecule. The reaction (R5.2) neutralizes only one hydronium ion per one calcite molecule.

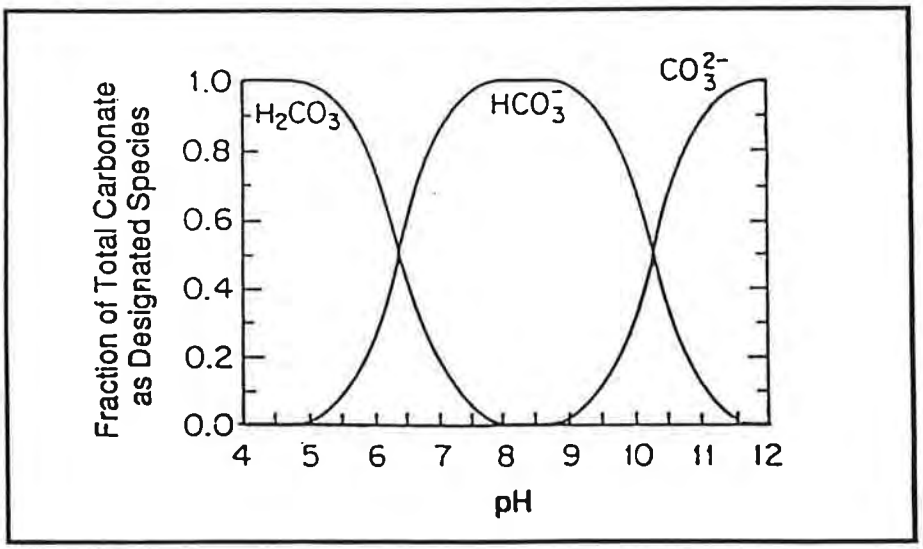

Fig. 2.11. Relationship of pH to relative concentrations of carbonate species (from Freeze and Cherry [FrC].

Iron carbonates provide no net consumption of acid [Lap], [MoC]. The initial dissolution of one mole of iron carbonate consumes one or two moles of acid:

$$FeCO_3 + H^+ = HCO_3^- + Fe^{2+} \ , \qquad (2.49)$$

$$FeCO_3 + 2H^+ = H_2CO_3^- + Fe^{2+} \ . \qquad (2.50)$$

Under environmental conditions one mole of ferrous iron released is oxidized to ferric iron which precipitates as ferric hydroxide. The oxidation and precipitation yield two moles of acid. Thus, iron carbonate does not contribute to acid consumption.

II.4. Solubility of oxygen in water

In the previous paragraphs, we have summarized the experimental results on the temperature dependent rates of the chemical and biological reactions involved in pyrite oxidation. Chemical factors are primarily responsible for the generation of acid and dissolved metal ions. Reaction rates are also controlled by several physical factors like temperature, solubility of oxygen in water, rates of energy and mass transport, surface properties of rock, etc.

Inside large waste rock piles the oxygen concentration varies as a function of the distance from the pile boundaries. Near the pile boundaries the oxygen concentration in the gas phase is about 21% and may decrease to almost 0% far from the boundaries. This nonhomogeneous oxygen distribution depends on the rates of chemical reactions and on the rates of mass and energy transport through a porous pile. When the pile porosity is small, mass transport is slow and reaction rates are greatly reduced because of the small concentration of oxygen inside a pile. In this way the reaction rates are controlled by the mass transport rates. We leave a detailed analysis of the interplay between chemical, biological and physical factors for a future project. To construct a realistic waste rock model we need, however, quantitative information on the reaction rates as a function of oxygen concentration.

Table I presents data on the concentrations of oxygen dissolved in water, $[O_2]$ as a function of the temperature and oxygen concentration in the gas phase, $[O_2]_{gas}$. The temperature values correspond to those observed in waste rock piles. $[O_2]$ increases slightly faster than linearly with $[O_2]_{gas}$ at constant temperature. At 60°C and $[O_2]_{gas}=21\%$, $[O_2]$ is less than 50% of its value at 10°C. In this way we observe a competitive effect of temperature and dissolved oxygen concentration on the reaction rates. A detailed analysis of temperature dependence of reaction rates will be presented in our numerical analysis.

As we mentioned before, the values of activation energies for pyrite oxidation by dissolved oxygen have been determined by compensating for the effect of decreasing $[O_2]$ with increasing temperature. We can thus use the activation energy values without further corrections.

The values in Table I are obtained for water without any dissolved iron or sulphate ions. Unfortunately we do not have any experimental data on the concentrations of

T °C	$[O_2]_{gas}$=21%		$[O_2]_{gas}$=15%		$[O_2]_{gas}$=10%		$[O_2]_{gas}$=5%		$[O_2]_{gas}$=1%	
	mg	µmol	mg	µmol	mg	µmol	mg	µmol	mg	µmol
5	12.79	399.6	9.60	299.9	6.02	188.1	2.92	91.2	0.50	15.6
10	11.30	353.0	8.03	250.9	5.31	165.9	2.59	80.9	0.41	12.8
15	10.11	315.9	7.16	223.7	4.72	147.5	2.27	70.9	0.32	10.0
20	9.12	284.9	6.45	201.5	4.23	132.2	2.01	62.8	0.23	7.2
25	8.30	259.3	5.86	183.1	3.77	117.8	1.82	56.8	0.14	4.4
30	7.60	237.5	5.33	166.5	3.44	107.5	1.56	48.7	0.05	1.6
35	7.00	218.7	4.88	152.5	3.12	97.5	1.43	44.7	0.00	0.0
40	6.47	202.1	4.47	139.7	2.81	87.8	1.15	35.9	0.00	0.0
45	6.00	187.5	4.10	128.1	2.52	78.7	0.94	29.4	0.00	0.0
50	5.57	174.0	3.75	117.2	2.25	70.3	0.74	23.1	0.00	0.0
55	5.17	161.5	3.55	110.9	1.96	61.2	0.50	15.6	0.00	0.0
60	4.89	152.8	3.38	105.6	1.64	51.2	0.25	7.8	0.00	0.0

Table I. Saturation concentrations of dissolved oxygen in water, $[O_2]$, at atmospheric pressure (1013.25 hPa) for different oxygen concentrations in the gaseous phase $[O_2]_{gas}$. The solubilities of oxygen are defined in terms of the mass of oxygen dissolved in one litre of the water in equlibrium with an atmosphere saturated with water vapour at various temperatures. The data are calculated following Benson and Krause [BeK] and using a computer program published by Beer [Be].

dissolved oxygen in the presence of iron and sulphate ions at various pH values. We will simply assume that the maximum concentration of oxygen dissolved in water does not depend on pH. This assumption is supported by the fact that the order of reaction (R3) with respect to oxygen does not depend on pH, as discussed by McKibben and Barnes [McK].

In our numerical analysis we use values of $[O_2]$ instead of $[O_2]_{gas}$ used previously in most experimental and modelling studies. This choice is motivated by a strong dependence of $[O_2]$ on temperature, as illustrated by data in Table I. A future waste rock model should use an empirical formula describing the nonlinear dependence of $[O_2]$ on temperature for various concentrations of $[O_2]_{gas}$ in waste rock piles.

III. Mathematical Analysis of Chemical Kinetics

This chapter presents results of our mathematical analysis of a set of kinetic equations constructed on the basis of experimental data obtained independently for reactions (R1)-(R5) and B(1)-(B3), as discussed in previous paragraphs. The purpose of our analytical and numerical analysis is to establish the relative importance of individual factors responsible for acid rock drainage. When useful, we also derive closed form formulae which may be helpful in designing and interpreting some new experiments. Our kinetic equations are ordinary differential equations and we do not analyze explicitly the processes of mass and energy transport, which after a sufficiently long time control reaction rates in large waste rock piles. The only physical factors involved in the present analysis are temperature and oxygen concentration. Mass and energy transport will be described in our future project by means of nonlinear partial differential equations which will describe the spatially nonhomogeneous distribution of oxygen, water, reaction products and temperature as a function of physical and mineralogical properties such as pile porosity, oxygen diffusion and convection, thermal conductivity, water infiltration rates, water evaporation, rock neutralizing potential, etc.

We want to obtain quantitative results which would allow us to understand better the complex chemistry of ARD as a function of two physical parameters: concentration of dissolved oxygen and temperature. Most experimental results were obtained for small samples of less than ten grams of pyrite and times shorter than ten hours. We use the available experimental data to obtain information on chemical and physical behaviour of greater masses of pyrite and water during several weeks. This initial information should be useful for a future reliable waste rock model. After achieving the necessary understanding of the chemical processes involved, a waste rock model should concentrate on the physical and geochemical processes and should provide the understanding of physico-chemical behaviour of much greater masses of waste rock (greater than 10^5 tons) over time intervals of several years.

Discharge of contaminants from waste rock sites shows temporal variations. One of the key questions is whether these variations are related to (i) an oscillatory nature of

chemical and biological reactions or (ii) result from an interplay between local chemical processes and mass and energy transport. In case (i), a future model including transport processes would be very complicated and one would have to use sophisticated numerical methods to obtain reliable results. If no chemical oscillations are detected for a set of ordinary differential equations, we will be able to reduce the number of coupled nonlinear differential equations and deal with a relatively simple model.

We have analyzed acid generation, discharge of iron ions, oxygen and water depletion for different scenarios corresponding to various situations in waste rock piles and our results are presented in Sections III.1 and III.2.

III.1. Pyrite oxidation without bacteria and without neutralization (Reactions (R1), (R2) and (R3) at low pH values and reactions (R1), (R2) and (R4) at high pH values).

III.2. Pyrite oxidation with neutralization in the absence of bacteria (reactions (R1), (R2), (R4) and (R5).

Bacterial oxidation is analyzed in Chapter IV.

Numerical results are presented for different values of temperature, pH and concentration of dissolved oxygen. Numerical analysis has been performed for two types of conditions:

(i) when oxygen concentration is constant in time

(ii) when oxygen concentration evolves in time from an initial value corresponding to the atmospheric conditions

Condition (i) simulates the situation near the pile boundary. Condition (ii) simulates the situation far from the boundaries at the initial stage after a waste rock pile is formed.

The main results of our analysis can be summarized by the following points:

1. The coupled chemical reactions do not produce temporal oscillations of concentrations of final and transient products. No chaotic behaviour or limit cycles are detected.

2. At low pH below four, the rate of oxidation of ferrous iron (Fe^{2+}) to ferric iron (Fe^{3+}) controls the rate of pyrite oxidation by ferric iron. This is a qualitative feature known before.

We have obtained a closed form formula for the rate of pyrite oxidation by ferric iron, expressed in terms of the rate constant governing the oxidation of ferrous iron. In the absence of bacteria the concentration of ferric iron does not affect qualitative features of temporal changes of concentrations of other species.

3. The oxidation of ferrous iron leads to concentrations of ferric iron given by the quasi-equilibrium principle applied to the chemical network.

4. For constant in time oxygen concentrations at pH values between four and seven, and without neutralization, the rate of pyrite oxidation is practically time independent. The amount of oxidized pyrite and concentrations of iron, hydronium and sulphate ions increase linearly with time.

5. Application of neutralizing compounds leads to fast rates of oxidation of ferrous iron to ferric iron and subsequent formation of ferric hydroxide which precipitates and slows the oxidation process when pH is greater than four.

6. At high pH values the concentration of ferrous iron converges to a quasi-equilibrium value which increases when pH values become lower.

7. We estimated the amount of neutralizing material necessary to maintain high pH values. There is a stoichiometric incompatibility between acid-generating processes and acid-neutralizing processes. The values obtained for quantities of neutralizing material are different from the values suggested in the literature.

8. In every case we have obtained quantitative results for pyrite oxidation rates as a function of oxygen concentration, temperature, the ratio between active surface area and the volume of water, for various initial conditions. In our computation we have used existing data on the concentration of oxygen dissolved in water, which decreases when temperature increases. Despite this, in the absence of bacteria the pyrite oxidation rate increases monotonically with temperature. This temperature effect is dramatic - for temperatures between 273K and 323K the rate of pyrite oxidation accelerates ten times per 20K.

9. We have derived simple scaling relations which allow the translation of results obtained for one set of entry data, into results for a different set of entry data (without computation).

10. The results of our analysis are essential for establishing the hierarchy of characteristic time scales for chemical and biological reactions and transport processes. This knowledge should be used in a future comprehensive waste rock model. These results can also be used for modelling of acid generation at underwater disposal sites.

Before we proceed with presenting the results of our numerical analysis, we briefly discuss in the next paragraph the numerical values of parameters governing the rates of individual chemical reactions. We include this analysis because some papers which provide fundamental experimental data, contain erroneous values of rate constants and other parameters essential for our study.

III.0. Preliminary analysis of experimental data on abiotic oxidation

In Chapter II we have reviewed experimental results pertaining to the elementary chemical and biological processes contributing to pyrite oxidation and responsible for acidic drainage. Unfortunately, some papers contain erroneous values of rate constants for chemical reactions. The purpose of this section is to determine the correct numerical values of chemical and physical parameters. Experimental results are reproduced by solving kinetic differential equations with proper values of rate constants and other parameters. Both numerical and analytical results are presented.

III.0.1. *Pyrite oxidation by dissolved oxygen*

Rate equations for the reaction (R1) depend on the pyrite surface area, S and the volume, V of water with dissolved oxygen.

$$\frac{d[O_2]_{(R1)}}{dt} = -\frac{7S}{2V} k_1(T)\,[O_2]^{1/2} \tag{3.0.1}$$

$$\frac{d[Fe^{2+}]_{(R1)}}{dt} = \frac{S}{V} k_1(T)\,[O_2]^{1/2} \tag{3.0.2}$$

For the dissolved oxygen concentration in molar units and the specific rate in units of moles of pyrite cm^{-2} min^{-1}, Mc Kibben and Barnes [McK p. 1514] give the rate constant value of $10^{-6.77}$ $moles^{0.5}$ $cm^{-0.5}$ min^{-1} at 30°C. This value is incorrect (by 3 orders of magnitude) and does not reproduce McKibben and Barnes's experimental results. (This has also been pointed out by Nicholson [Ni], p.12]). The correct value of k_1 at T_o=303 K and $[O_2]$ in units M=mol/litre, is:

$$k_1(T_o) = 2.83 \cdot 10^{-8} M^{1/2} m^{-2} s^{-1}. \tag{3.0.3}$$

We will use chemical units M=mol/litre and physical units following the SI standard.

Figs. 3.0.1(a) and 3.0.1(b) compare experimental data obtained by McKibben and

Barnes [McK p.1513] with our solution of eq.(3.0.2) . We have used the rate constant given by (3.0.3).

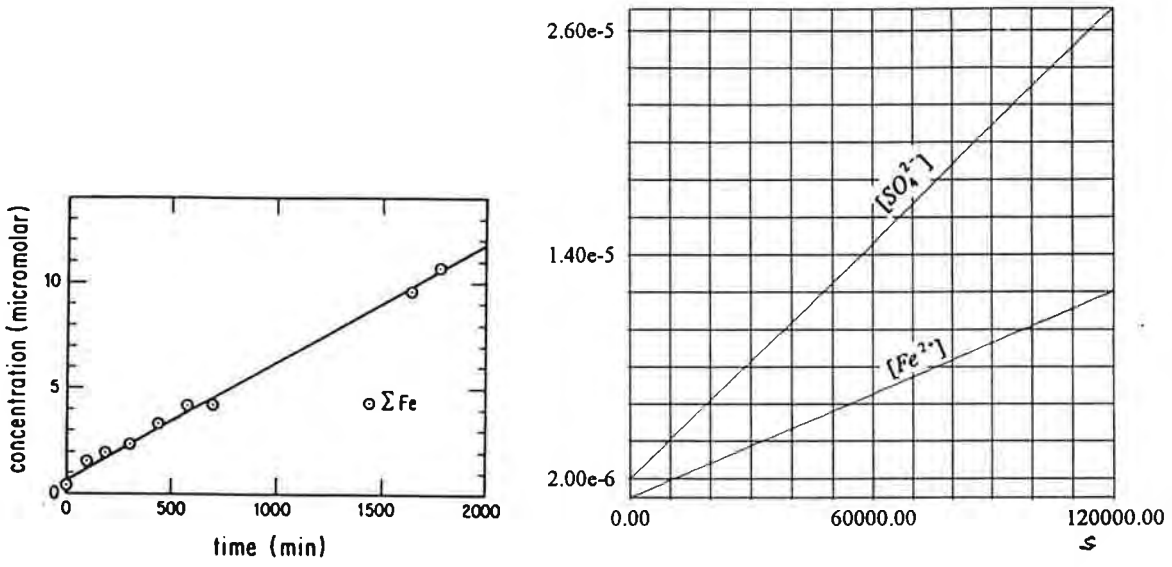

(a) (b)

Fig. 3.0.1. (a) Experimental data [McK, Fig.6] on the oxidation of pyrite at 303 K, $[O_2]=1.260$ mM, pH=1.89. Line indicates fit of linear regression equation used to determine rates. (b) Plot of the solution to eq. (3.0.2) giving the concentration of ferrous ions (in moles per litre) as a function of time. At constant temperature and constant oxygen concentration, the solution has the form given by eq. (3.0.4). Horizontal axis: time (120000s=200m); vertical axis: concentration (millimolar in Fig. (a), molar in Fig. (b), M=mol/litre.

For the time independent concentration of dissolved oxygen, eq. (3.0.2) has a trivial solution

$$[Fe^{2+}(t)] = [Fe^{2+}(t_o)] + \frac{S}{V} k_1(T)[O_2]^{1/2}(t - t_o) \qquad (3.0.4)$$

We want to mention again, that Nicholson et al. [NiG] give the Longmuir-type rate expression based on a profound analysis of the adsorption mechanism involved in the process of oxidation by dissolved oxygen. Both formulae reproduce experimental data within an experimental error. While the Longmuir expression is more appropriate from a general

physical and chemical point of view, we prefer to use expressions (3.0.1) and (3.0.2) because they have the same form of a power law as other expressions for abiotic oxidation and it is easier to analyze some scaling relations (see paragraph III.1.3).

III.0.2. *Oxidation of ferrous iron*

The experimental data presented in Fig.2.3 and other experimental data presented by Millero et al. [MiS] were analyzed recently by Wehrli [We]. Experimental data for a wide range of pH values can be approximated by the expression

$$R = (r_1 + r_2 K_2^* / [H^+] + r_3 \beta_3^* / [H^+]^2)[Fe^{2+}] \qquad (3.0.5)$$

$$= r[Fe^{2+}]$$

with the constants

$$r_1 = 1.0 \cdot 10^{-8} s^{-1}, \quad r_2 = 3.2 \cdot 10^{-2} s^{-1}, \quad r_3 = 1.0 \cdot 10^{-4} s^{-1},$$

$$K_2^* = 10^{-9} M \ , \ \beta_3^* = 10^{-20.6} M^2 \ . \qquad (3.0.6)$$

Eq.(3.0.5) with constants (3.0.6) provides the formula for oxidation rates at 298 K and partial oxygen pressure, $P(O_2)=1$ atm. In our numerical analysis we allow the oxygen concentration to vary and we need an expression for the rate constant independent of oxygen concentration. This approach will make our numerical results more useful for a later physical waste rock model which will have to take into account both spatial and temporal variation of oxygen concentration. Because the reaction (R2) is of the first order with respect to oxygen, this can be easily done by simply dividing the values determined by Wehrli by 1.26 mM. 1.26 mM is the equilibrium concentration of dissolved oxygen, $[O_2]$ at T=298 K and oxygen partial pressure of 1 atm. With rate constants independent of oxygen concentration we do not have to use Henry's law providing a linear dependence of dissolved oxygen on partial oxygen pressure $P(O_2)$ or oxygen concentration $[O_2]_{gas}$ in the gas phase surrounding the water solution in which reactions take place. Henry's law is a good approximation only at low temperatures and high $[O_2]_{gas}$ values and in our analysis we prefer to use more the accurate values listed in Table I.

We have converted the values of the constants (3.0.6) (which reproduce experimental data according to eq. (3.0.5)) to values which reproduce the same experimental data when we use the equation

$$\frac{d[Fe^{3+}]_{(R2)}}{dt} = (k_{21}(T) + k_{22}(T)[H^+]^{-1} + k_{23}(T)[H^+]^{-2})[O_2][Fe^{2+}] \ . \qquad (3.0.7)$$

The rate constants have the form

$$k_{2i}(T) = k_{2i}(T_o)e^{\frac{E_{2i}(T-T_o)}{RTT_o}} \ , \qquad i = 1,2,3; \qquad (3.0.8)$$

with the values

$$k_{21}(T_o) = 1.30 \cdot 10^{-5} M^{-1} s^{-1} \ , \quad k_{22}(T_o) = 1.41 \cdot 10^{-8} s^{-1} \ , \quad k_{21}(T_o) = 3.78 \cdot 10^{-14} M s^{-1} \ . \qquad (3.0.9)$$

at T_o=303 K. The values of activation energies E_{21}, E_{22} and E_{23} are given by eqs. (2.19)-(2.21).

We define

$$k_2(T) = k_{21}(T) + k_{22}(T)[H^+]^{-1} + k_{23}(T)[H^+]^{-2} \qquad (3.0.10)$$

as an effective pH dependent rate coefficient. Fig.3.0.2a presents the experimental results compiled by Wehrli, and the products $k_2(T)[O_2]$ as a function of pH for various concentrations of dissolved oxygen and various temperatures.

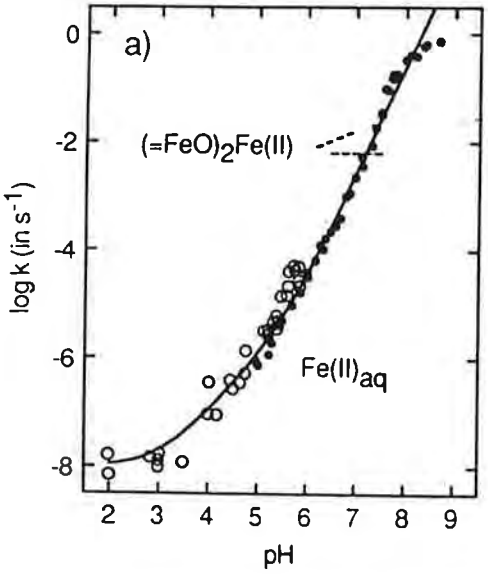

(a)

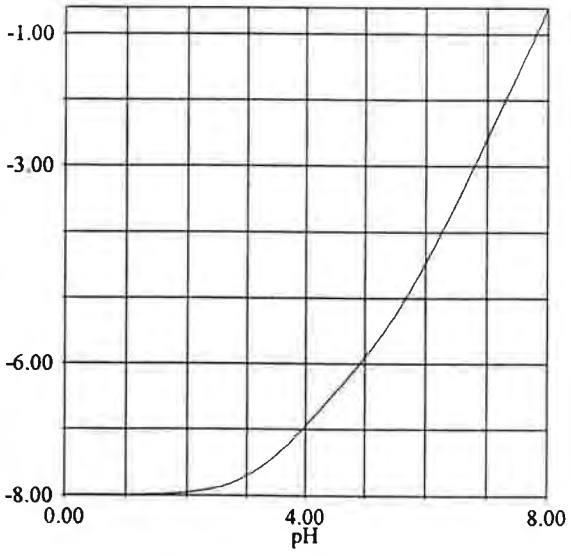

(b)

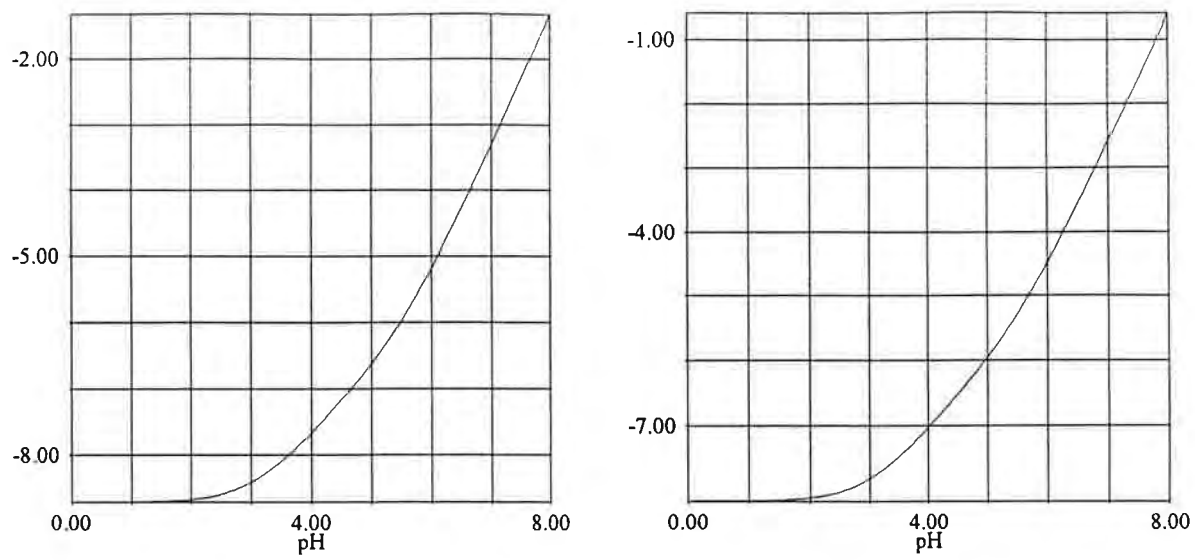

(c) (d)

Fig. 3.0.2. (a) The oxidation rate coefficient r for $[O_2]=1.26$ mM at T=298 K. Open circles represent data by Singer and Stumm [SiS], dots are data from Millero et al. [MiS]. The solid line was calculated with eq. (3.0.5) by Wehrli [We]. The diagram reproduced from p. 326 in [We]. (b) $k_2[O_2]$ at T=298K and $[O_2]=1264\mu$M corresponding to $P(O_2)=1$atm at 298K. (c) $k_2[O_2]$ at T=283K and $[O_2]=353\mu$M corresponding to $P(O_2)=0.21$atm at 298K. (d) $k_2[O_2]$ at T=313K and $[O_2]=202\mu$M corresponding to $P(O_2)=0.21$atm at 313K. (Horizontal axis: pH values; vertical axis: log ($k_2[O_2]$) in s^{-1}).

The oxidation rates show a strong temperature dependence by accelerating about 3.5 times per every 10 K increase in temperature. This temperature effect will be discussed more extensively in paragraph 3.1.3, where scaling properties of time dependent solutions to the kinetic equations are analyzed.

III.0.3. Pyrite oxidation by ferric iron

Rates of pyrite oxidation by ferric iron depend on the chemically active surface area, S of pyrite reacting with dissolved oxygen. Concentrations of reaction products depend on the volume, V of water solution in contact with pyrite. For this reason the chemical rate is proportional to S/V.

Again, we could not reproduce the fundamental experimental data published by McKibben and Barnes [McK] by using their rate constant $k_3=10^{-9.74}$ moles cm^{-2} min^{-1} at 30°C.

We have also found that the formulae

$$\frac{d[Fe^{3+}]_{(R3)}}{dt} = -\frac{S}{V} k_3(T)\,[Fe^{3+}]^{3/5}\,[H^+]^{-1/2} \qquad (3.0.11)$$

$$\frac{d[Fe^{2+}]_{(R3)}}{dt} = \frac{15S}{14V} k_3(T)\,[Fe^{3+}]^{3/5}\,[H^+]^{-1/2} \qquad (3.0.12)$$

provide a better fit to the experimental data of McKibben and Barnes in Fig. 3.0.3. In eqs. (3.0.11) and (3.0.12) we use the 0.6 instead of often used 0.5 order with respect to the ferric iron. (This is a minor modification, however)

For a constant pH, eq.(3.0.11) can be solved analytically and we obtain the expressions:

$$[Fe^{3+}(t)]_{(R3)} = \{\ [Fe^{3+}(t_o)]^{2/5} - \frac{2S}{5V} k_3 [H^+]^{-1/2}\,(t-t_o)\ \}^{5/2}\ , \qquad (3.0.13)$$

$$[Fe^{2+}(t)]_{(R3)} = [Fe^{2+}(t_o)] + \frac{15}{14}[Fe^{3+}(t)] \qquad (3.0.14)$$

for time dependent concentrations of ferric and ferrous iron. McKibben and Barnes give the rate law with the exponent 0.58 ± 0.09 for the rate dependence on ferric iron concentration. Their value was determined by measuring the effect of initial ferric iron molarity on the initial oxidation rate of pyrite by ferric iron. We have determined the value of 3/5 by fitting the theoretical results to experimental data in Fig.2 of ref. [McK]. As the exponent 3/5 is very close to 0.58, our analysis of the order with respect to ferric iron essentially confirms

the conclusion by McKibben and Barnes.

In order to reproduce the experimental results, we have to use the constant

$$k_3(T_o) = 8.72 \cdot 10^{-7} mol^{0.9}\, m^{-2} s^{-1} \quad at \quad T_o = 303K \qquad (3.0.14)$$

which is significantly different from the value given by McKibben and Barnes. Our analytical results are presented in Fig. 3.0.3b.

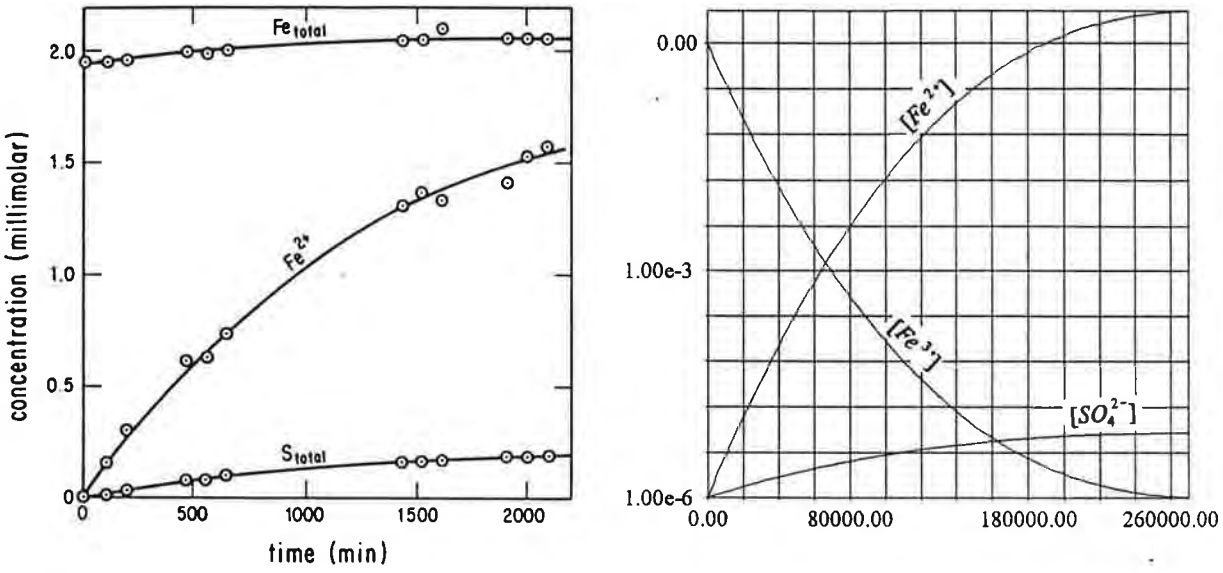

(a) (b)

Fig. 3.0.3. (a) Experimental data on oxidation of pyrite by millimolar initial concentrations of ferric iron at pH 1.89, temperature 298 K [McK, Fig.2]. Curves are not mathematical solutions but indicate a fit of the second order power series used to determine initial rates. Note that total iron concentration increases by the amount required by the stoichiometry of the reaction (R3). (b) The theoretical curves obtained for molar concentrations by solving the kinetic equations for the same initial conditions as in the experiment; time in seconds (260 000s=3 days).

The experimental evidence of an increasing total iron concentration in Fig. 3.0.3a, is a strong argument supporting the stoichiometry postulated by eq. (R1). Theoretical results in Fig. 3.0.3a show that for every 14 ferric ions disappearing from the water solution there are 15 ferrous irons produced by the reaction (R3). This stoichiometry does not depend on

the hydronium ions concentration. The analytical solution (3.0.13) is valid only for constant in time low pH values for which the reaction of oxidation of ferrous iron is very slow. The relation (3.0.14) is valid for arbitrary conditions and must be satisfied by numerical solutions when pH varies with time.

Eq.(3.0.13) also provides a prescription for measuring the effective reactive surface area for rocks with pyrite. The experiment could use the relation

$$\frac{S}{V} = \frac{2[H^+]^{1/2}}{5k_3(t-t_o)}\{[Fe^{3+}(t_o)]^{2/5} - [Fe^{3+}(t)\}^{2/5}) \quad . \tag{3.0.15}$$

In an experiment under anaerobic conditions one would measure the difference between the initial concentration of ferric iron, $[Fe^{3+}(t_o)]$ and the final concentration of ferric iron $[Fe^{3+}(t)]$ after a time interval $(t-t_o)$ at constant pH values. At low temperatures and low pH values the oxidation of ferrous iron even in the presence of oxygen can be neglected (in the absence of bacteria) and the change in $[Fe^{3+}]$ is almost entirely due to oxidation of pyrite by ferric iron. Under stirred conditions, the reaction should be completed after time

$$t - t_o = \frac{2k_3V}{5S}[H^+]^{1/2}[Fe^{3+}(t_o)]^{2/5} \tag{3.0.16}$$

Thus the experiment should not last longer than 20-200 minutes for S/V between 1 m^2/l and 10 m^2/l and millimolar initial concentrations of Fe^{3+} at pH=2. Interpretation of experimental results depends, of course, on a presence of compounds other than pyrite, which may also react with ferric iron.

III.1. Abiotic chemical oxidation of pyrite without neutralization

In this section the set of kinetic equations corresponding to reactions (R1)-(R4) is analyzed separately pH values between 4 and 7, and for those below 4. This distinction is made because at pH values above 4 the ferric hydroxide precipitates .

III.1.1. Oxidation at pH between 4 and 7

The set of coupled kinetic differential equations has the form

$$\frac{d[Fe^{2+}]}{dt} = \frac{S}{V}k_1(T)[O_2]^{1/2} - k_2(T,[H^+])[Fe^{2+}][O_2] \ , \qquad (D1.1)$$

$$\frac{d[Fe(OH)_3]}{dt} = k_2(T,[H^+])[Fe^{2+}][O_2] \ , \qquad (D1.2)$$

$$\frac{d[H^+]}{dt} = \frac{2S}{V}k_1(T)[O_2]^{1/2} + 2k_2(T,[H^+])[Fe^{2+}][O_2] \ , \qquad (D1.3)$$

$$\frac{d[O_2]}{dt} = -\frac{7S}{2V}k_1(T)[O_2]^{1/2} - \frac{1}{4}k_2(T,[H^+])[Fe^{2+}][O_2] \ , \qquad (D1.4)$$

$$\frac{d[SO_4^{2-}]}{dt} = \frac{2S}{V}k_1(T)[O_2]^{1/2} \ , \qquad (D1.5)$$

$$\frac{d[H_2O]}{dt} = -\frac{S}{V}k_1(T)[O_2]^{1/2} - \frac{5}{2}k_2(T,[H^+])[Fe^{2+}][O_2] \ . \qquad (D1.6)$$

The last two equations are "slave" equations because the concentrations of sulphate and water do not appear on the right-hand side of the kinetic equations. Water is consumed at rates which do not affect, in a significant way, the ratio of S/V during the time intervals discussed in our present study (which does not consider transport processes). In a future waste rock

model, the total amount of water should no longer be a parameter but should become an important variable. Still, water consumption in chemical processes will be relatively small, but changes due to water transport will be significant. The time dependent concentrations of sulphate and the changes in the amount of water can be determined from stoichiometric relations after we find solutions to the first four equations.

Eq.(D1.2) assumes that the precipitation of ferric hydroxide is much faster than the rate of oxidation of ferrous iron. We also assume that ferric hydroxide precipitates fast enough, so that the oxidation of pyrite by ferric iron does not take place at high pH values. In this way the rate of formation of ferric hydroxide becomes equal to the rate of oxidation of ferrous iron and we disregard terms proportional to k_3.

The total amount of dissolved pyrite, $[FeS_2]_R$ satisfies the stoichiometric relations (R1) and (R3):

$$[FeS_2]_R = \frac{1}{2}[SO_4^{2-}] \quad . \tag{3.1.1}$$

At high pH values $[FeS_2]_R$ follows the differential equation

$$\frac{d[FeS_2]_R}{dt} = \frac{S}{V} k_1(T)[O_2]^{1/2} \quad . \tag{3.1.2}$$

The last equation is proportional to the eq. (D1.5) and we do not include it in a set of independent equations (D1).

The numerical factors in the kinetic equations result from the stoichiometric relations (R1), (R2), (R3) and (R4) which are the conservation laws for the species involved.
The rate coefficient $k_2(T_o,[H^+])$ is defined in eq.(3.0.10). Rate constants in equations (D1) have the form

$$k_i(T) = k_i(T_o)\exp[\frac{E_i(T-T_o)}{RTT_o}] \; ; \; i = 1, 21, 22, 23 \, . \tag{3.1.3}$$

These have been discussed before on p. 12.

The coefficient S/V describes both the characteristic rates of the chemical processes taking place on the pyrite surface and the chemical activity as a function of physical factors such as the pyrite reactive surface area, crystalline structure, pyrite content, rock porosity

and pore size, water content, etc. Because of the complex nature of the physical and chemical factors determining the values of S/V, a reliable waste rock model will have to use site-specific experimental values of these quantities. In our numerical analysis we used different values of S/V ranging from $0.1 m^2/l$ to $100 m^2/l$, which correspond to the different physico-chemical properties of the pyrite containing rock and the different quantities of water in contact with the pyrite. We present results for both constant and variable concentrations of dissolved oxygen.

(i) *oxidation of pyrite at constant concentrations of dissolved oxygen*

Figures (3.1.1)-(3.1.3) present numerical solutions to the set of kinetic equations (D1) for various temperatures and different concentrations of oxygen. We have analyzed the network of chemical reactions at different temperatures ranging from 283 K to 333 K. Typically temperature inside a waste rock pile does not exceed 323 K. As we mentioned before, when the oxygen concentration in the gas phase is lower than 2%, the concentration of dissolved oxygen at temperatures higher than 323 K becomes infinitesimally small (see Table I on p. 42) and no thermal energy is released. This implies that the maximum temperature inside a waste rock pile with low oxygen content should not exceed 323 K.

We have used initial conditions corresponding to the situation when water of pH=7 comes in contact with a dry pyritic rock.

From plots in figures 3.1.1 and 3.1.2 it is evident that at T=303K the oxidation rate slows down about three times when the concentration of oxygen in the gas phase decreases from 21% (0.21 atm. partial pressure) to 2%. This effect is a direct consequence of the "square-root" dependence of the oxidation rate on the concentration of dissolved oxygen.

At circumneutral pH and millimolar concentrations of ferrous iron, the oxidation of ferrous iron (reaction (R2)) proceeds with a rate comparable to that of reaction (R1). While oxidation of pyrite by dissolved oxygen produces 1 hydronium ion per 1 sulphate ion, the subsequent reactions of the oxidation of ferrous iron and precipitation of ferric hydroxide add 2 hydronium ions per one sulphate ion. The oxidation of ferrous iron slows down dramatically, however, when pH decreases from the initial conditions used in Figs. 3.1.1 and 3.1.2 (it becomes much slower than the rate of pyrite oxidation by dissolved oxygen).
(The bracketed numbers (11), (12) refer to rows and columns in Fig. 3.1.1 and other figures)

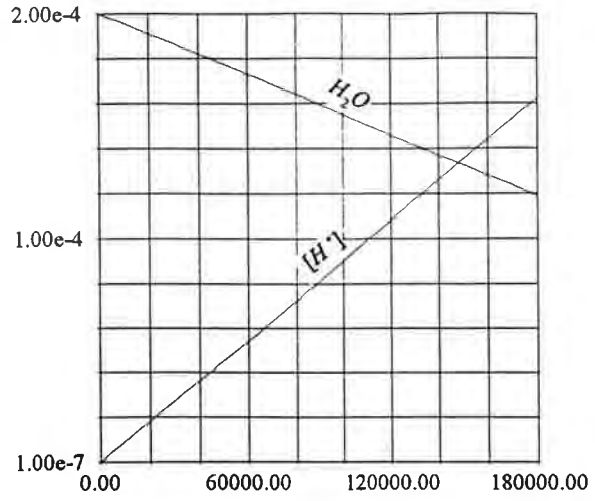

(11)

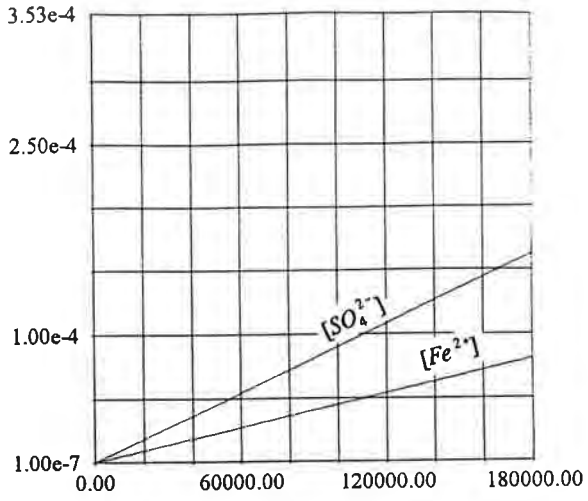

(12)

T=283K

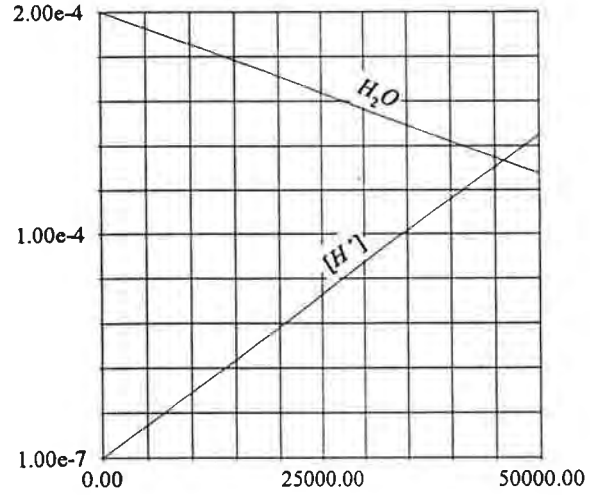

(21)

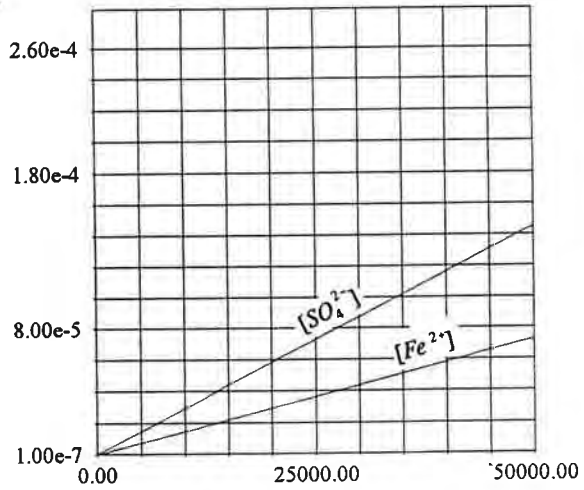

(22)

T=293K

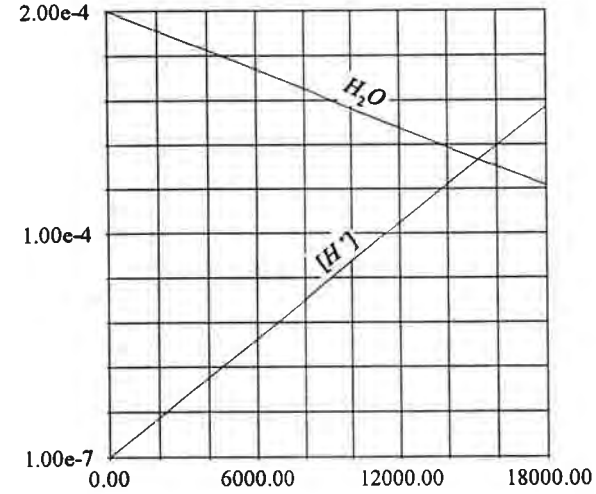

(31)

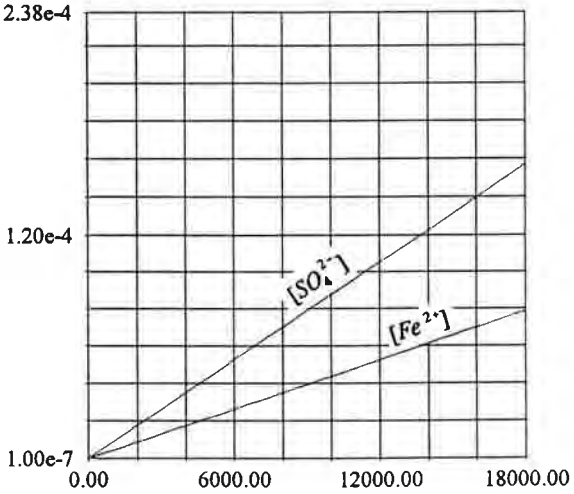

(32)

T=303K

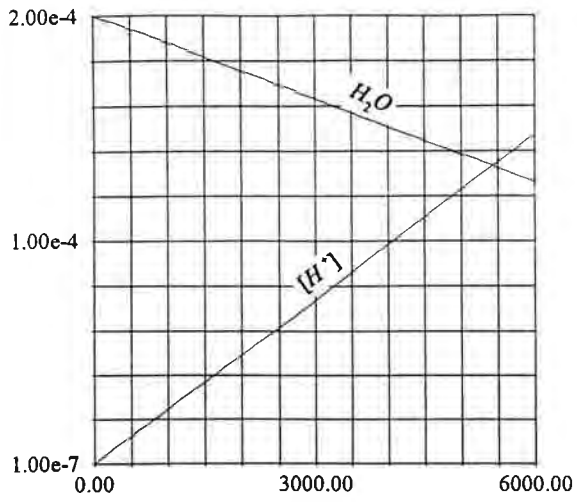

(41)

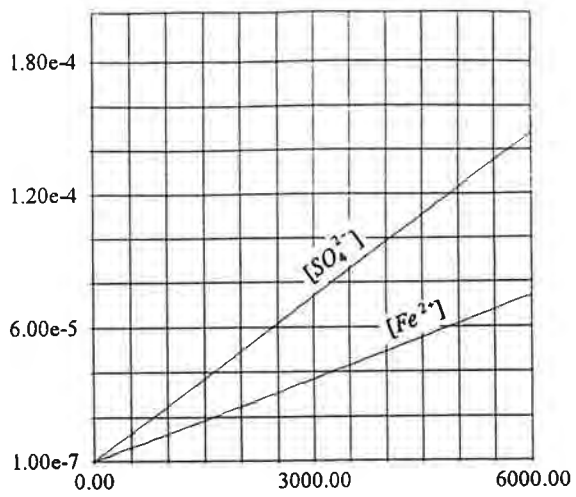

(42)

T=313K

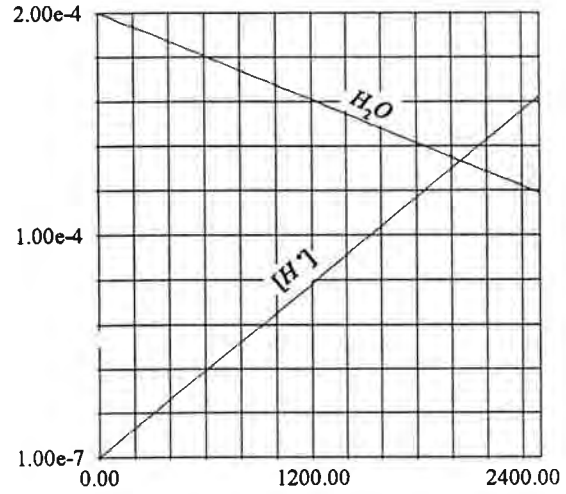

(51)

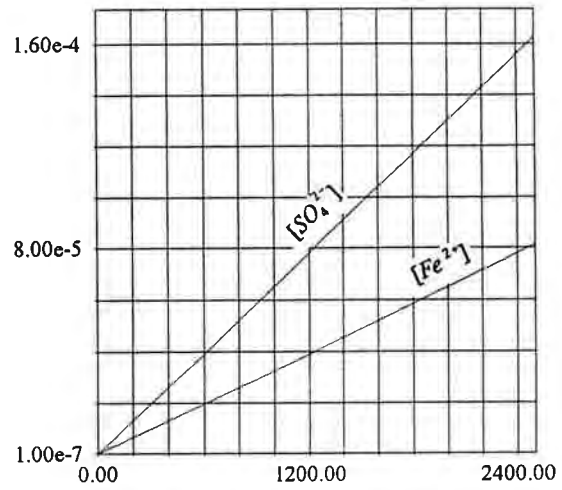

(52)

T=323K

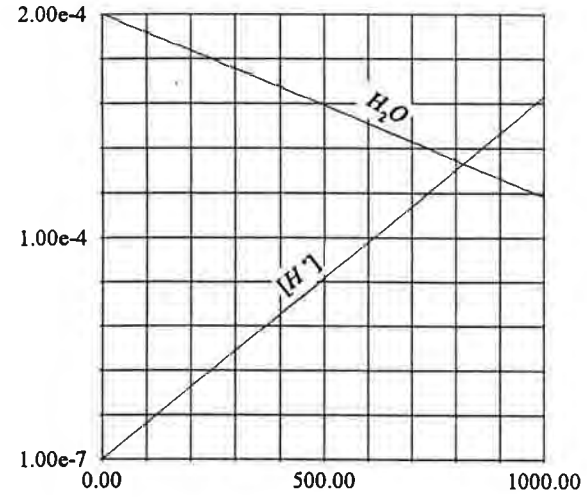

(61)

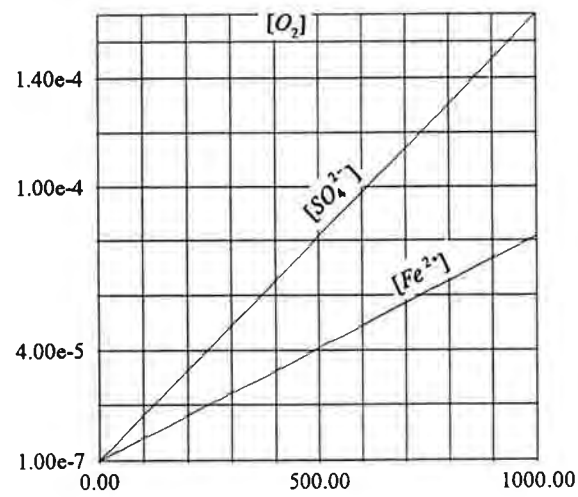

(62)

T=333K

Fig. 3.1.1. The oxidation kinetics due to reactions (R1)-(R4) for different temperatures, S/V=10 m^2/l and the initial conditions: $[Fe^{2+}(t=0)]=0$, $[SO_4^{2-}(t=0)]=0$, $[Fe(OH)_3(t=0)]=0$ and $pH(t=0)=7$. Constant in time concentration of dissolved oxygen, $[O_2]$ for $[O_2]_{gas}=21\%$ Horizontal axis: time in seconds, vertical axis-concentration in moles per litre. (180 000 sec.= 5 hours).

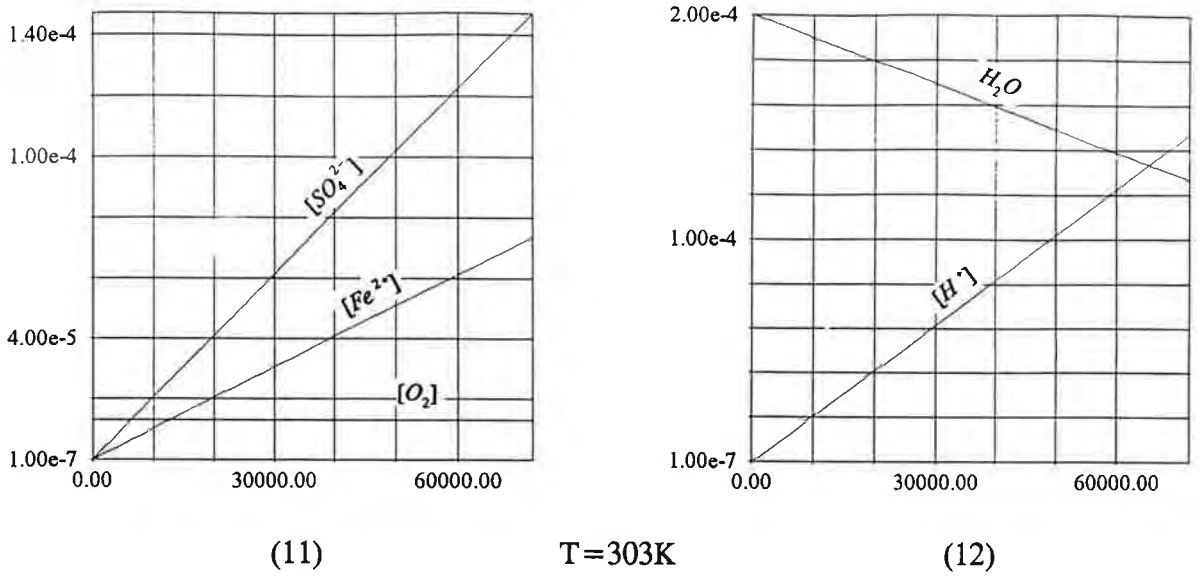

(11) T=303K (12)

Fig. 3.1.2. The oxidation kinetics due to reactions (R1), (R2), (R3) and (R4) for different temperatures, $S/V=10m^2/l$ and the initial conditions: $[Fe^{2+}(t=0)]=0$, $[SO_4^{2-}(t=0)]=0$, $[Fe(OH)_3(t=0)]=0$ and $pH(t=0)=7$. Constant in time but temperature dependent concentration of dissolved oxygen, $[O_2]$ for $[O_2]_{gas}=2\%$ Horizontal axis: time in seconds, vertical axis: concentration in moles per litre. (60 000 sec.= 17 hours).

According to eqs. (D1.1) and (D1.2), for very small initial concentrations of hydronium and ferrous ions the term proportional to $[Fe^{2+}]$ decreases in time. This happens because at high pH values $k_2(T,[H^+])$ is proportional to $[H^+]^{-2}$, and both concentrations $[Fe^{2+}]$ and $[H^+]$ increase with similar rates. For large concentrations of dissolved oxygen and large values of S/V, the rate of the oxygenation of ferrous iron will always remain much slower than the rate at which pyrite is oxidized by dissolved oxygen when initial concentrations of hydronium and ferrous ions are both small. This explains why for all temperatures the concentrations of products of pyrite oxidation show linear time dependence and are proportional to the rate constant k_1. Fig.3.1.3 gives the cumulative concentrations of ferric iron formed in the reaction (R2) for two different values of $S/V=0.1m^2/l$ and $S/V=1m^2/l$. At high pH values ferric iron reacts very quickly with water and forms ferric hydroxide which precipitates and subsequently is dissolved when pH drops below 4.

The plots labelled "H_2O" show molar water consumption per one litre of solution (as a difference between arbitrary initial and final states).

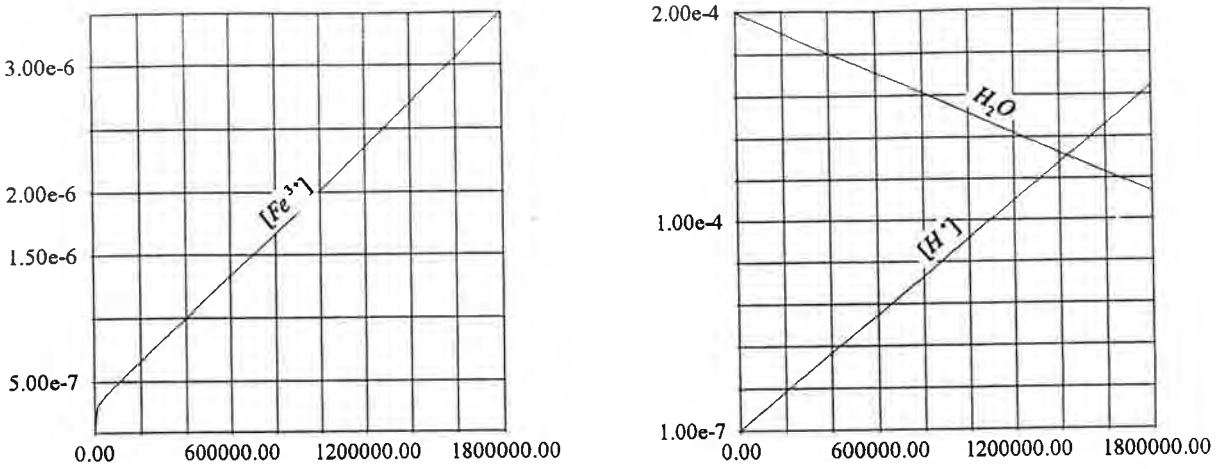

(a)

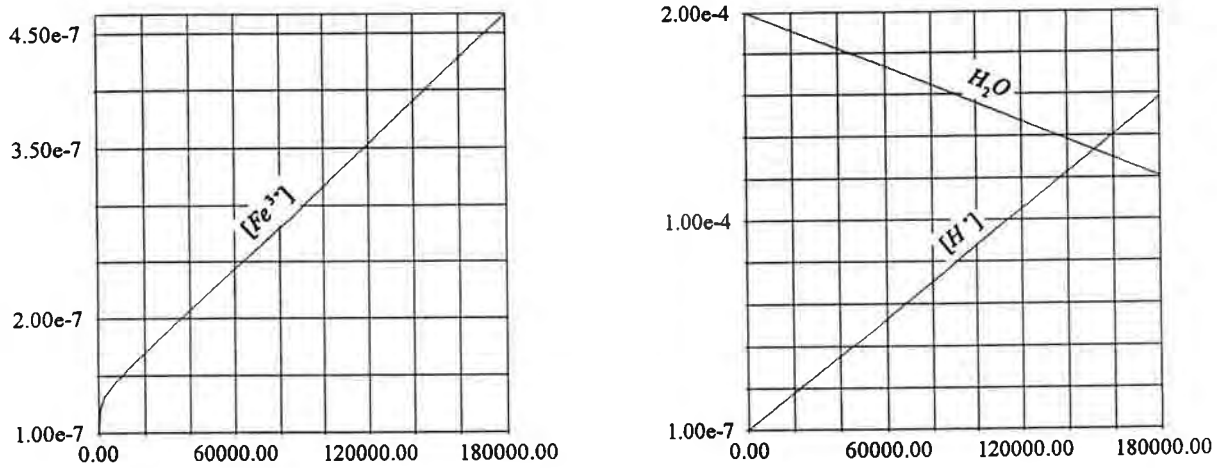

(b)

Fig. 3.1.3. Cumulative values of concentrations of $[Fe^{3+}]$ (left) and $[H^+]$ (right) formed at T=303 K when pyrite is oxidized without neutralizing minerals and pH decreases rapidly. (a) S/V=0.1m²/l; (b)S/V=1m²/l.(Horiz. axis: time in seconds; vert. axis-concentration in moles/l)

Our results indicate that at temperature 303K in the absence of neutralizing minerals acidic conditions with pH=4 develop after about 2 weeks for S/V=0.1m²/l and after 32 hours for S/V=1m²/l. The total amount of ferric hydroxide is very small in both cases. It is also worth of note that the initial rates of oxidation of ferrous iron are high at pH=7 .

If the initial concentration of ferrous iron is large (or S/V very small), then the

reactions (R2) and (R4) proceed with rates comparable to (R1). This happens also when circumneutral pH values are stabilized for a long time (i.e. when the factor $[H^+]^{-2}$ is small (see eq. (3.0.10) and Fig. 3.0.2). Because reaction (R4) generates hydronium ions, there is a positive feedback between the neutralizing reactions and the formation of hydronium ions. Hydronium ions formed in the reaction (R4) are, of course, subsequently neutralized. We discuss this phenomenon in more detail in Section III.2, where we analyze effects of neutralizing compounds.

(ii) *oxidation of pyrite at variable oxygen concentration*

In this paragraph we analyze depletion rates of dissolved oxygen during oxidation of pyrite at pH values between 4 and 7. We analyze oxygen depletion rates under extreme conditions when there is no transfer of oxygen from the surrounding atmosphere into water. In reality, even when we seal a waste rock pile completely, there will be a large initial amount of gaseous oxygen inside a pile to provide enough dissolved oxygen for about 100 oxidation cycles discussed here. The value of results presented in this paragraph is two-fold:

- upper limits for depletion rates of dissolved oxygen are established
- the oxygen depletion rates are indicative of the values oxygen fluxes necessary to maintain given concentrations of oxygen.

The last information may be useful for designing and estimating effectiveness of covers limiting access of oxygen and water.

Fig. 3.1.4 presents our results for oxygen depletion rates and time-dependent concentrations of other species involved in acidic drainage. The initial amount of oxygen ranges from 3.53×10^{-4}M at 293K to 1.83×10^{-4}M at 333K and is consumed in about 110 hours (400 000s) at 293K (see Fig. 3.1.4(12) and about 15 minutes at 333K (Fig. 3.1.4(62). For each value of $[O_2]$, the slope of curves defining the time dependence of $[O_2]$ defines the flux of oxygen necessary to maintain given concentration of dissolved oxygen. This information is useful for estimating the effectivenes of low-permeability covers.

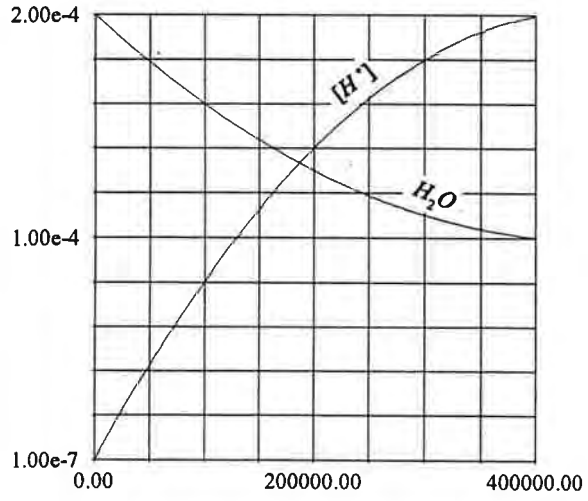

(11)

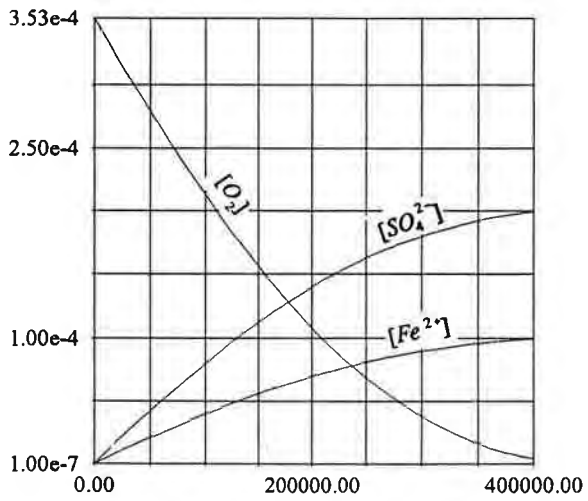

(12)

T=283 K

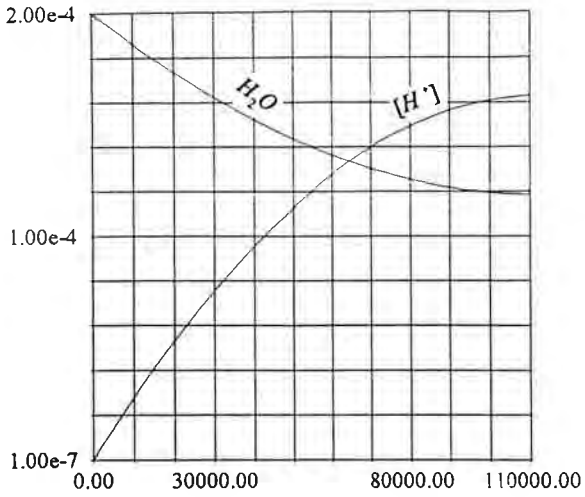

(21)

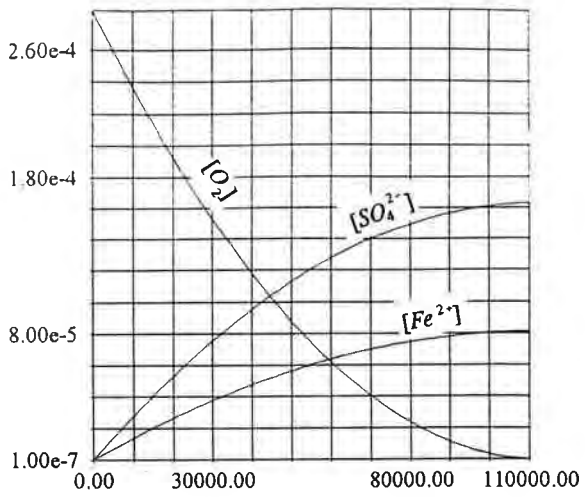

(22)

T=293 K

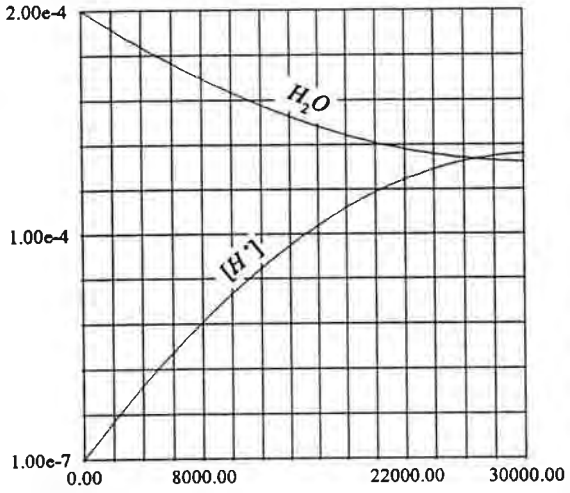

(31)

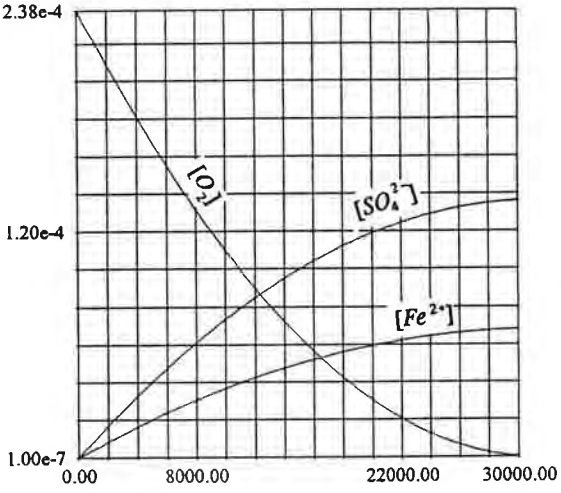

(32)

T=303 K

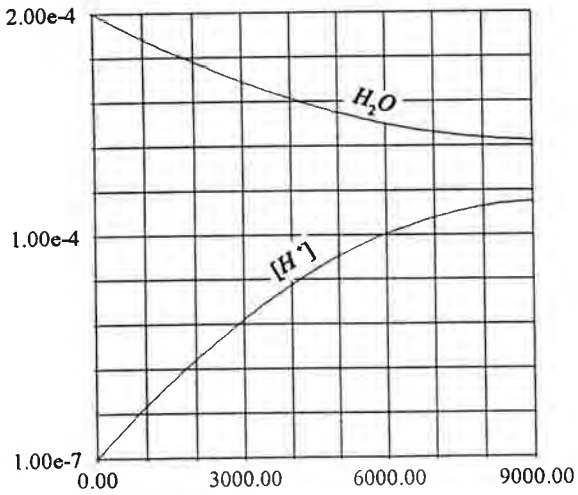

(41)

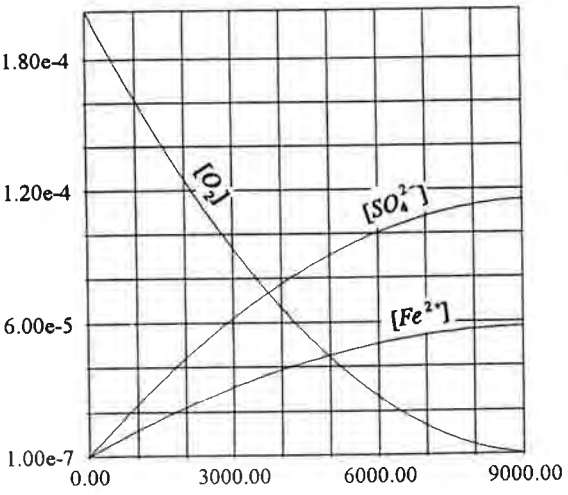

(42)

T=313 K

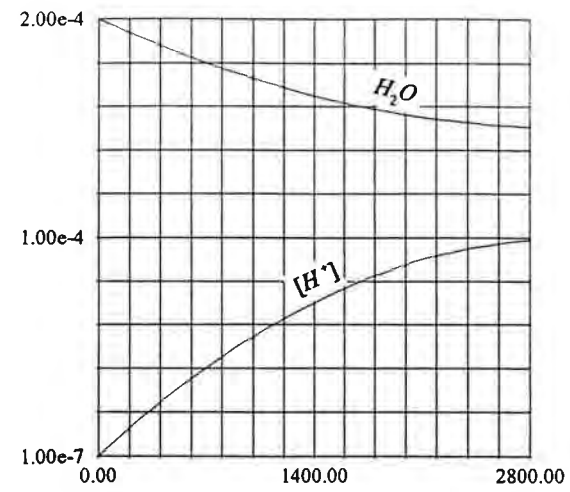

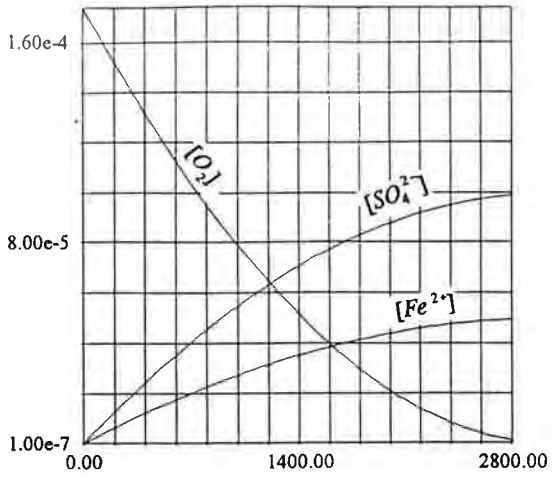

(51) T=323 K (52)

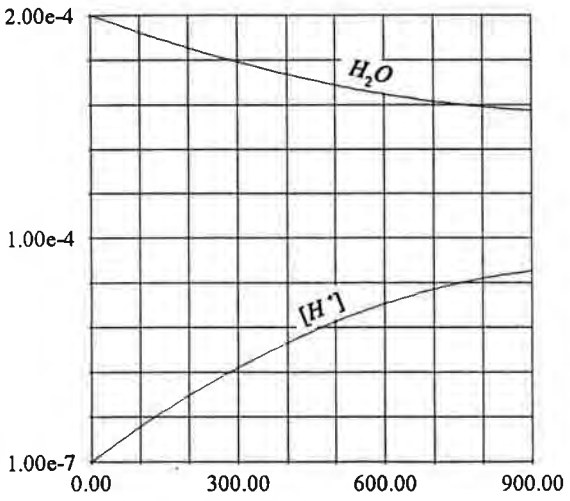

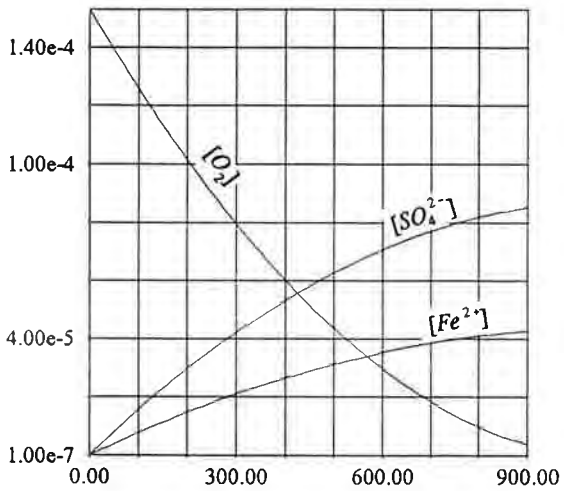

(61) T=333 K (62)

Fig. 3.1.4. Oxygen depletion and concentrations of species involved in acidic drainage as a function of time (in seconds) for temperatures between 283 K and 333 K; S/V=10m^2/l. Horizontal axis: time in seconds; vertical axis: concentration in moles/litre. (400 000s=111h, 900s=15min.)

III.1.2. *Oxidation at pH less than 4*

At low pH values ferric hydroxide does not precipitate if concentrations of ferric iron are sufficiently small (see Fig.2.6 on p. 27). This means that the ferric iron, Fe^{3+} (which is formed by oxidation of ferrous iron) oxidizes pyrite according to the reaction (R3). The set of coupled kinetic differential equations has the form

$$\frac{d[Fe^{2+}]}{dt} = \frac{S}{V}k_1(T)[O_2]^{1/2} - k_2(T,[H^+])[Fe^{2+}][O_2] + \frac{15S}{14V}k_3[Fe^{3+}]^{3/5}[H^+]^{-1/2} , \qquad (D2.1)$$

$$\frac{d[Fe^{3+}]}{dt} = k_2(T,[H^+])[Fe^{2+}][O_2] - \frac{S}{V}k_3(T)[Fe^{3+}]^{3/5}[H^+]^{-1/2} , \qquad (D2.2)$$

$$\frac{d[H^+]}{dt} = \frac{2S}{V}k_1(T)[O_2]^{1/2} - k_2(T,[H^+])[Fe^{2+}][O_2] + \frac{8S}{7V}k_3(T)[Fe^{3+}]^{3/5}[H^+]^{-1/2} , \qquad (D2.3)$$

$$\frac{d[O_2]}{dt} = -\frac{7S}{2V}k_1(T)[O_2]^{1/2} - \frac{1}{4}k_2(T,[H^+])[Fe^{2+}][O_2] , \qquad (D2.4)$$

$$\frac{d[SO_4^{2-}]}{dt} = 2k_1(T)[O_2]^{1/2} + \frac{S}{7V}k_3(T)[Fe^{3+}]^{3/5}[H^+]^{-1/2} , \qquad (D2.5)$$

$$\frac{d[H_2O]}{dt} = -\frac{S}{V}k_1(T)[O_2]^{1/2} + \frac{1}{2}k_2(T,[H^+])[Fe^{2+}][O_2] - \frac{4S}{7V}k_3(T)[Fe^{3+}]^{3/5}[H^+]^{-1/2} . \qquad (D2.6)$$

At low pH values the process of pyrite oxidation by ferric iron may play an important role. There are at least two possible scenarios under which significant amounts of ferric iron may be formed.

(1). Ferric iron can be formed at high rates in the presence of Thiobacillus ferrooxidans at low pH values.

(2). At high pH values the process of oxidation of ferrous iron is also relatively fast and leads to the formation of ferric hydroxide. If neutralization agents are not applied in a sufficient amount, further pyrite oxidation may lead to lower pH values at which ferric hydroxide dissolves and provides ferric iron for the accelerated oxidation of pyrite.

The neutralization process and bacterial oxidation will be discussed in Section 3.2 and Chapter IV. In this paragraph we concentrate on the oxidation of pyrite by ferric iron as such, independently of accompanying circumstances.

The total amount of dissolved pyrite $[FeS_2]_R$ satisfies the stoichiometric relations (R1) and (R3):

$$[FeS_2]_R = \frac{1}{2}[SO_4^{2-}]$$

and follows the differential equation

$$\frac{d[FeS_2]_R}{dt} = \frac{S}{V}k_1(T)[O_2]^{1/2} + \frac{S}{14V}k_3[Fe^{3+}]^{3/5}[H^+]^{-1/2} \quad . \tag{3.1.4}$$

The last equation is proportional to eq. (D2.5) and we do not include it in a set of independent equations (D2).

There are two competitive effects associated with the process of pyrite oxidation by ferric iron. As shown in Fig. 2.6, the solubility of ferric iron increases when pH decreases. On the other hand the rate of oxidation decreases when pH decreases. These two effects do not play a dominant role, however, in determining the rate of pyrite oxidation by ferric iron. By comparing the values of rate constants, it becomes evident that in the absence of bacteria the rate of reaction (R3) is controlled by the rate of reaction (R2) which produces ferric iron.

It turns out that independently of its initial value, the concentration of ferric iron converges after a relatively short time to its quasi-equilibrium value defined by the condition $d[Fe^{3+}]/dt=0$. From the condition $d[Fe^{3+}]/dt=0$ imposed on equation (D2.2) we obtain the quasi-equilibrium value of the ferric iron concentration, $[Fe^{3+}]_{qeq}$:

$$[Fe^{3+}]_{qeq} = \{\frac{k_2(T,[H^+])\,V}{k_3(T)\,S}\,[H^+]^{1/2}[O_2][Fe^{2+}]\}^{5/3} \quad . \qquad (3.1.5)$$

The concept of quasi-equilibrium for transient species produced by non-equilibrium chemical and physical processes is discussed in Section III.3. In this paragraph we present only quantitative results without discussing the mathematical properties of the differential equations governing the time evolution of the chemical system.

For pH between 2 and 4, $[O_2]=2x10^{-4}$ M, $[Fe^{2+}]=10^{-2}$M, S/V=1m^2/l the concentration of ferric iron are below a critical value at which the precipitation of ferric hydroxide takes place. Fig.3.1.5 gives the values of $[Fe^{3+}]_{qeq}$ as a function of pH=-log $[H^+]$.

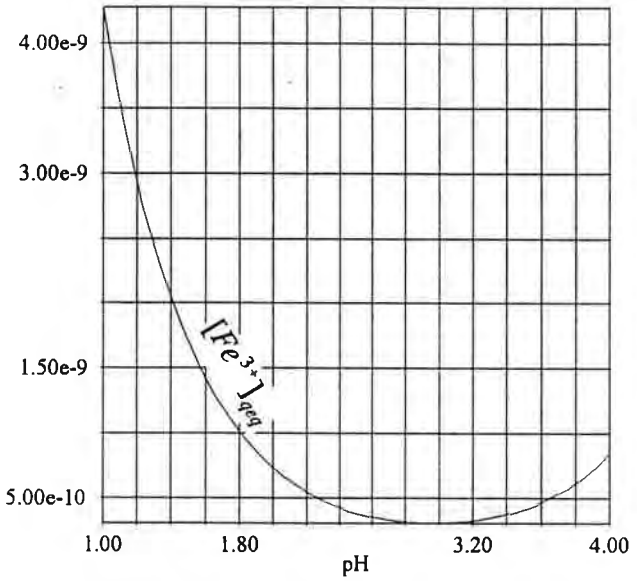

Fig.3.1.5 The quasi-equilibrium values of the concentration of ferric iron as a function of pH for $[O_2]=2x10^{-4}$ M, $[Fe^{2+}]=10^{-2}$M, S/V=1 m^2/l, T=303K. Vertical axis: concentration in moles per litre.

For small concentrations of ferric iron reaction (R3) is slow and pyrite oxidation is mainly due to reaction (R1) - see Fig. 3.1.6. We present results on pyrite oxidation at low pH values for two situations: when the concentration of dissolved oxygen is time independent and when oxygen is depleted.

(i) *oxidation at time-independent concentrations of dissolved oxygen*

By comparing terms on the right-hand side of eq.(D2.5) we conclude that for the oxidation of pyrite by ferric iron to be faster than the oxidation by dissolved oxygen, the ferric iron concentration would have to satisfy the condition

$$[Fe^{3+}] \geq \{\frac{14k_1(T)}{k_3(T)}\}^{5/3} [O_2]^{5/6} [H^+]^{5/6} . \qquad (3.1.6)$$

For pH=4 and $[O_2]=2.38\text{x}10^{-4}$ M at 303 K we obtain $[Fe^{3+}]\geq 2.6\text{x}10^{-4}$. According to eq. (3.1.6) this condition cannot be satisfied in waste rock piles in the absence of bacteria because the quasi-equilibrium value of ferric iron concentration $[Fe^{3+}]_{qeq}$ is four orders of magnitude smaller even for S/V=0.1m^2/l. (Note that the relation (3.1.6) does not depend explicitly on S/V, but $[Fe^{3+}]_{qeq}$ defined by eq. (3.1.5) does.)

The maximum rate of pyrite oxidation by ferric iron can be obtained after substituting eq. (3.1.5) into eq.(3.1.4), and is given by the relation

$$\frac{d[FeS_2]_{R3}}{dt} = \frac{1}{14} k_2(T,[H^+])\,[O_2][Fe^{2+}] \qquad (3.1.7)$$

Eq. (3.1.7) does not depend explicitly on S/V or $[Fe^{3+}]$, it gives the rate of pyrite oxidation by ferric iron contained in one litre of water.

For the ratio between the rates of reactions (R3) and (R1) we obtain the expression

$$\frac{\frac{d[FeS_2]_{R3}}{dt}}{\frac{d[FeS_2]_{R1}}{dt}} = \frac{V}{14S}\frac{k_2(T,[H^+])}{k_1(T)}[O_2]^{1/2}[Fe^{2+}] \qquad (3.1.8)$$

For $[O_2]=2\text{x}10^{-4}$ M, $[Fe^{2+}]=10^{-2}$M, S/V=1 m^2/l. In the absence of bacteria the rate of pyrite oxidation by ferric iron is three orders of magnitude slower than the rate of pyrite oxidation by dissolved oxygen according to the reaction (R1). In this way the reaction (R2) controls the rate of the reaction (R3). The relation (3.1.8) is plotted in Fig.3.1.6.

Underwater disposal offers lower oxidation rates overall - mainly because high pH values can be maintained and oxygen diffusion in water is much slower than in air, becoming

a strong limiting factor leading to a much slower oxidation of pyrite. Pyrite disposed under water, however, may be oxidized quickly by ferric iron.

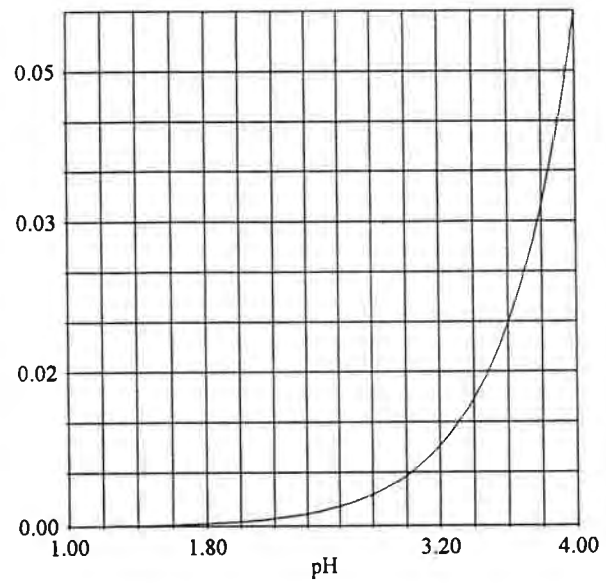

Fig.3.1.6. Ratio between rates of reactions (R3) and (R1) for $[O_2]=2x10^{-4}$ M, $[Fe^{2+}]=10^{-2}$M, T=303K, S/V=1 m^2/l as a function of pH.

Figures 3.1.7 and 3.1.8 present numerical solutions to the set of kinetic equations (D2). Eq. (D2.4) is eliminated because it is assumed that the rate of oxygen consumption is balanced by the rate at which oxygen is transferred from the surrounding atmosphere. Two sets of numerical results for two different concentrations of dissolved oxygen corresponding to $[O_2]_{gas}=21\%$ and $[O_2]_{gas}=5\%$ are presented. Figures 3.1.6, 3.1.7 and 3.1.8 demonstrate that, in the absence of bacteria, practically all pyrite is oxidized by oxygen according to the reaction (R1). At low pH values the oxidation of ferrous iron proceeds at rates which are several orders of magnitude slower than the oxidation of pyrite by dissolved oxygen (reaction (R1)).

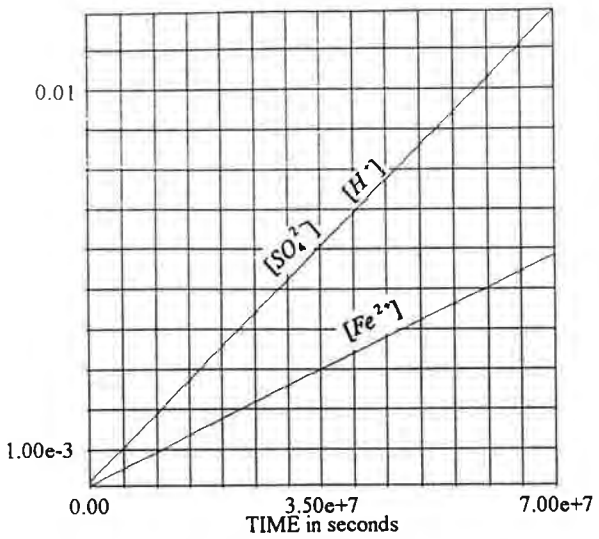

(11)

S/V=0.78m²/l, T=283K

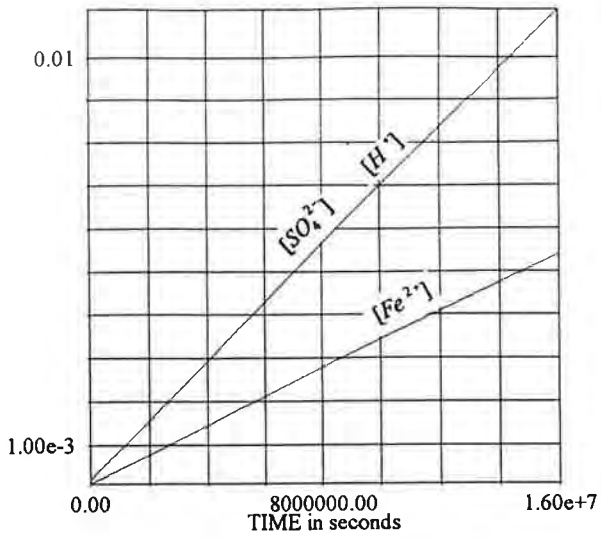

(12)

S/V=0.78m²/l, T=303K

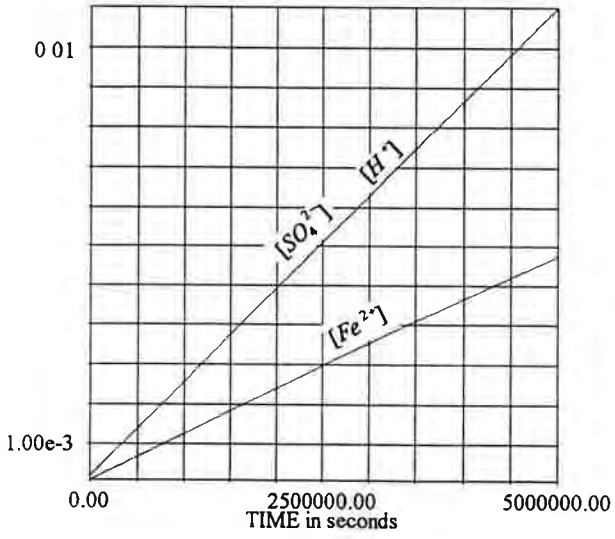

(21)

S/V=0.78m²/l, T=323K

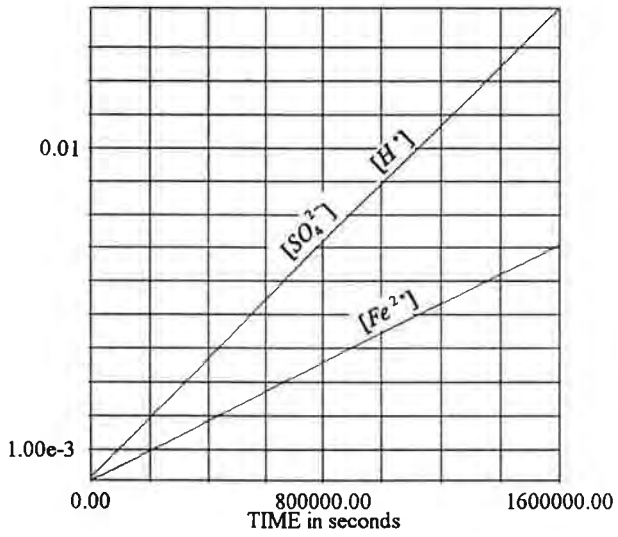

(22)

S/V=10m²/l, T=303K

Fig.3.1.7. The oxidation kinetics due to reactions (R1) - (R3) for various temperatures and S/V values. Constant in time concentration of dissolved oxygen, $[O_2]$ for $[O_2]_{gas}=21\%$. The initial conditions: $[Fe^{2+}(t=0)]=10^{-4}M$, $[SO_4^{2-}(t=0)]=2x10^{-4}M$, $[Fe^{3+}(t=0)]=0$ and $pH(t=0)=4$. Horizontal axis: time in seconds, vertical axis-concentration in moles per litre. ($7x10^7$ sec. = 27 months).

In Chapter IV we will use the same value S/V=0.78m²/l for the bacterial oxidation.

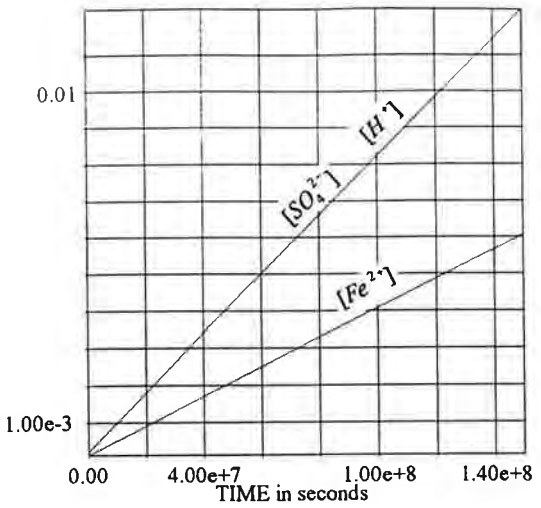

(11)

S/V=0.78m²/l, T=283K

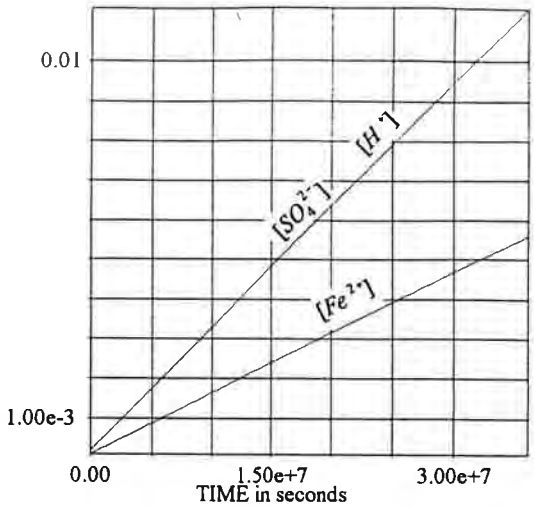

(12)

S/V=0.78m²/l, T=303K

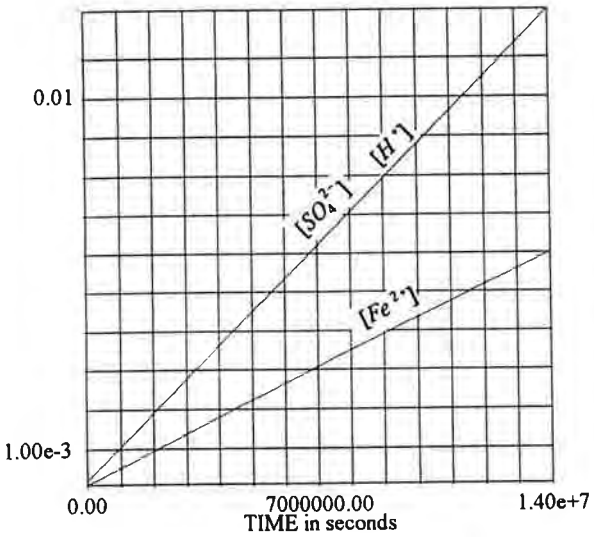

(21)

S/V=0.78m²/l, T=323K

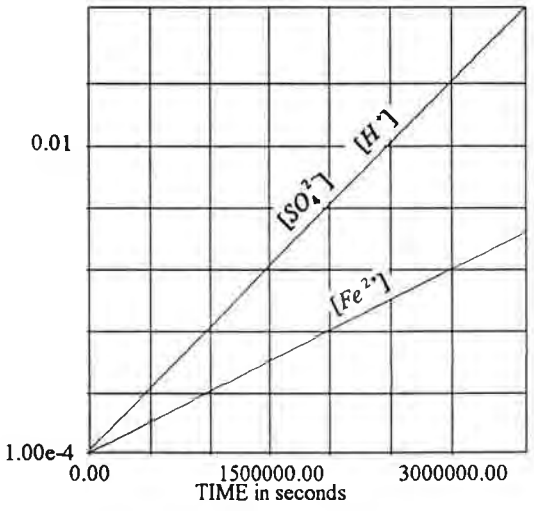

(22)

S/V=10m²/l, T=303K

Fig. 3.1.8. The oxidation kinetics due to reactions (R1) - (R3) for various temperature and S/V values. Constant in time concentration of dissolved oxygen, $[O_2]$ for $[O_2]_{gas}=5\%$. The initial conditions: $[Fe^{2+}(t=0)]=10^{-4}M$, $[SO_4^{2-}(t=0)]=2x10^{-4}M$, $[Fe^{3+}(t=0)]=0$ and $pH(t=0)=4$. Horizontal axis: time in seconds, vertical axis-concentration in moles per litre. ($1.5x10^8$ sec.= 57 months).

In Chapter IV the same value S/V=0.78m²/l for the bacterial oxidation is used.

We see that in figures 3.1.7 and 3.1.8 the changes of concentrations are linear in time. This is an obvious property because for small concentrations of ferric iron, terms proportional to k_2 and k_3 are very small and the concentrations can be approximated by

$$[Fe^{2+}(t)] \simeq [Fe^{2+}(t_o)] + \frac{S}{V} k_1(T)[O_2]^{(1/2)}(t - t_o) \ , \tag{3.1.9}$$

$$[H^{+}(t)] \simeq [H^{+}(t_o)] + \frac{2S}{V} k_1(T)[O_2]^{(1/2)}(t - t_o) \ , \tag{3.1.10}$$

$$[SO_4^{2-}(t)] \simeq [SO_4^{2-}(t_o)] + \frac{2S}{V} k_1(T)[O_2]^{(1/2)}(t - t_o) \ . \tag{3.1.11}$$

Fig. 3.1.10 provides further insight into the interplay between reactions (R1), (R2) and (R3) for high initial concentrations of ferric iron. By comparing time intervals over which the concentration of ferrous iron increases by 0.01 M, we conclude that at high concentrations of ferric iron the reaction of pyrite oxidation by ferric iron is much faster than the oxidation of pyrite by dissolved oxygen. Therefore it is very important to keep the levels of ferric iron as low as possible. In particular, sufficient amounts of neutralizing minerals should be used, so that pH always remains high and ferric hydroxide formed at high pH values does not dissolve. The neutralization process is analyzed in Section 3.2.

(ii) *oxidation at variable concentrations of dissolved oxygen*

We analyze the depletion rates of dissolved oxygen under ideal conditions, when there is no transfer of oxygen from the surrounding atmosphere. Although this is not a realistic situation, we obtain some useful information about reduced values of oxygen fluxes sufficient to slow down the long-term oxidation process below required levels. We analyze reactions (R1), (R2) and (R3) for two sets of different initial concentrations of dissolved oxygen at temperatures from 283 K to 333 K. The two sets of initial concentrations are saturation concentrations corresponding to two different concentrations of gaseous oxygen: 21% and 2%. For each temperature, the slope of $[O_2(t)]$ gives a value of oxygen fluxes per one litre of water, necessary to maintain the concentration of dissolved oxygen at a given level. This information should be useful for estimating the permeability of covers used in order to reduce the access of oxygen. It can also be used for estimates of oxygen depletion rates for underwater disposal where lower oxygen concentration is expected to be observed near the pyrite surface. In Chapter IV we will perform a similar analysis for much higher oxidation rates due to bacterial processes.

According to eq. (D2.4), the rate of oxygen depletion is proportional to $[O_2]^{1/2}$. This means that when low-permeability covers are used and oxygen concentration decreases n times, the rate of pyrite oxidation by dissolved oxygen decreases only $n^{1/2}$ times. We arrive at a similar conclusion when we use the formula:

$$\frac{d[O_2]}{dt} = -\frac{[O_2]}{1+\kappa[O_2]} \qquad (3.1.12)$$

given by Nicholson et al. [NiG]. Eq. (3.1.12) also describes a slower than linear increase of the oxygen depletion rates with an increasing concentration of dissolved oxygen. In the next paragraph we discuss the general scaling properties of the chemical processes responsible for acid rock drainage.

We analyze oxygen depletion rates at various temperatures. When the rate of reaction (R2) is very slow, we may neglect the second term in eq. (D2.4) and obtain the approximate analytical solution

$$[O_2(t)] \simeq \{[O_2(t_o)]^{1/2} - \frac{7S}{4V}k_1(T)(t-t_o)\}^2 . \qquad (3.1.13)$$

Other concentrations can be obtained after we substitute the solution (3.1.13) into equations (D2):

$$[Fe^{2+}(t)] \simeq [Fe^{2+}(t_o)] + \frac{S}{V}k_1(T)\{[O_2(t_o)]^{1/2}(t-t_o) - \frac{7S}{8V}k_1(T)(t-t_o)^2\} , \qquad (3.1.14)$$

$$[H^+(t)] \simeq [H^+(t_o)] + \frac{2S}{V}k_1(T)\{[O_2(t_o)]^{1/2}(t-t_o) - \frac{7S}{8V}k_1(T)(t-t_o)^2\} , \qquad (3.1.15)$$

$$[SO_4^{2-}(t)] \simeq [SO_4^{2-}(t_o)] + \frac{2S}{V}k_1(T)\{[O_2(t_o)]^{1/2}(t-t_o) - \frac{7S}{8V}k_1(T)(t-t_o)^2\} . \qquad (3.1.16)$$

The form of the above solutions is very simple, showing a quadratic time dependence. (We have also obtained solutions for the rate equation proposed by Nicholson et al. [NiG]. The mathematical form of the solution is more complicated in that case and we do not present it in this report).

We want to stress again that the formulae (3.1.13) - (3.1.16) are valid only when the rate of oxidation of ferrous iron in the reaction (R2) is much slower than the rate of reaction (R1). Fig.3.1.9 presents our results for time dependence of concentrations according to eqs. (D2). As discussed in Chapter IV, the rates of pyrite oxidation become considerably faster in the presence of bacteria and formulae (3.1.13)-(3.1.16), which are valid for negligibly slow reaction (R2), cannot be applied.

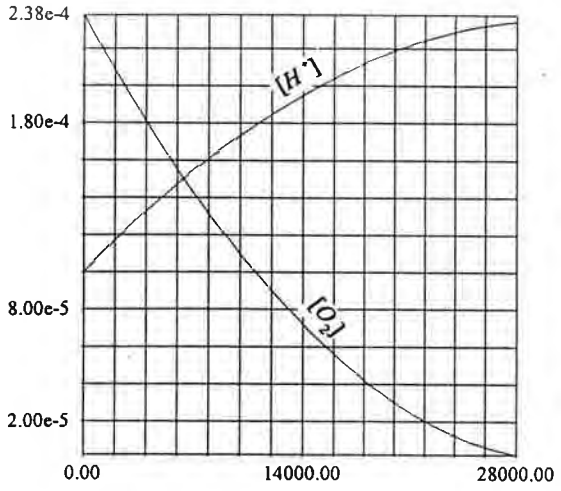

S/V=10m²/l, T=303K

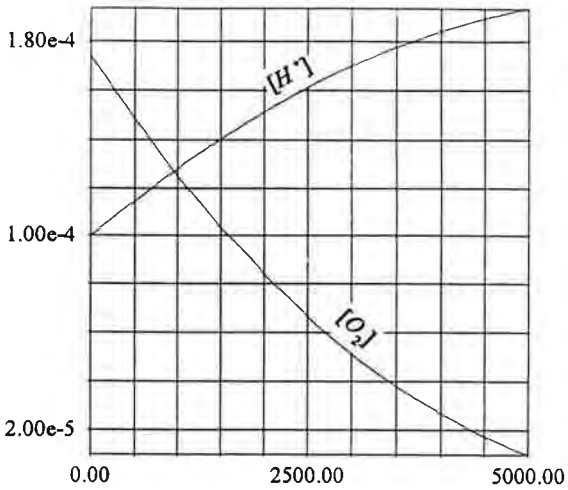

S/V=10m²/l, T=323K

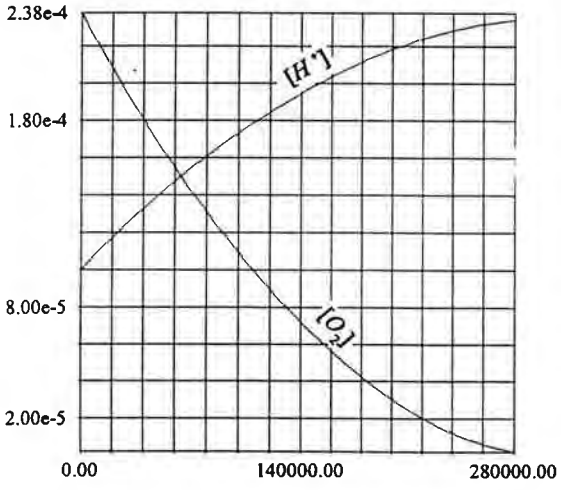

S/V=1m²/l, T=303K

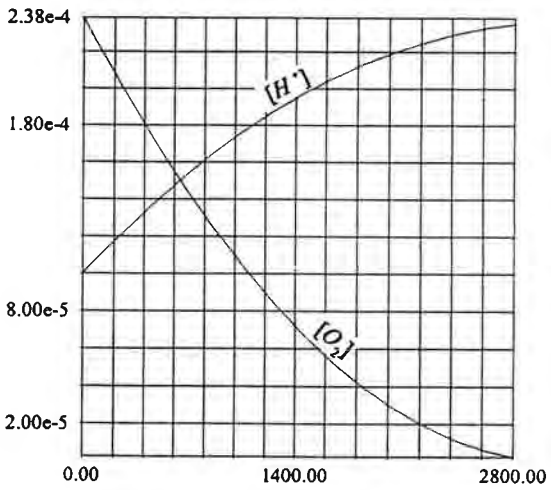

S/V=100m²/l, T=323K

Fig.3.1.9. The rate of oxygen depletion and increasing acidity for different values of S/V and temperature. Initial concentrations $[Fe^{2+}(t=0)]=[Fe^{3+}(t=0)]=[H^{+}(t=0)]=10^{-4}$M. Horizontal axis: time in seconds; vertical axis: concentration in moles per litre (280 000 sec.=78 hours).

III.2. Oxidation of pyrite in the presence of neutralizing minerals

Acid neutralization reduces the environmental impact of acid generation by stabilizing high pH values. At high pH values ferrous ions react with oxygen and water, and then precipitate from the water. The typical neutralizing minerals are calcite ($CaCO_3$), dolomite ($CaMg(CO_3)_2$), ankerite ($CaFe(CO_3)_2$, and many others. As mentioned before we can distinguish three different scenarios for neutralization:

1° Acid-generating and acid-neutralizing minerals react simultaneously with water and oxygen. During this process high pH values above 5.5 can be maintained, if a sufficient amount of neutralizing mineral is used.

2°. Water and oxygen react with acid generating minerals first, and then flow over acid neutralizing minerals. In this case, the results of the previous paragraphs apply to the acid generation phase.

3°. The water flows over neutralizing minerals and by dissolving a portion of the minerals accumulates alkalinity and then reacts with acid generating minerals.

Maintaining high pH values has beneficial environmental effects: a large portion of iron precipitates and remains in a waste rock pile, the reaction (R3) does not take place, and the reactions (R2) and (R4) do not produce sulphate ions which are formed in the reaction (R3) at low pH values; at the same time hydronium ions formed in the reaction (R4) are neutralized.

If neutralizing minerals are consumed completely before the acid-generating minerals are consumed, acid drainage may occur at accelerated rates. This may happen both in scenario 1° and scenario 3°. There are two factors which may contribute to this undesirable effect:

(a) At high pH values ferrous iron is oxidized to ferric iron at high rates and precipitates as ferric hydroxide (reactions (R2) and (R4)).

(b) When pH decreases below 4, ferric hydroxide becomes soluble and the dissolved ferric ions react quickly with pyrite (reaction (R3)).

The net result is an increased rate of acid generation. Because the reaction (R3) does not require oxygen, this effect may be very severe far from waste pile boundaries, where the oxygen concentration is usually low.

As in the previous paragraphs, we present results obtained for different temperatures and oxygen concentrations constant in time as well as oxygen concentrations that are time dependent .

We solve numerically the following set of coupled kinetic differential equations:

$$\frac{d[Fe^{2+}]}{dt} = \frac{S}{V}k_1(T)[O_2]^{1/2} - k_2(T,[H^+])[Fe^{2+}][O_2] \ , \qquad (D3.1)$$

$$\frac{d[Fe(OH)_3]}{dt} = k_2(T,[H^+])[Fe^{2+}][O_2] \ , \qquad (D3.2)$$

$$\frac{d[H^+]_R}{dt} = \frac{2S}{V}k_1(T)[O_2]^{1/2} + 2k_2(T,[H^+])[Fe^{2+}][O_2] \ , \qquad (D3.3)$$

$$\frac{d[O_2]}{dt} = -\frac{7S}{2V}k_1(T)[O_2]^{1/2} - \frac{1}{4}k_2(T,[H^+])[Fe^{2+}][O_2] \ , \qquad (D3.4)$$

$$\frac{d[SO_4^{2-}]}{dt} = \frac{2S}{V}k_1(T)[O_2]^{1/2} \ , \qquad (D3.5)$$

$$\frac{d[H_2O]}{dt} = -\frac{S}{V}k_1(T)[O_2]^{1/2} - \frac{5}{2}k_2(T,[H^+])[Fe^{2+}][O_2] \ . \qquad (D3.6)$$

Eqs. (D3) describe the concentrations of the species produced in the reactions (R1), (R2) and (R4) at constant pH values which are maintained due to the neutralization process. In eqs. (D3) the neutralization process is included implicitly by the imposed condition of time-independent pH. $[H^+]_R$ in eqs. (D3) has a different sense than $[H^+]$ in the definition of $k_2(T,[H^+])$ and in eqs. (D1) and (D2). In equations (D1) and (D2) the concentration $[H^+]$ of hydronium ions also defined pH ($pH=-\log([H^+])$. In equations (D3), $[H^+]_R$ corresponds to the number of hydronium ions produced in the reactions (R1), (R2) and (R4) and $[H^+]_R$ does not define pH. A time independent total concentration of the hydronium ions $[H^+]$ is assumed to be maintained by neutralizing reactions. In this way there is no logical inconsistency

between constant pH and variable $[H^+]_R$ in equations (D2).

We focus our attention on the relative rates of formation of hydronium and sulphate ions in reactions (R1), (R2) and (R4) at high pH values maintained due to the neutralizing reactions (R5.1) or (R5.2). This information is significant for designing the most efficient and cost-effective neutralization methods which should produce a minimum amount of sludge.

The relative rates of formation of the hydronium and sulphate ions are different for different pH values because the rate coefficient $k_2(T,[H^+])$ for the reaction (R2) increases dramatically with pH. The reactions (R2) and (R4) produce hydronium ions but do not produce sulphate ions.

(i) *pyrite oxidation by time-independent concentrations of dissolved oxygen*

We present three sets of results for three different time-independent pH values: 5.5, 6.3 and 6.9. These values correspond to the range of equilibrium pH for calcium-based carbonates used as neutralizing minerals in field and laboratory studies [Mo], [MoJ], [Re]. At pH values close to 6.3 $H_2CO_3^*$ and HCO_3^- are similar in concentrations and according to the diagram on p. 40, strong buffering occurs, which stabilizes the pH value despite the addition of acidity or alkalinity. We use a simplified approach to the neutralization process and focus our attention on a long term effect of high pH values on reactions (R1), (R2) and (R4). While this approach seems to be well justified for pH=6.3 at which strong self-buffering occurs, it should be considered as an approximation for other pH values. A more realistic model should take into account the kinetics of carbonate species as a function of pH. Such an analysis goes beyond the scope and limited time of this study. We will analyze this problem in future. In paragraph III.2(iii), we discuss two important aspects of the neutralization process, which merit further attention.

Figures 3.2.1, 3.2.2 and 3.2.3 present our results for acid drainage at different temperatures for three different pH values and temperature dependent concentrations of dissolved oxygen corresponding to the oxygen partial pressure of 0.21 atm. At high pH values the concentration of ferrous iron shows very similar behaviour to the concentration of ferric iron at low pH values.

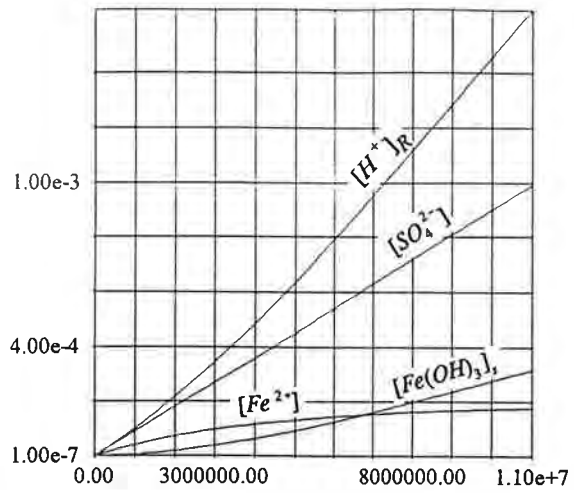

(11) T=283K

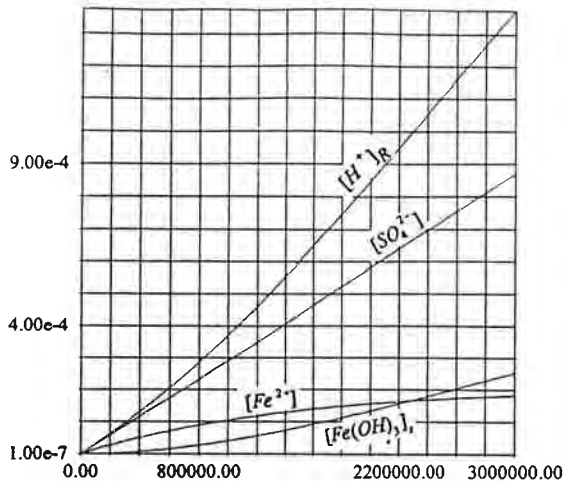

(12) T=293K

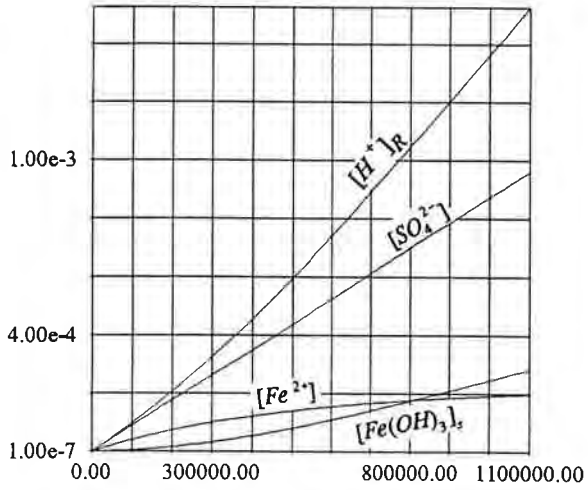

(21) T=303K

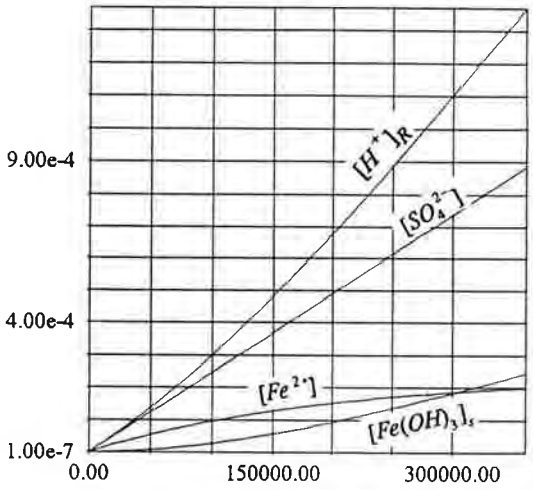

(22) T=313K

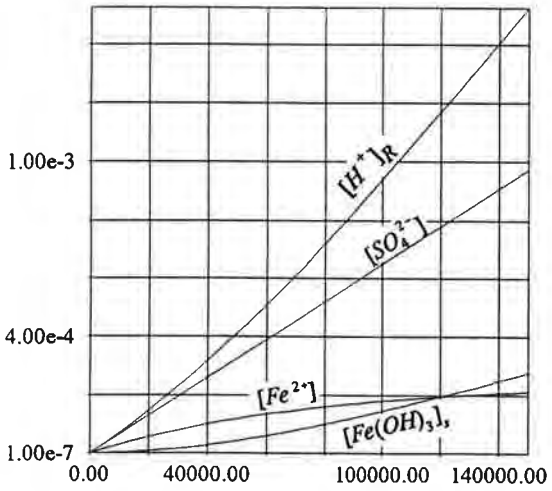

(31) T=323K

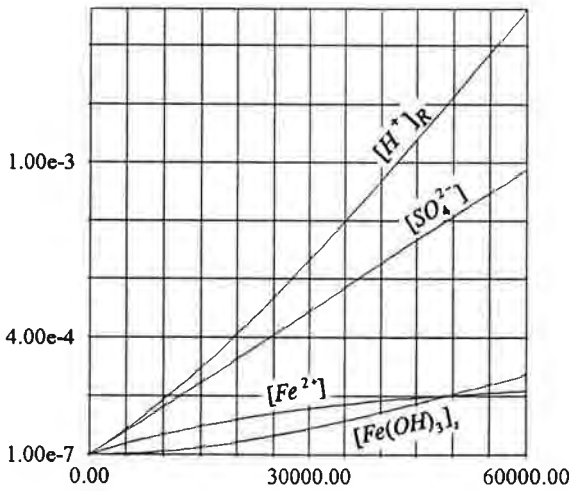

(32) T=333K

Fig. 3.2.1. The oxidation kinetics due to reactions (R1)-(R4) for different temperatures, S/V=1 m^2/l; the initial conditions: $[Fe^{2+}(t=0)]=0$, $[SO_4^{2-}(t=0)]=0$, $[Fe(OH)_3(t=0)]=0$. Constant in time pH=5.5 and concentration of dissolved oxygen, $[O_2]$ for $[O_2]_{gas}=21\%$. Horizontal axis:time in seconds, vertical axis: concentration in moles per litre. (11 000 000 sec.= 127 days).

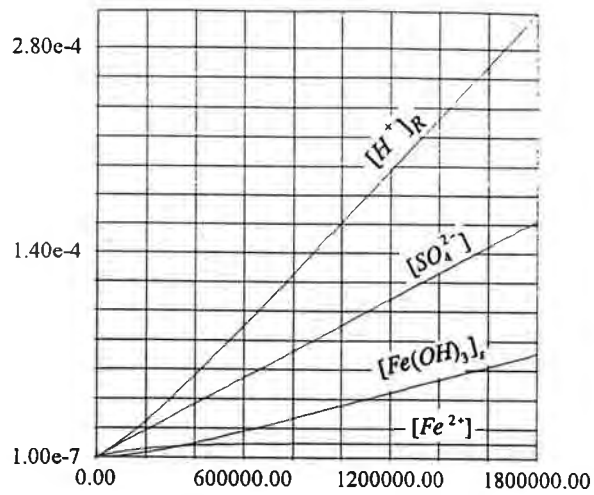

(11) T=283K

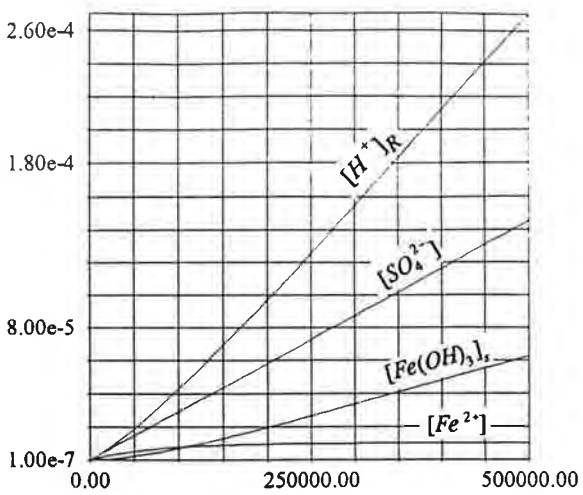

(12) T=293K

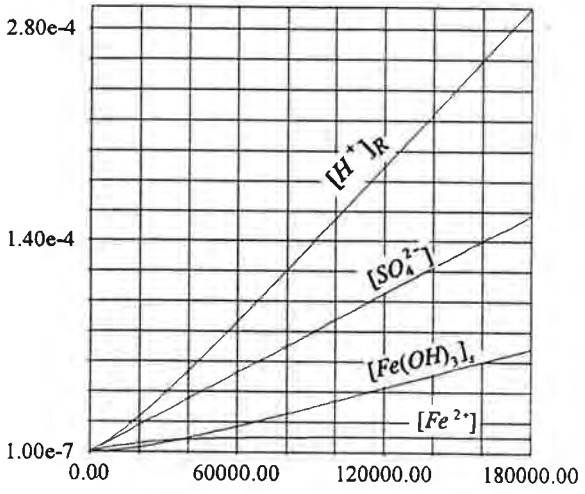

(21) T=303K

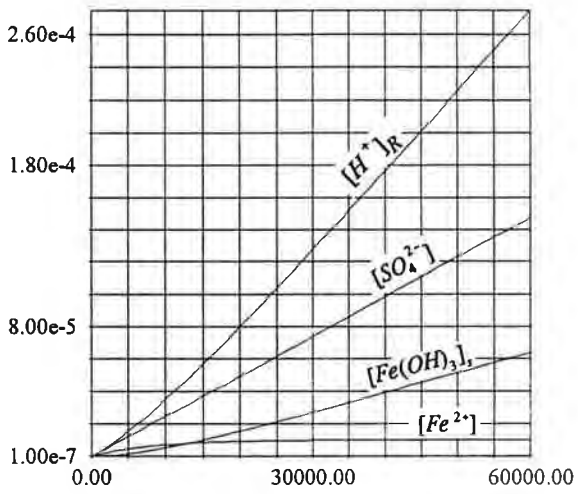

(22) T=313K

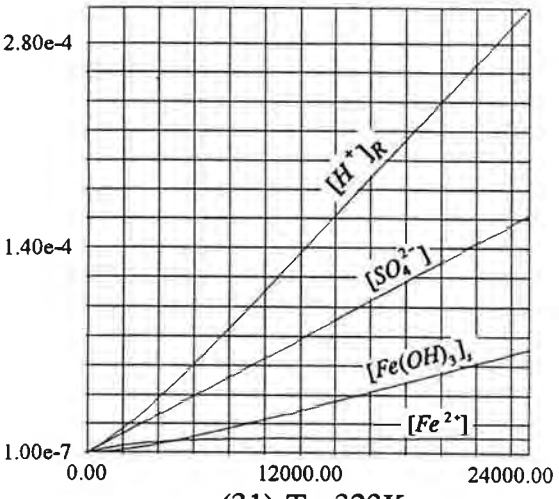

(31) T=323K

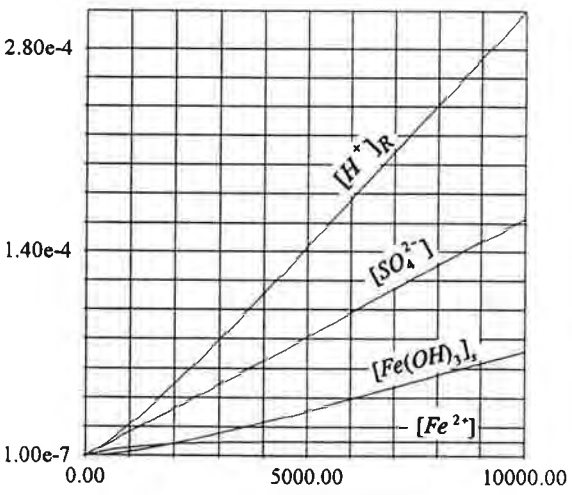

(32) T=333K

Fig. 3.2.2. The oxidation kinetics due to reactions (R1)-(R4) for different temperatures, S/V=1 m^2/l; the initial conditions: $[Fe^{2+}(t=0)]=0$, $[SO_4^{2-}(t=0)]=0$, $[Fe(OH)_3(t=0)]=0$. Constant in time pH=6.3 and concentration of dissolved oxygen, $[O_2]$ for $[O_2]_{gas}=21\%$. Horizontal axis: time in seconds, vertical axis: concentration in moles per litre. (1 800 000 sec. = 3 weeks).

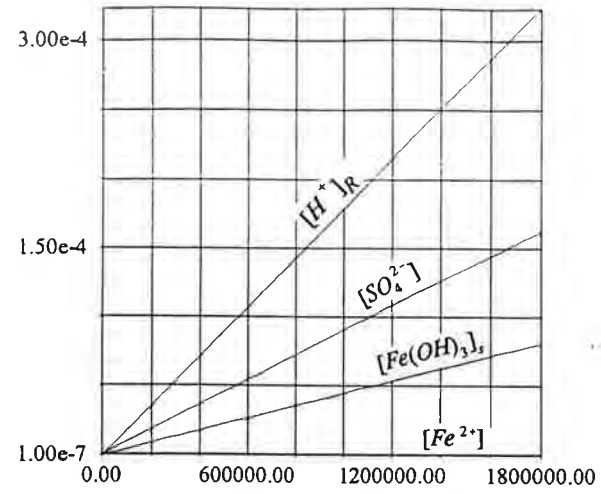

(11) T=283K

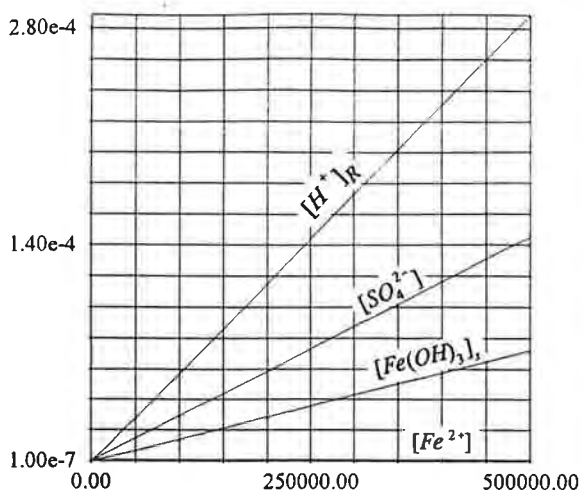

(12) T=293K

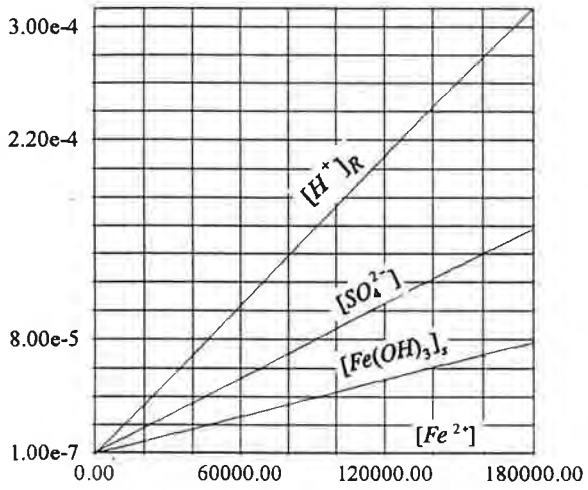

(21) T=303K

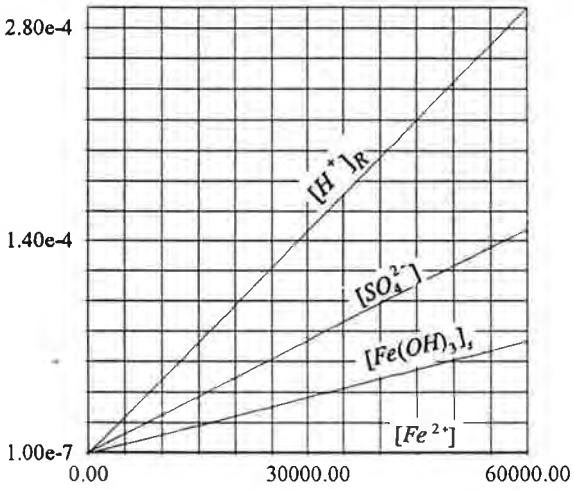

(22) T=313K

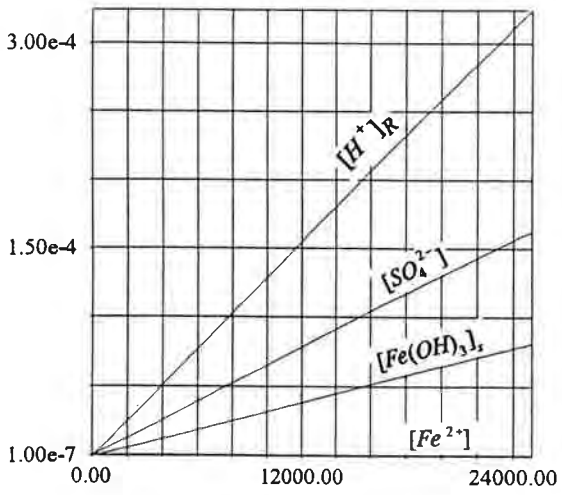

(31) T=323K

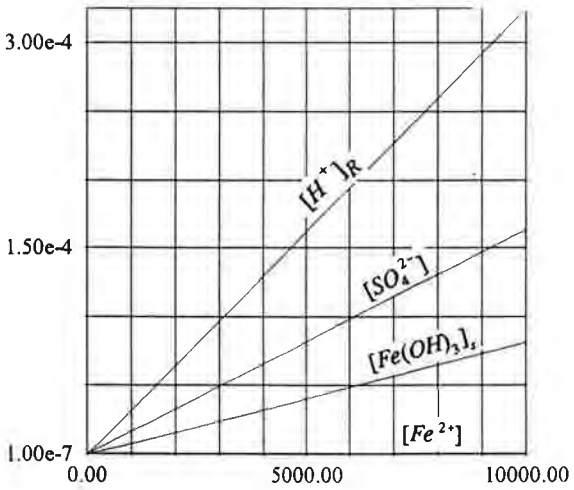

(32) T=333K

Fig. 3.2.3. The oxidation kinetics due to reactions (R1)-(R4) for different temperatures, S/V = 1 m^2/l; the initial conditions: $[Fe^{2+}(t=0)]=0$, $[SO_4^{2-}(t=0)]=0$, $[Fe(OH)_3(t=0)]=0$. Constant in time pH=6.9 and concentration of dissolved oxygen, $[O_2]$ for $[O_2]_{gas}=21\%$.Horizontal axis:time in seconds, vertical axis: concentration in moles per litre. (1 800 000 sec.= 3 weeks).

By decreasing pH values, the ratio between the concentrations of hydronium and sulphate ions, $[H^+]_R/[SO_4^{2-}]$ decreases from almost 2.0 at pH=6.9 to about 1.9 at pH=6.3. At pH=5.5 the ratio $[H^+]_R/[SO_4^{2-}]$ is close to 1 for a few days and than approaches a value above 1.5 after a few weeks. This phenomenon can be understood by analyzing eq. (D3.1).

For time independent oxygen concentrations, the concentration of ferrous iron converges to a quasi-equilibrium value $[Fe^{2+}]_{qeq}$ defined by pH and the concentration of dissolved oxygen:

$$[Fe^{2+}]_{qeq} = \frac{S}{V}\frac{k_1(T)}{k_2(T,[H^+])}[O_2]^{-1/2} \ , \qquad (3.2.1)$$

Fig. 3.2.4 illustrates how $[Fe^{2+}]_{qeq}$ changes as a function of pH and oxygen concentration, $[O_2]$ at T=303 K.

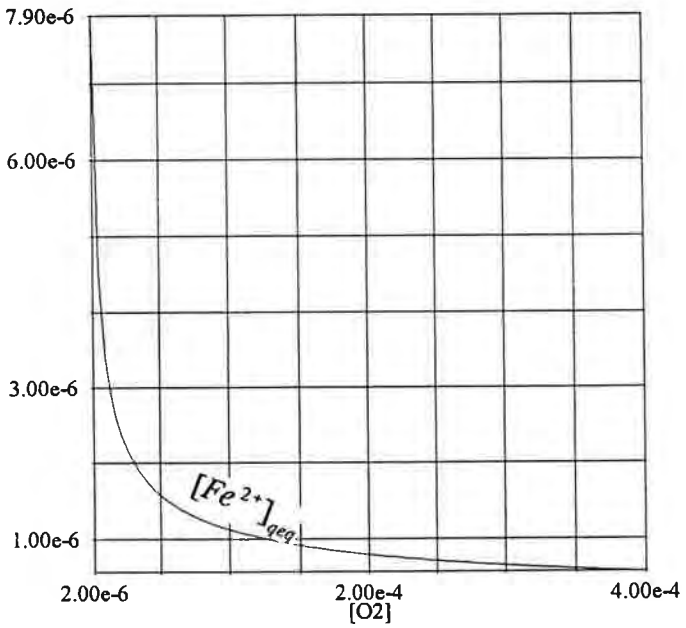

(a)

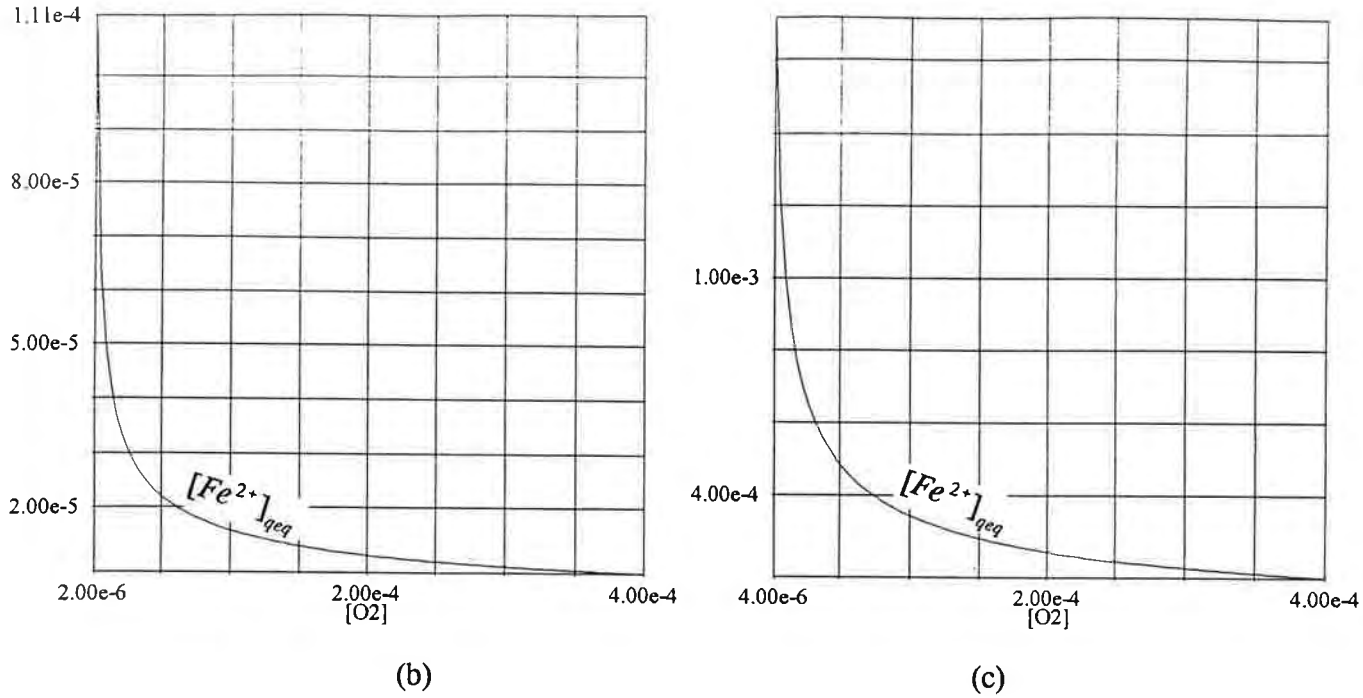

Fig. 3.2.4. Values of $[Fe^{2+}]_{qeq}$ as a function of the concentration of dissolved oxygen, $[O_2]$ at T=303 K for three different pH values: (a) pH=6.9; (b) pH=6.3; (c) pH=5.5. Horizontal axis: dissolved oxygen in moles per litre; vertical axis: quasi-equilibrium concentration of ferrous iron in moles per litre.

The quasi-equilibrium concentration of ferrous iron decreases with an increasing concentration of the dissolved oxygen. The asymptotic values of $[Fe^{2+}]$ at T=303 K in Figs.3.2.1 - 3.2.3 are the same as the values of $[Fe^{2+}]_{qeq}$ for appropriate concentrations of dissolved oxygen in Fig. 3.1.3. Concentration of ferrous iron converges to $[Fe^{2+}]_{qeq}$ with rates which depend on pH. This property is illustrated in Figs. 3.2.5, 3.2.6 and 3.2.7. The values of $[Fe^{2+}]_{qeq}$ do not depend on concentrations of ferric iron, $[Fe^{3+}]$.

The value of $[Fe^{2+}]_{qeq}$ defines a stable value of concentration of ferrous iron for pH greater than 4. In a similar way $[Fe^{3+}]_{qeq}$ defines a stable value of the concentration of the ferric iron for pH less than 4. Note that the formula (3.1.14) relates the quasi-equilibrium concentration of ferric iron to the concentration of ferrous iron. Even when both pH and $[O_2]$ are time-independent, the value of $[Fe^{3+}]_{qeq}$ follows the temporal changes of $[Fe^{2+}]$. The convergence to quasi-equilibrium concentrations is much faster than the non-equilibrium process of pyrite decay.

The results presented in Fig. 3.2.5 are obtained by solving numerically the full set of eqs. (D3). The asymptotic values of $[Fe^{2+}]$ in Figs. 3.2.5 (a)-(c) are the same as the values of $[Fe^{2+}]_{qeq}$ given by eq. (3.2.1). This agreement between the analytical result (3.2.1) and the numerical solutions justifies the concept of quasi-equilibrium.

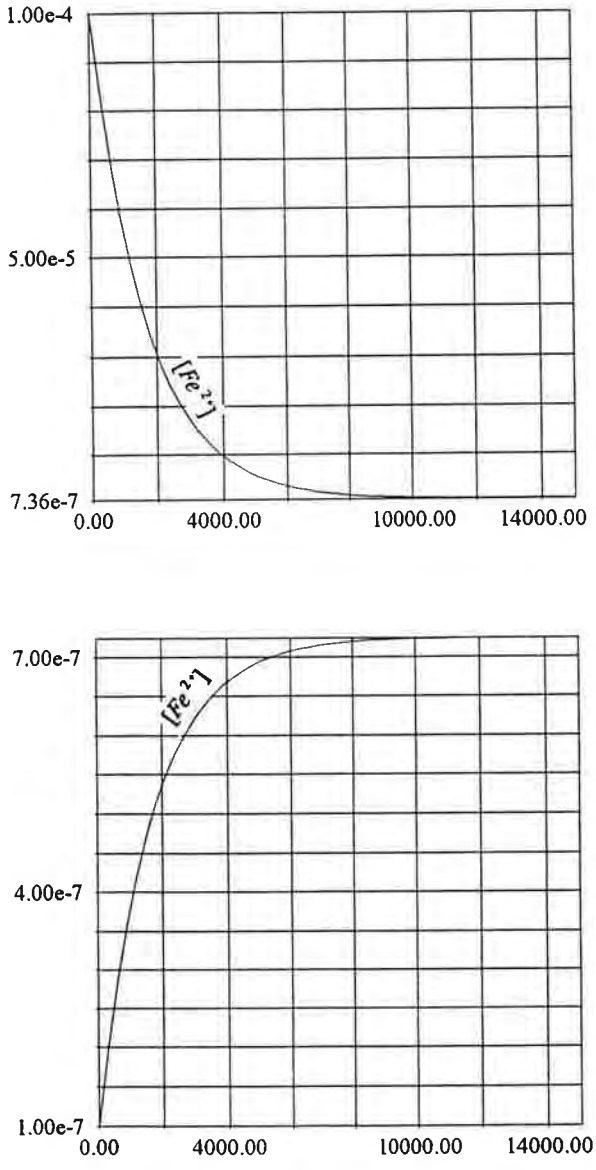

(a)

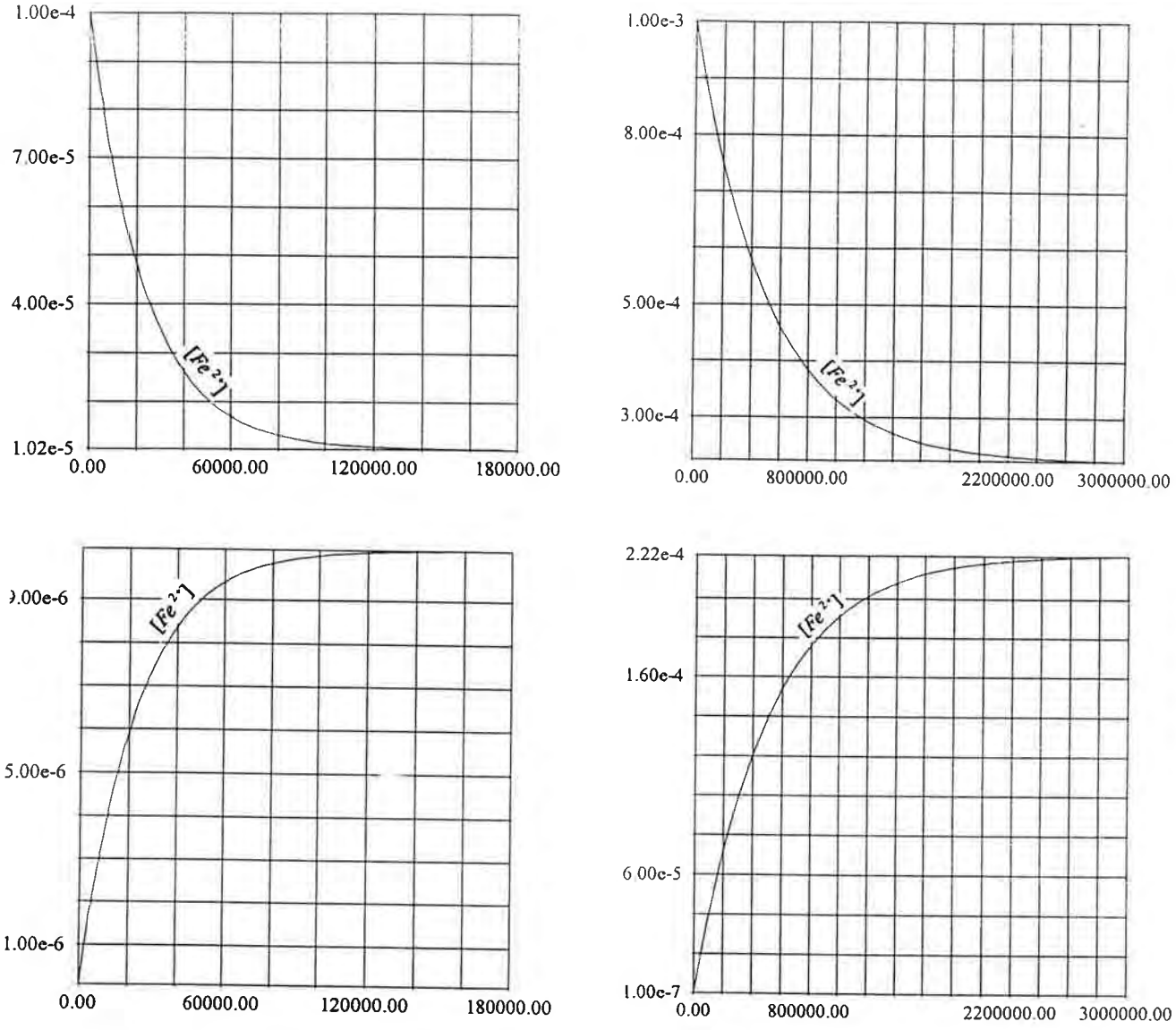

(b) (c)

Fig. 3.2.5. The temporal evolution of the concentration of ferrous iron, $[Fe^{2+}]$ during pyrite oxidation at a constant oxygen partial pressure of 0.21 atm and T=303 K. The diagrams illustrate the stability property and convergence rates for different pH values: (a) pH=6.9; (b) pH=6.3 (left); (c) pH=5.5 (right)

(ii) *oxygen depletion during oxidation of pyrite*

We analyze the oxygen depletion rates and the inhibition of acid generation at different temperatures for three different pH values analyzed in point III.2 (i). Our numerical results for different values of S/V and pH are presented in Figs. 3.2.6 and 3.2.7 . It is evident that increasing the value of S/V has the same effect on the ratio $[H^+]_R/[SO_4^{2-}]$ as decreasing pH values. By increasing the value of the active surface area per water volume, we observe increasing rates of reaction (R1) in which one hydronium iron is produced per every sulphate ion.

In Figs. 3.2.6 and 3.2.7 oxygen depletion rates accelerate with temperature in a similar way because we use similar values for the activation energies E_1, E_{22} and E_{23}. In saline water, however, the activation energy for the oxidation of ferrous iron is lower than E_{23}=96 kJ/mol used in our analysis [MiS], [Nip]. (We are grateful to R. Nicholson for bringing ref. [MiS] to our attention).

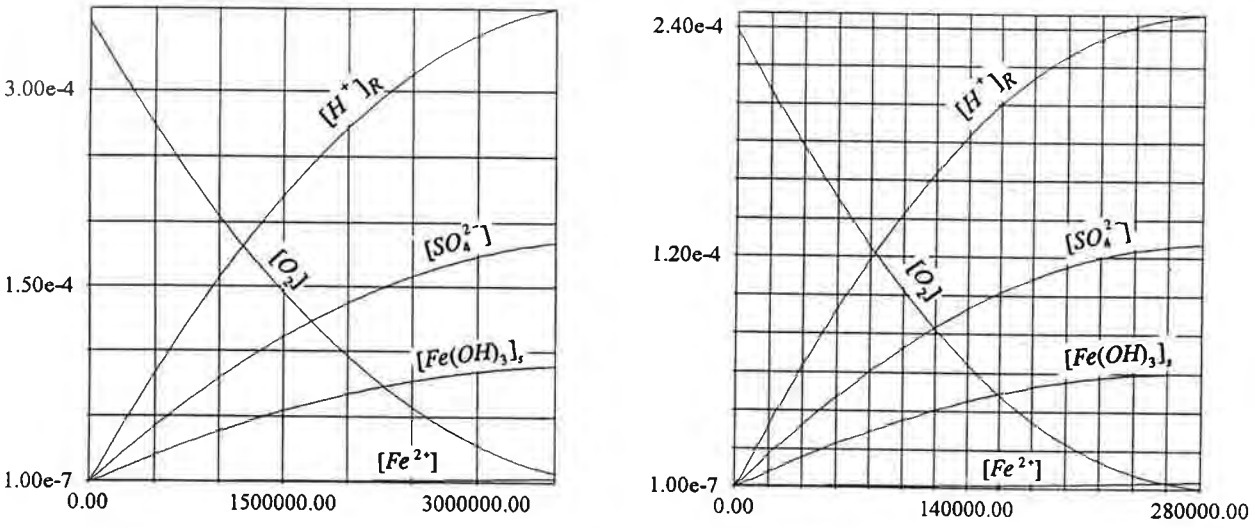

(a) (b)

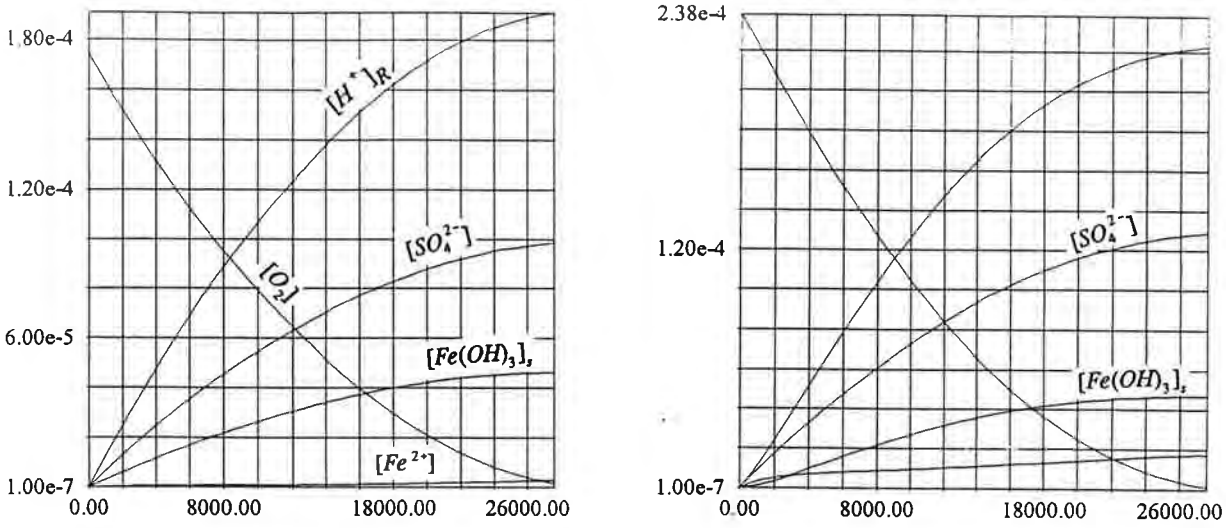

(c) (d)

Fig. 3.2.6. The consumption of dissolved oxygen at pH=6.9 for different values of S/V and different temperatures. (a) S/V=1m²/l, T=283 K; (b) S/V=1m²/l, T=303 K; (c) S/V=1m²/l, T=323; (d) S/V=10m²/l, T=303 K. Horizontal axis: time in seconds; vertical axis: concentration in moles per litre (3 000 000s=35 days).

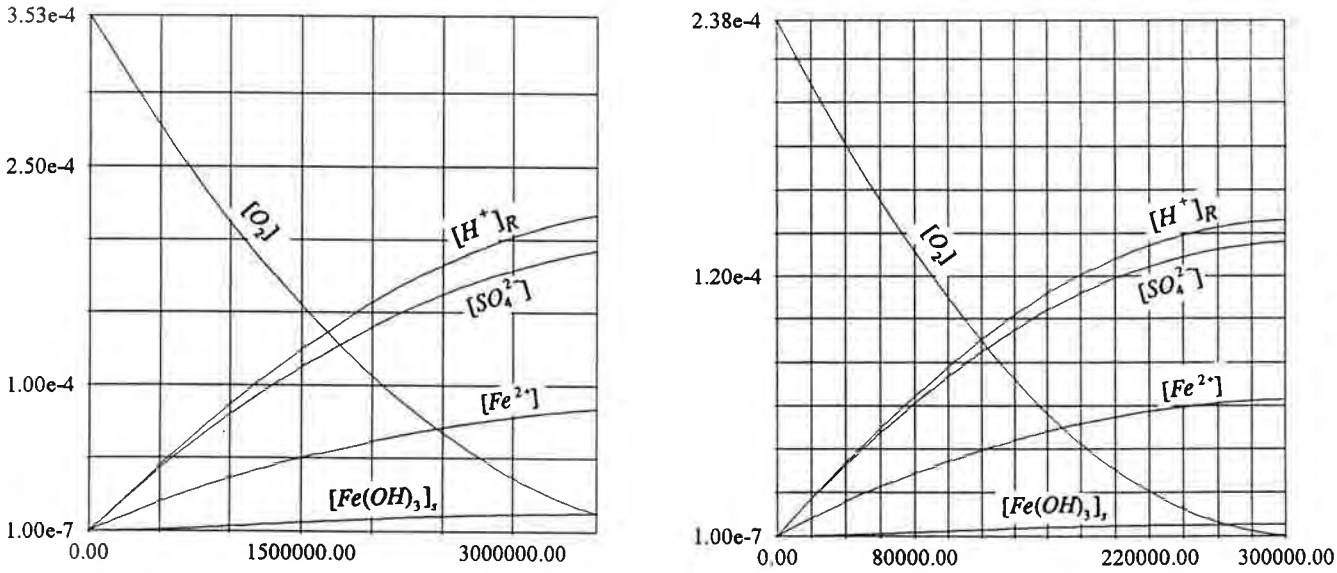

(a) (b)

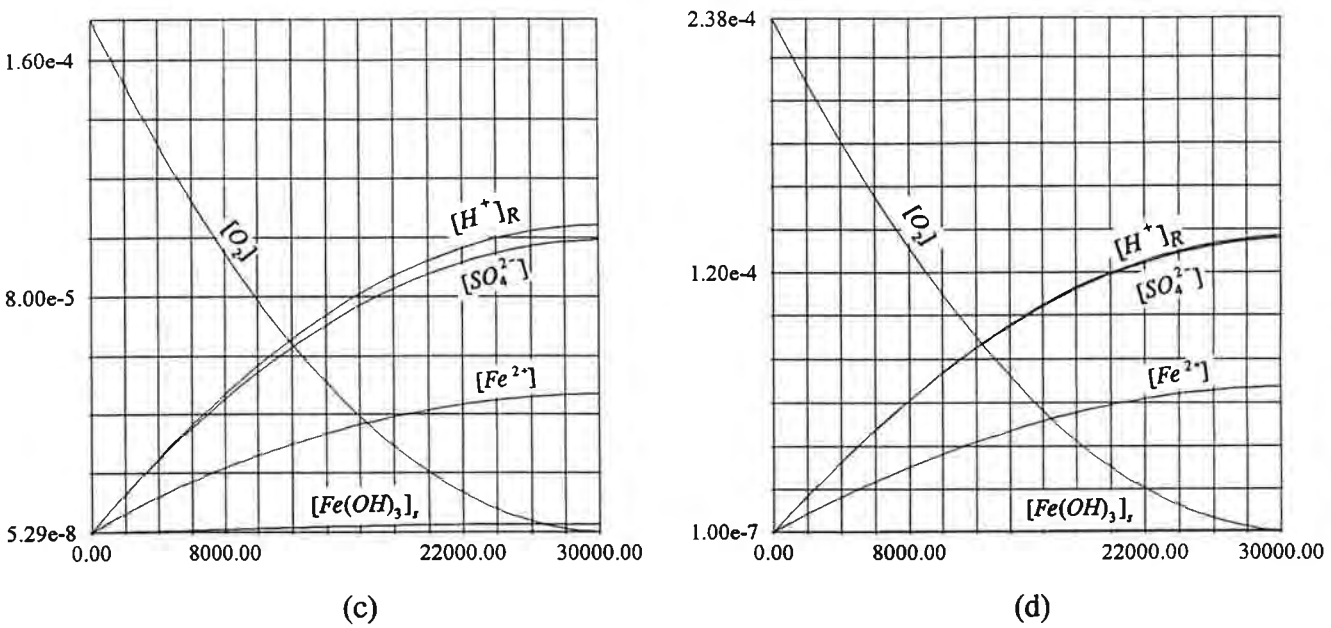

Fig. 3.2.7. The consumption of dissolved oxygen at pH=5.5 for different values of S/V and different temperatures. (a) S/V=1m^2/l, T=283 K; (b) S/V=1m^2/l, T=303 K; (c) S/V=1m^2/l, T=323; (d) S/V=10m^2/l, T=303 K. Horizontal axis: time in seconds; vertical axis: concentration in moles per litre (3 000 000s=35 days).

(iii) *stoichiometric incompatibility of acid-generating and acid-neutralizing reactions*

Reactions (R2) and (R4) at pH=7 are over ten times faster than at pH=6 and produce 4 hydronium ions per one ferrous ion. At the same time the reaction (R1) generates 2 hydronium ions per one ferrous ion. The reaction (R1) produces 2 sulphate ions per one ferrous iron. In this way the ratio $[H^+]_R/[SO_4^{2-}]$ increases from 1 at low pH values, to a number close to 2 at high pH values. The neutralization reactions show an opposite tendency. At pH values below 6 $H_2CO_3^\circ$ is stable and the neutralization process proceeds mainly according to the scheme (R5.1) in which 2 hydronium ions are consumed together with one sulphate ion. In this way calcium carbonate neutralizes the hydronium ions more efficiently than the sulphate ions (hydronium ions are generated practically at the same rate

as sulphate ions at pH below 6). We observe an opposite tendency at pH=7. At pH=7 HCO_3^- is stable and the neutralization process proceeds mainly according to the scheme (6.2) in which only 1 hydronium ion is consumed per 1 sulphate ion. Because at pH=7 the hydronium ions are produced faster than the sulphate ions we conclude that the neutralization process becomes inefficient and expensive. In order to eliminate both the hydronium and sulphate ions we have to use more neutralizing agents at pH=7 than at pH=6. This results in a larger amount of sludge which also has a negative environmental impact. At the same time it is environmentally desirable to maintain high values of pH close to 7 in effluent water. To solve this dilemma, it seems that a two-step neutralization process should be used. At first, neutralization should take place according to scenario 1°, then the effluent (weakly acidic) water should be further neutralized to reach an environmentally friendly pH value.

The two competitive stoichiometric effects associated with the neutralization process and affecting the cost efficiency, are not the only effects which should be considered in a future study. It was suggested that ferric hydroxide precipitates on mineral surfaces and leads to slower rates of pyrite oxidation [NiG]. The neutralizing minerals become coated by secondary precipitates as well. This may lead to a lower neutralizing potential. The process of formation and precipitation of ferric hydroxide (as described by reactions (R3) and (R4)) is faster at higher pH values. Other precipitates like siderite ($FeCO_3$) also affect (indirectly) rates of acid generation and neutralization. One should be able to estimate the importance of this effect in relation to the efficiency of the neutralization process discussed above.

We could not find in the literature systematic quantitative experimental results on the effectiveness of the neutralization process as a function of pH values, stoichiometry of hydronium and sulphate formation and coating by precipitating compounds (see [MoJ] and references therein). These aspects seem to merit further experiments and modelling studies which may result in practical decisions leading to reduced quantities of sludge.

III.3. Quasi-equilibrium evolution of concentrations of ferric and ferrous iron and the absence of chemical oscillations

One of the working ideas which motivated this study was the hypothesis about chemical oscillations and the possible chaotic behaviour of time dependent concentrations of species formed during pyrite oxidation [Go]. Indeed, the diagram presented on page 5 suggests indeed that the feedback mechanism between the reactions of oxidation of ferrous iron and pyrite oxidation by ferric iron might be responsible for chemical oscillations. There are known examples of model chemical systems in which a similar feedback leads to an oscillatory behaviour [Pr], [NiP], [Ty], [An]. Because the number of chemical species involved in pyrite oxidation is greater than three, one might expect a chaotic behaviour [An], [Ty].

A classical example of a chemical system exhibiting nonlinear oscillations is the Brusselator defined by the stoichiometric relations [NiP]:

$$(1): A \rightarrow X \ , \quad (2): B + X \rightleftharpoons Y + D \ , \quad (3): 2X + Y \rightleftharpoons 3X \ , \quad (4): X \rightarrow E \ . \qquad (BR1)$$

and the rate equations:

$$\frac{d[X]}{dt} = k_1[A] - (k_2[B] + k_4)[X] + k_{-2}[D][Y] + k_3[X]^2[Y] - k_{-3}[X]^3 \ ,$$

$$\frac{d[Y]}{dt} = k_2[B][X] - k_{-2}[D][Y] - k_3[X]^2[Y] + k_{-3}[X]^3 \ . \qquad (BR2)$$

The coefficients k_i and k_{-i} are the rate constants for the direct (from left to right) and the reverse (from right to left) reactions described by the stoichiometric relations (BR1). The model describes a reactor with the final products D and E removed from the reaction space as soon as they are formed. The concentrations of species A and B are in excess. In this way the kinetic equations for [A], [B], [D], and [E] can be disregarded. Both the Brusselator and the acid rock drainage model describe non-equilibrium processes. The fact that we deal with a chemical system at non-equilibrium does not exclude by itself the possibility of chemical

oscillations. As a matter of fact the values of concentrations [A] and [B] in eq. (BR2) must be different from zero for oscillations to exist. The parameters k_1 and k_2 describe the rates of decomposition of chemical compounds which are in excess and whose concentrations do not change significantly over time. A key property of equations (BR2), which leads to chemical oscillations, is the presence of a so called focal point in the phase space, which becomes unstable when the concentration [B] exceeds a certain critical value. This property results from a particular form of the nonlinear terms in the kinetic equations for (BR2) [NiP], [OtL].

There is some analogy between the Brusselator and the pyrite oxidation problem. We have a large initial amount of pyrite and nonlinear terms in eqs. (D1)-(D3), but they do not produce oscillations. We do not present mathematical details in this report, instead, we use illustrative numerical results which show that the concentration of ferric iron and ferrous iron converge to the quasi-equilibrium values defined by eqs.(3.1.5) and (3.2.1). We call the concentrations $[Fe^{3+}]_{qeq}$ and $[Fe^{2+}]_{qeq}$ defined by eqs.(3.1.5) and (3.2.1) quasi-equilibrium states for the following reasons:

(i) concentrations of ferric and ferrous iron evolve to quasi-equilibrium values both when the initial concentration is greater than the quasi-equilibrium value and when the initial concentration is less than the quasi-equilibrium values

(ii) the initial relative evolution rates $(d[Fe^{3+}]/dt)/[Fe^{3+}]$ and $(d[Fe^{2+}]/dt)/[Fe^{2+}]$ for the concentrations of ferric and ferrous iron are much greater than the relative rate $(d[FeS_2]_R/dt)/[FeS_2]$ at which pyrite is oxidized ($[FeS_2]_R$ denotes the total amount of pyrite reacted per one litre of water, $[FeS_2]$ denotes the total amount of unreacted pyrite).

(iii) the quasi-equilibrium values evolve according to the equations (3.1.5) and (3.2.1) which describe a slow adiabatic evolution of the ferric and ferrous species

Properties (i) - (iii) are illustrated in Fig. 3.2.4 where the full set of equations (D3) is solved numerically for two different initial values of $[Fe^{2+}]$. A good measure of the relative rates are the quantities $(d[Fe^{3+}]/dt)/[Fe^{3+}]$, $(d[Fe^{2+}]/dt)/[Fe^{2+}]$ and $(d[H^+]/dt)/[H^+]$. Fig.3.2.4 demonstrates that the concentration $[Fe^{2+}]$ evolves to the value $[Fe^{2+}]_{qeq}$ and that $[Fe^{2+}]_{qeq}$ follows the slowly evolving values of the concentrations of other species, according to eqs. (D3). The observed behaviour is a direct consequence of the fact that the derivative

$d[Fe^{2+}]/dt$ changes its sign at $[Fe^{2+}]=[Fe^{2+}]_{qeq}$. $d[Fe^{2+}]/dt$ is negative for $[Fe^{2+}]>[Fe^{2+}]_{qeq}$, and positive for $[Fe^{2+}]<[Fe^{2+}]_{qeg}$ (i.e. the concentration increases when it is initially below the quasi-equilibrium value and decreases when it is above the quasi-equilibrium value). The concentration of ferrous iron after a relatively short time converges to $[Fe^{2+}]_{qeq}$ which shows only a weak time dependence in comparison with the initial change. A rigorous mathematical stability analysis of the set of kinetic equations for pyrite oxidation will be presented in our forthcoming publications [Otp].

IV. BACTERIAL OXIDATION OF PYRITE

This chapter presents the results of our analysis of the experimental data on bacterial oxidation at pH values less than 4. The processes involved in bacterial oxidation are treated in a similar way as the abiotic reactions. An important new element in our analysis is the introduction of coupling between all the elementary abiotic and bacterial processes. In previous modelling efforts [Se] abiotic and bacterial processes were characterized by an overall rate of pyrite oxidation expressed as

$$R_{tot} = R_{chem} + R_{bact}$$

Such an approach is often appropriate for the kinetics characterized by linear processes. Unfortunately the experimental data reviewed in Chapter II indicate that pyrite oxidation involves strongly nonlinear processes which require a consistently nonlinear approach. The bacterial oxidation cannot be considered as independent from the abiotic processes. A direct consequence of the nonlinear coupling between the individual chemical reactions is the presence of quasi-equilibrium concentrations of transient species, which define the total rates of pyrite oxidation. Proper understanding of the complex chemical kinetics is necessary for the development of a reliable physical model which may become a useful tool for prediction, prevention and monitoring of acid mine drainage.

The main results presented in this chapter can be summarized as follows:

1. The anaerobic bacterial oxidation of pyrite by ferric iron (reaction (B3)) is introduced for the first time to the kinetic model. The rate constant governing the reaction (B3) and a kinetic equation are derived and provide a good agreement with experimental data. At 30°C the anaerobic pyrite oxidation by ferric iron is accelerated by about 250% when Thiobacillus ferrooxidans are present at concentrations of 1 gram per litre.

2. The kinetic formula for the bacterial oxidation of ferrous iron, introduced previously by Suzuki et al. [SuL], is modified and gives a satisfactory quantitative description of

competitive inhibition observed at bacterial concentrations between 0.1 g and 1.0 g of cells per litre. In the presence of Thiobacillus ferrooxidans the reaction of the oxidation of ferrous iron is over a million times faster than in the analogous abiotic reaction.

3. The rate constant for pyrite oxidation by dissolved oxygen is determined. At a concentration of 1 gram of cells per litre, the bacterial reaction (B3) is three hundred times faster than the analogous abiotic reaction (R1).

4. A realistic formula is proposed for the temperature dependence of rate constants governing the bacterial processes.

5. Kinetic equations for reactions (B1), (B2) and (B3) are derived and included in a kinetic model together with the abiotic reactions (R1), (R2) and (R3).

6. The kinetic model is analyzed for various temperatures and various concentrations of dissolved oxygen. The coupled chemical and bacterial reactions do not produce temporal oscillations of the transient and final products. During the nonequilibrium process of pyrite oxidation the concentrations of ferric and ferrous iron evolve to quasi-equilibrium values which depend on pH, concentration of dissolved oxygen, concentration of bacteria, temperature and other factors. (This conclusion is valid only in the absence of the transport processes and does not exclude the possibility of nonlinear oscillations as the result of a competition between the chemical and biological reactions and processes of mass and energy transport which should be included in a future physical model).

7. The reactions (B2) and (B3) provide a negative feedback mechanism which is responsible for a negative response of the chemical system when the concentration of oxygen decreases. A decreasing oxygen concentration results in an increased quasi-equilibrium concentration of ferrous iron. Because the rate of oxidation of ferrous iron is proportional to the concentration of ferrous iron and also controls the rate of anaerobic pyrite oxidation by ferric iron, the effect of lowering oxygen concentration, while still significant, is much weaker than previously expected.

8. Oxygen consumption rates during bacterial oxidation of pyrite are very high and are

controlled by the oxygen transport to a much greater extent than abiotic oxidation. In underwater disposal, oxygen diffusion in water seems to be an even more significant factor limiting oxidation rates more effectively than in waste rock piles.

9. The negative feedback mechanism is also responsible for maintaining moderately low pH values during bacterial activity. Thiobacillus ferrooxidans exhibit a chemistatic action by maintaining moderately low pH values at which the pyrite oxidation is very fast. This is a strong nonlinear effect resulting directly from the form of pH and temperature dependence of the bacterial activity. Because hydronium ions are consumed during the reaction of oxidation of ferrous iron, and ferric iron reaches high concentrations, pH values decrease relatively slowly and remain for a long time at the optimum level for bacterial processes. Consequently, the bacterial activity takes place longer than one would expect by analyzing a simplified model in which reactions (B1), (B2) and (B3) are not included as separate processes.

10. At a high concentration of bacteria, the concentration of ferric iron may become even greater than the concentration of ferrous iron. The ferric iron may then oxidize pyrite after bacterial activity decreases when pH becomes very low. This may be viewed as a delayed bacterial oxidation of pyrite.

11. At 30°C and a bacteria concentration on the order of 1 gram of bacteria per one litre of water, the overall process of bacterial oxidation of pyrite is over a thousand times faster than at the same temperature in the absence of bacteria - the bacterial oxidation during one week has an environmental impact greater than the abiotic oxidation during one year (see Figs. 4.1.1, 4.1.2 , 3.1.7 and 3.1.8).

12. The bacterial oxidation at temperatures between 20°C and 40°C is much faster than the abiotic oxidation at temperatures twenty degrees higher.

13. We do not know of any experimental data on the rates of bacterial oxidation of ferrous iron for concentrations $[Fe^{2+}] < 1mM$ and on the dependence of reactions (B1) and (B3), on oxygen concentration and the ratio between active pyrite surface area, S and cell concentration [cell]. It seems quite possible that reactions (B1) and (B3) show effects of

competitive inhibition when the bacteria concentration increases. Further experiments may provide useful information which may lead to modifications in our model.

We have extrapolated the laboratory results to longer times, with oxygen concentrations and temperatures different than in previous experiments. We have used experimental data obtained under laboratory conditions which may be significantly different than field conditions. In particular, Eh and pe values were not monitored in previous experiments and may be important for bacterial processes. Some of the assumptions introduced in our model require verification by further experiments. The results obtained by computer simulation should be confronted with the available field data and calibrated before the kinetic model developed here is used as part of a comprehensive physical waste rock model.

In paragraphs IV.0.0 -IV.0.3, a detailed quantitative analysis of experimental data on bacterial oxidation is presented and elementary kinetic equations for individual reactions are derived and solved. The full set of coupled kinetic equations is analyzed in paragraphs 4.1.1 and 4.1.2. The model is constructed in a modular form which provides a high level of flexibility to include new information.

IV.0. Analysis of experimental data on bacterial oxidation of pyrite

In Chapter II we have reviewed experimental data on bacterial oxidation. According to our previous discussion the kinetic model which includes the bacterial processes, has the form:

$$\frac{d[Fe^{2+}]}{dt} = K_1(T,[H^+])[O_2]^{1/2} - K_2(T,[H^+])[Fe^{2+}][O_2] + \frac{15}{14}K_3(T,[H^+])[Fe^{3+}]^{3/5}[H^+]^{-1/2}, \quad (DB.1)$$

$$\frac{d[Fe^{3+}]}{dt} = K_2(T,[H^+])[Fe^{2+}][O_2] - K_3(T,[H^+])[Fe^{3+}]^{3/5}[H^+]^{-1/2}, \quad (DB.2)$$

$$\frac{d[H^+]}{dt} = 2K_1(T,[H^+])[O_2]^{1/2} - K_2(T,[H^+])[Fe^{2+}][O_2] + \frac{8}{7}K_3(T,[H^+])[Fe^{3+}]^{3/5}[H^+]^{-1/2}, \quad (DB.3)$$

$$\frac{d[O_2]}{dt} = -\frac{7}{2}K_1(T,[H^+])[O_2]^{1/2} - \frac{1}{4}K_2(T,[H^+])[Fe^{2+}][O_2], \quad (DB.4)$$

$$\frac{d[SO_4^{2-}]}{dt} = 2K_1(T,[H^+])[O_2]^{1/2} + \frac{1}{7}K_3(T,[H^+])[Fe^{3+}]^{3/5}[H^+]^{-1/2}, \quad (DB.5)$$

$$\frac{d[H_2O]}{dt} = -K_1(T,[H^+])[O_2]^{1/2} + \frac{1}{2}K_2(T,[H^+])[Fe^{2+}][O_2] - \frac{7}{4}K_3(T,[H^+])[Fe^{3+}]^{3/5}[H^+]^{-1/2}. \quad (DB.6)$$

The rate constants $K_1(T,[H^+])$, $K_2(T,[H^+])$ and $K_3(T,[H^+])$ describe the simultaneous abiotic and bacterial processes described by the stoichiometric relations (R1)-(R3) and (B1)-(B3):

$$K_1(T,[H^+]) = \frac{S}{V}k_1(T) + \frac{S}{V}k_{1b}(T_m,[H^+]_m,[cell])B([H^+])B(T), \quad (4.0.1)$$

$$K_2(T,[H^+]) = k_2(T,[H^+]) + k_{2b}(T_m,[H^+]_m,[cell])B([H^+])B(T), \quad (4.0.2)$$

$$K_3(T,[H^+]) = \frac{S}{V}k_3(T) + \frac{S}{V}k_{3b}(T_m,[H^+]_m,[cell])B([H^+])B(T) \quad . \qquad (4.0.3)$$

The rate constants k_1, k_2 and k_3 govern the abiotic reactions and are defined in Chapters II and III. The rate coefficients k_{1b}, k_{2b} and k_{3b} for the bacterial processes assume their maximum values at temperature T_m, and the hydronium ions concentration $[H^+]_m$. The optimum conditions for bacterial activity of Thiobacillus ferrooxidans are strain dependent. The value of T_m is usually between 298K and 313K. Optimum pH values (defined by $pH_m = -\log([H^+]_m)$) vary between 2 and 3. The coefficients k_{1b}, k_{2b} and k_{3b} depend also on bacterial cell concentration, [cell]. The coefficients B(T) and B([H^+]) describe temperature and pH dependence of bacterial activity. In paragraphs IV.0.0 - IV.0.3 experimental data are used to determine values of rate coefficients for the bacterial processes.

In paragraph 4.0.0, we discuss the pH and temperature dependence of the bacterial activity. This analysis is followed by a discussion of the elementary kinetic equations for reactions (B1)-(B3). We proceed in a different order than in Chapter III and analyze in paragraph 4.0.1, the anaerobic reaction (B3). In paragraph 4.0.2 the reaction (B2) is analyzed. The rate constant for the reaction (B1) cannot be measured directly but can be determined indirectly from the quantitative information on reactions (B2) and (B3) as described in paragraph 4.0.3.

IV.0.0. ***Temperature and pH dependence of bacterial activity***

The coefficients B(T) and B([H^+]) are defined as

$$B(T) = \exp[-c(T-T_m)]^{1.4}\{1 - th[d(T-T_m)^3]\}, \qquad (4.0.3)$$

$$B([H^+]) = (1 + 10^{b_1-b_m} + 10^{b_m-b_2})(1 + 10^{b_1-pH} + 10^{pH-b_2})^{-1}, \qquad (4.0.4)$$

where $b_m=(b_1+b_2)/2$.

The coefficient B(T) has its maximum value $B(T_m)=1$ at a temperature T_m which is different for different strains of bacteria. The coefficient B([H]) has its maximum value $B([H]=0.005)=1$ at $pH=-\log[H]=2.3$. The rate constants k_{ib} define maximum rates for reactions (B1), (B2) and (B3). We assume that the bacterial activity for each of the elementary reactions shows the same temperature and pH dependence. We do not have, however, a confirmation of this assumption by independent experiments.

The coefficient B(T) is obtained by fitting the formula (4.0.3) to the experimental data presented in Fig.2.9. (The coefficient B(T) is different than the one used in RATAP model [Se]). In Fig. 4.0.1 we illustrate the coefficients B(T) for two different sets of fitting parameters in eq. (4.0.3). In Fig. 4.0.1a B(T) is defined by

$$c=0.05, \quad d=0.0005 \qquad (4.0.5)$$

and has its maximum at $T_m=303K$ (30°C). In Fig. 4.0.1b

$$c=0.04, \quad d=0.002 \qquad (4.0.6)$$

and B(T) has two maxima as the upper experimental curve in Fig.2.9. The powers 1.4 and 3 in the expression (4.0.3) can be changed to fit other experimental data. Because B(T) depends on the difference $T-T_m$, a change in the value of T_m results in shifting the plots in Fig. 4.0.1.

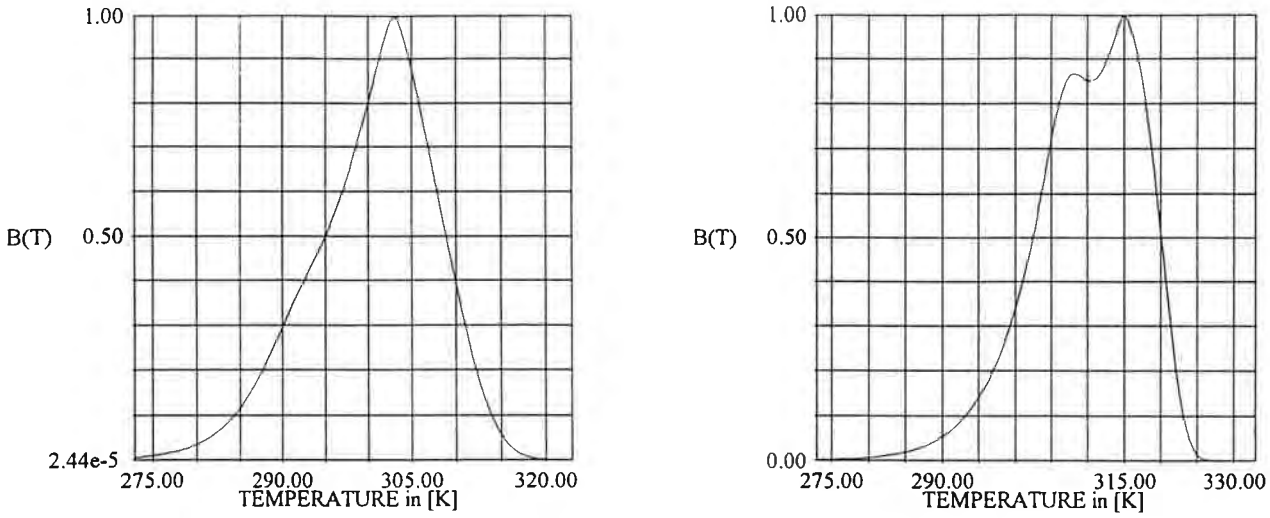

(a) (b)

Fig. 4.0.1. (a) Values of the temperature coefficient B(T) fitted to experimental data for Thiobacillus ferrooxidans used in this study (b) Values of B(T) with two maxima characteristic for a thermophilic culture (not used in this study).

The coefficient B([H^+]) is defined in the same way as in previous studies [BeO], [Se].In Fig. 4.0.2 we present plots of B([H^+]) used in this study and in the RATAP model [Se]. We use experimental data obtained by Suzuki et al. [SuL] and Lizama and Suzuki [LiS4] for a particular strain SM-4 of Thiobacillus ferrooxidans which show the maximum activity at pH=2.3. Plot 4.0.2a is obtained for

$$b_1 = 2.2 \quad and \quad b_2 = 2.4 . \tag{4.0.6}$$

Fig. 4.0.2b illustrates the coefficients B([H^+]) used in the RATAP model [Se]. The arithmetic average of the coefficients b_1 and b_2 is equal to the value of pH=b_m at which the bacterial activity reaches its maximum. The plots in Fig. (4.0.2) are symmetrical with respect to b_m. Further modifications can be easily made if future experimental data would require asymmetrical dependence of B on pH.

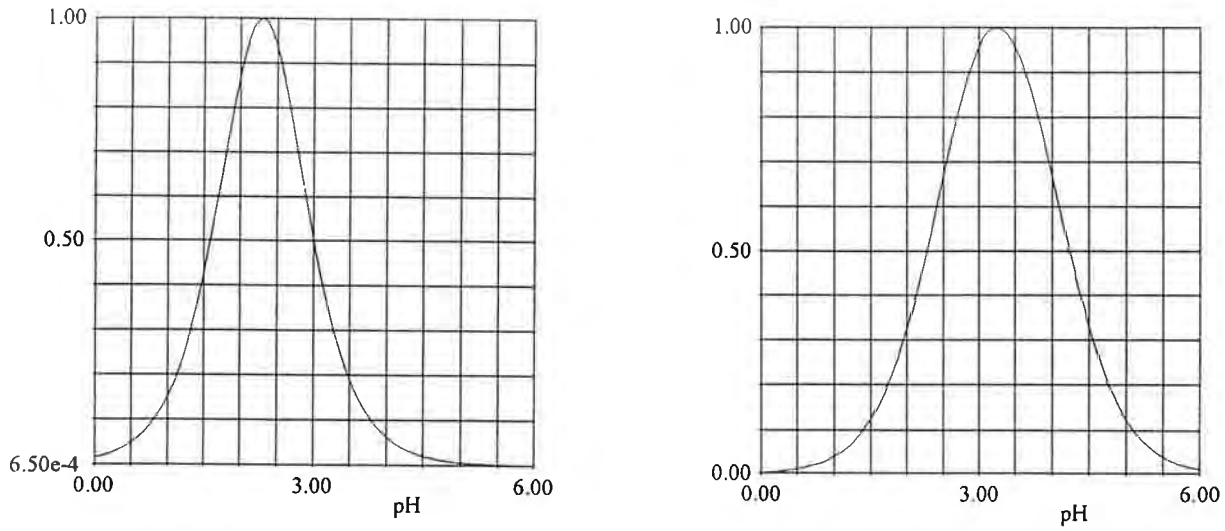

Fig. 4.0.2. (a) The pH dependence of the rate coefficient B([H^+]) used in this study (pH=-log([H^+]). (b) Plot of the coefficient B([H^+]) used previously in the RATAP model.

4.0.1. ***Anaerobic oxidation of pyrite by ferric iron.***

The process of anaerobic oxidation of pyrite by ferric iron has been documented recently in independent experiments [LiS4],[Pr],[Gu].In this paragraph we analyze experimental data on the anaerobic bacterial oxidation of pyrite obtained for a bacterial strain SM-4. Fig.2.9 presents experimental data obtained by Lizama and Suzuki [LiS4] during the anaerobic oxidation of 3.125 mg of pyrite in 1.2 ml of HP (high phosphate) solution. Fig.2.9 presents experimental data obtained by Lizama and Suzuki et al. [LiS4] during anaerobic oxidation of 3.125 mg of pyrite in 1.2 ml of HP (high phosphate) solution. We have found that a good quantitative agreement with experimental data is achieved if we use the kinetic equation

$$\frac{d[Fe^{2+}]}{dt} = \frac{15S}{14V}\{k_3(T) + k_{3b}(T_m,[H^+]_m,[cell])B([H^+])B(T)\}[Fe^{3+}]^{3/5}[H^+]^{-1/2} \qquad (4.0.7)$$

with the rate constant

$$k_{3b} = 2.18 \cdot 10^{-6} M^{0.9} lm^{-2} s^{-1} \quad for \quad T_m = 303K,\ [H^+]_m = 0.005M,\ [cell] = 1gl^{-1}. \qquad (4.0.8)$$

The rate constant k_{3b} defines the rate of the reaction (B3) at $S/V = 1m^2/l$ and bacteria cell concentration, [cell]=1 gram of cells per 1 litre.

Fig.4.0.3 presents results obtained by solving the kinetic equation for the same conditions as in Fig.2.8 presented by Lizama and Suzuki [LiS4] in their experimental work. Lizama and Suzuki used the pyrite particles of approximately the same size as in the kinetic study by McKibben and Barnes [McK]. This allows us to use the same value of the active surface area per unit mass of pyrite as in our analysis in Chapter III. In Fig. 4.0.3a , we show that the same kinetic equation describes reasonably well independent data for both experimental studies [McK] and [SuL]. This is an important result because anaerobic experiments require special precautions and quite often oxygen dissolved in nitrogen may distort experimental result [Ni]. The fact that the two independent experiments produce the same results, raises our confidence in using these data. Fig.4.0.3b presents our model results obtained by solving the kinetic equation (4.0.7) the same initial conditions as in Fig. 2.9, $T=T_m=303K$ and $S/V=0.78m^2/l$.

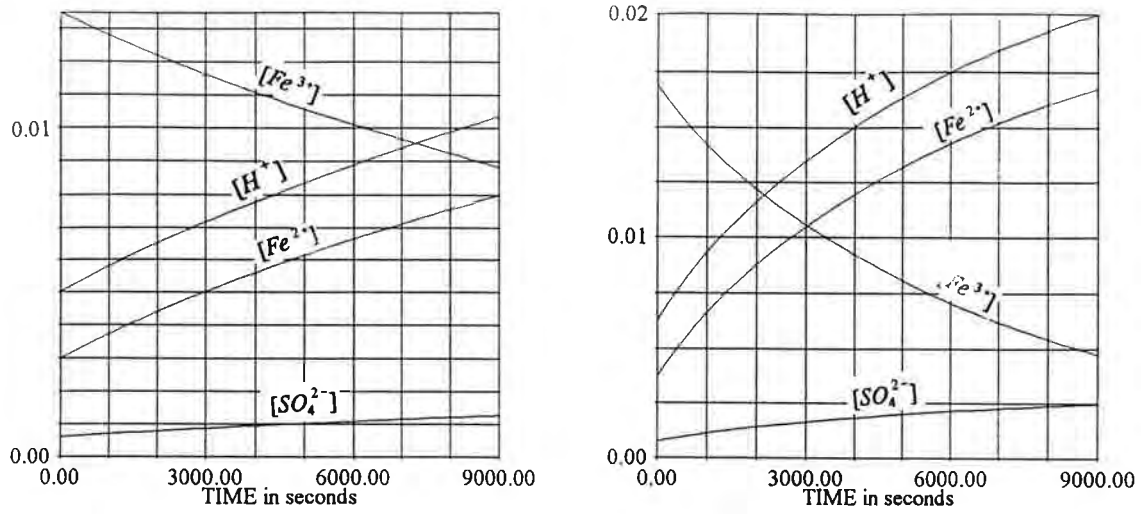

(a) (b)

Fig. 4.0.3. Molar concentrations of $[Fe^{2+}]$, $[Fe^{3+}]$, $[H^+]$ and $[SO_4^{2-}]$ obtained by solving the kinetic equation (4.0.8) for (a) abiotic oxidation of pyrite by ferric iron; (b) bacterial oxidation of pyrite by ferric iron. The initial conditions are the same as in the experiment by Lizama and Suzuki [LiS4]; $S/V=0.78m^2/l$, $T=303K$.(900s=15min., see Fig. 2.9).

A good agreement with the experimental data is obtained for the rate constant k_{3b} which is 2.5 times greater than the rate constant k_3 for the abiotic reaction (R3). This is a relatively small effect in comparison with the two other reactions (B1) and (B2). The reactions (R1) and (R2) are accelerated by bacteria by about 300 times and over a million times respectively.

We must stress that we could not find any experimental data which analyzed systematically the dependence of the reaction (B3) on S/V and [cell]. It is quite possible that both surface reactions (B3) and (B1) exhibit an effect of competitive inhibition in a similar way as the reaction (B2) discussed in the next paragraph. This aspect of the bacterial oxidation merits further experimental work which may provide information important for controlling the process of bacterial oxidation.

4.0.2. *Bacterial oxidation of ferrous iron*

Thiobacillus ferrooxidans have a very dramatic effect on the rate of the reaction (R2) which at millimolar concentrations of ferrous iron becomes over one million times faster due to the bacterial activity. The bacterial reaction (B2)

$$Fe^{2+} + 1/4\ O_2 + H^+ \xrightarrow{\text{bacteria}} Fe^{3+} + 1/2\ H_2O\ , \qquad \text{(B2)}$$

is responsible for the subsequent oxidation of pyrite by ferric iron. A competitive inhibition observed by increasing the bacteria concentration is a very important feature discovered by Suzuki et al. [SuL]. We have reanalyzed the experimental data and the empirical formula (2.35) obtained by Suzuki et al. [SuL]. A better agreement with the experimental data presented in Fig.2.8 is achieved when we use the formula

$$k_{2b}(T_m,[H^+]_m,[cell]) = C_2[cell]\{k_{2m}(1+[cell]^{2/3}/k_{2c})+[Fe^{2+}]\}^{-1} \qquad (4.0.9)$$

with the empirical constants

$$C_2 = 16.87\,Mlg^{-2}s^{-1},\ k_{2m} = 1.1\cdot 10^{-4}M,\ k_{2c} = 2.8\cdot 10^{-3}(l/g)^{2/3}\ . \qquad (4.0.10)$$

The above formula is only a slight modification of the formula proposed by Suzuki et al. We have used a simple dimensional analysis based on the property that the competitive inhibition is proportional to the second power of the number of cells and inversely proportional to the average distance between the cells (distance is proportional to $V^{-1/3}$; V-volume). This leads to the introduction of the term proportional to $[cell]^{2/3}$ instead of [cell] in the denominator of eq.(4.0.9). In Figs. 4.0.4 a-d we present plots of the rhs of eq.(4.0.9) for different bacteria concentrations. Plots in Figs. 4.0.4 reproduce experimental data presented before in Fig.2.8. One should expect a similar effect of competitive inhibition for the surface reactions (B1) and (B3). So far, however, we did not find in the literature any experimental data on the competitive inhibition, which could be used in our model of the surface reactions (B1) and (B2).

The effect of competitive inhibition is illustrated in Fig.4.0.5 which shows the dependence of the reaction rate on the concentration of Thiobacillus ferrooxidans at two different concentrations of ferrous iron $[Fe^{2+}]=0.01$ and $[Fe^{2+}]=0.0001$. The competitive inhibition manifests itself by a very small increase in the reaction rate when the cell

concentration exceeds 1g/l.

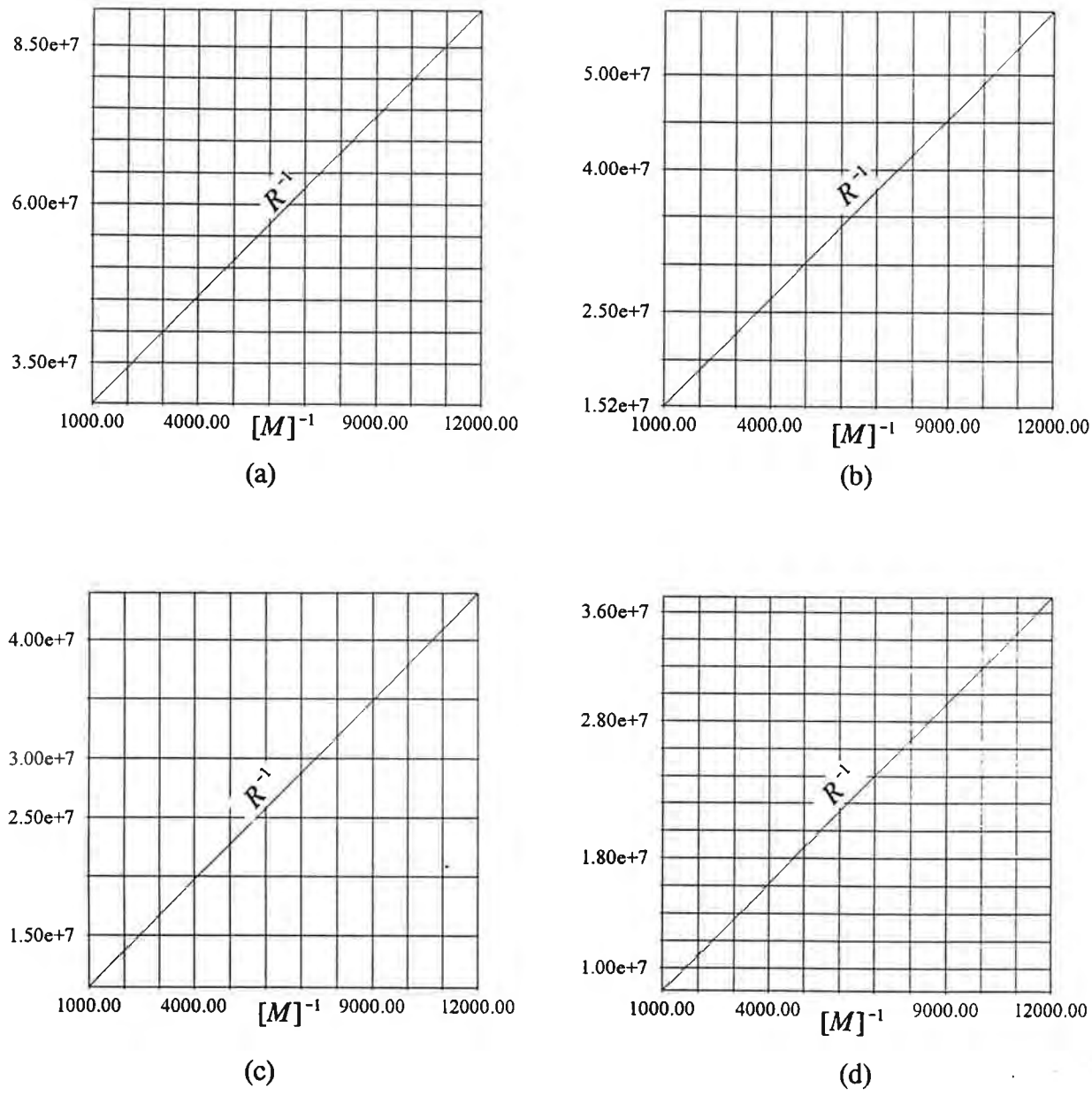

Fig. 4.0.4. The rates of the bacterial oxygenation of ferrous iron for different concentration of ferrous iron and different concentrations of bacteria. Cell concentrations are the same as in Fig.2.8. (a) [cell]=0.21g/l; (b) [cell]=0.42g/l; (c) [cell]=0.63g/l; (d) [cell]=0.83g/l. Vertical axis: inverse rate in $[M/min.]^{-1}$; horizontal axis: inverse concentration of ferrous iron in $[M]^{-1}$ =(moles per litre)$^{-1}$.

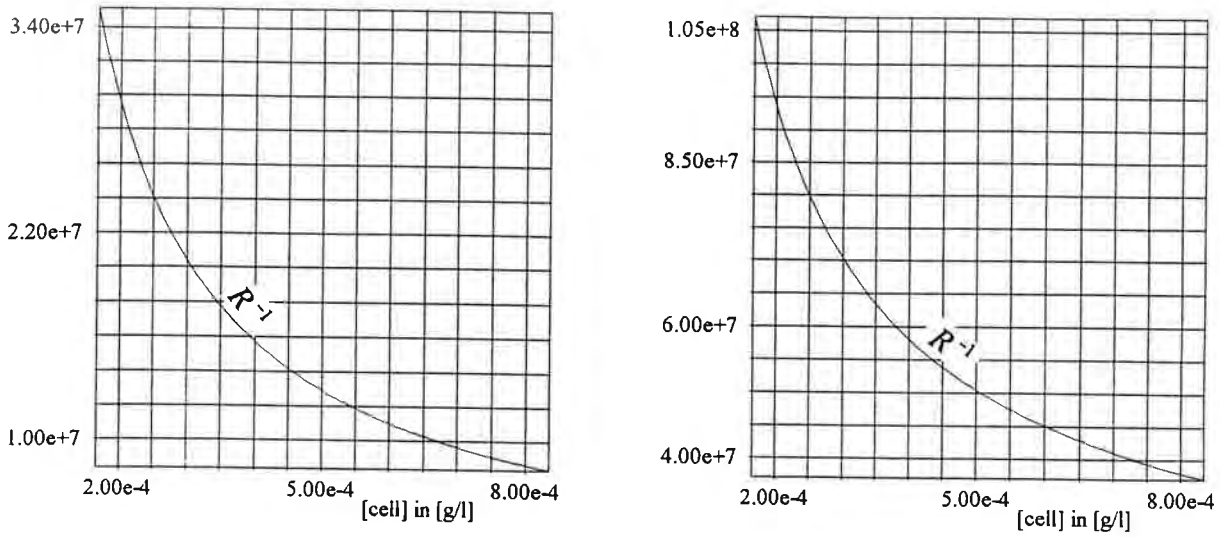

(a) (b)

Fig. 4.0.5. The effect of competitive inhibition for two different concentration of ferrous iron. (a) $[Fe^{2+}]=0.01M$; $[Fe^{2+}]=0.0001M$. Vertical axis: the inverse rate of oxidation of ferrous iron in $[M/min]^{-1}$; horizontal axis: concentration of bacterial cells in [g/l].

(The reaction rates in Figs. 4.0.4 and 4.0.5 are expressed in units of moles per minute in order to make comparison with the experimental results in Fig. 2.8 easier.)

4.0.3. *Bacterial oxidation by dissolved oxygen*

It is not possible to eliminate reactions (B2) and (B3) and measure directly the rates of bacterial oxidation of pyrite in the reaction (B1),

$$FeS_2(s) + 7/2\ O_2 + H_2O \xrightarrow{\text{bacteria}} Fe^{2+} + 2SO_4^{2-} + 2H^+ \ . \qquad \text{(B1)}$$

The information on the rate of reaction (B1) can be extracted by analyzing quantitative results on the overall rates of oxygen consumption during the bacterial oxidation due to the simultaneous reactions (B1), (B2) and (B3). If we assume that (B1), (B2) and (B3) are the only significant bacterial processes, we can obtain the value of the rate constant k_{1b} by solving the equations (DB) in which k_{1b} is a fitting parameter and the rate constants k_{2b} and k_{3b} are determined in independent experiments analyzed in paragraphs 4.0.1 and 4.0.2. We have optimized eqs. (DB) for the variable parameter k_{1b} and obtained

$$k_{1b} = 8.49 \cdot 10^{-6} M^{1/2} lm^{-2} s^{-1} \quad at \quad T = T_m = 303K,\ [H^+]_m = 0.005,\ [cell] = 1 g/l. \qquad (4.0.11)$$

The rate constant k_{1b} determined in our procedure is 300 times greater than the rate constant k_1 for the abiotic reaction (R1). In Fig.4.0.6b the rate of oxygen consumption is plotted together with concentrations of the hydronium ions $[H^+]$, ferrous iron $[Fe^{2+}]$, ferric iron $[Fe^{3+}]$ and sulphate $[SO_4^{2-}]$. The initial conditions used are the same as in Fig.2.7. We use the same form of $B([H^+])$ and B(T) for all three reactions and the accuracy of the value of k_{1b} is affected by the accuracy of the formulae for $B([H^+])$ and B(T) which cannot be confirmed experimentally for the reaction (B1). Further justification of the kinetic model defined by the set of equations (DB) could be provided by a systematic analysis of oxygen consumption rates at different pH values.

The problem of the bacterial oxidation of pyrite coated with ferric hydroxide seems to be very important. During the neutralization process, large quantities of ferrous iron are oxidized in a relatively fast abiotic reaction (R2) taking place at high pH values. In the absence of bacteria, at high pH values the formation of ferric iron is followed by a fast reaction of ferric iron with water and the precipitation of ferric hydroxide. Because the formation and precipitation of ferric hydroxide is very fast, the reaction (R3) of pyrite oxidation by ferric iron does not take place at high pH values. Part of the precipitated

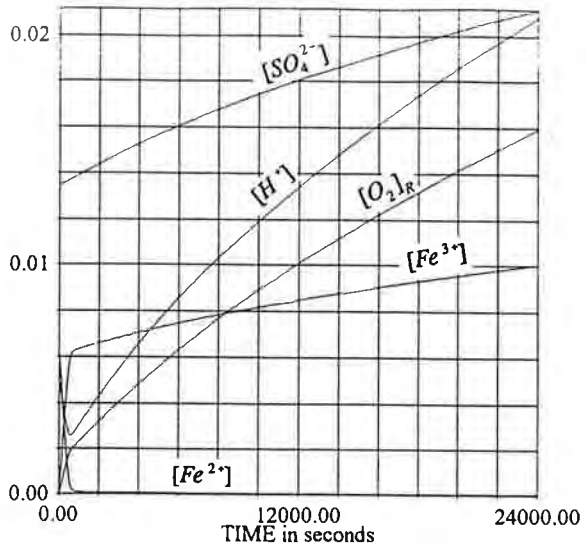

Fig. 4.0.6. Oxygen consumption, $[O_2]_R$ and temporal variation of concentrations of hydronium ions $[H^+]$, ferrous iron $[Fe^{2+}]$, ferric iron $[Fe^{3+}]$ and sulphate $[SO_4^{2-}]$ during the bacterial pyrite oxidation according to eqs.(DB). The conditions are the same as in the experiment by Lizama and Suzuki [LiS4] (see Fig.2.7): T=303K, $[Fe^{2+}(t=0)]$=6.25mM, $[O_2]$=238μM, S/V=0.78m^2/l. Vertical axis: molar concentrations; horizontal axis: time in seconds (24 000s=7 hours.

ferric hydroxide forms a protective coating on pyrite and is believed to slow-down the process of pyrite oxidation by dissolved oxygen. This discussion is valid for a well stirred reactor in which high pH values are maintained uniformly in the water solution and on the pyrite surface. In practice, during the natural process of pyrite oxidation in waste rock piles wet periods may be followed by dry periods during which the flow of water with dissolved calcite is limited and, at least locally, we may observe a limited neutralizing action resulting in lower pH values on the pyrite surface. This may create conditions for rapid bacterial oxidation due to high local concentrations of ferric iron formed from dissolved ferric hydroxide.

IV.1. Bacterial oxidation of pyrite at high concentrations of dissolved oxygen

During the bacterial oxidation of pyrite the ratio between concentrations of ferric iron and ferrous iron depends on the temperature, oxygen concentration, pH and the value of S/V. At temperatures close to T_m and high concentrations of dissolved oxygen the model for bacterial oxidation predicts much higher concentrations of ferric iron than in the absence of bacteria. For small values of S/V the concentration of ferric iron may be even greater than the concentration of ferrous iron. The combined effect of reactions (B2) and (B3) is much more severe than the direct oxidation of pyrite by dissolved oxygen according to the reaction (B1). Fig. 4.1.1 illustrates the temperature dependence of pyrite oxidation due to all the reactions (B1), B(2) and (B3) taking place simultaneously according to eqs. (BD). In our computer simulation the concentration of dissolved oxygen was at the saturation level corresponding (according to Table I on p.40) to 0.21 atm. of oxygen partial pressure for different temperatures. The symbol $[O_2]_R$ denotes the total cumulative amount of consumed oxygen, measured in moles per litre at constant in time temperature and constant concentration of dissolved oxygen $[O_2]$. The initial conditions of pH=4, $[Fe^{2+}]=0.0001$, $[Fe^{3+}]=0$ correspond to the situation in which moderately acidic conditions have developed from neutral initial conditions.

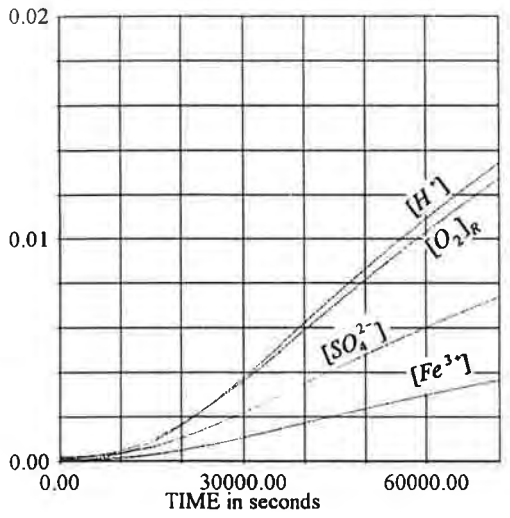

(11)

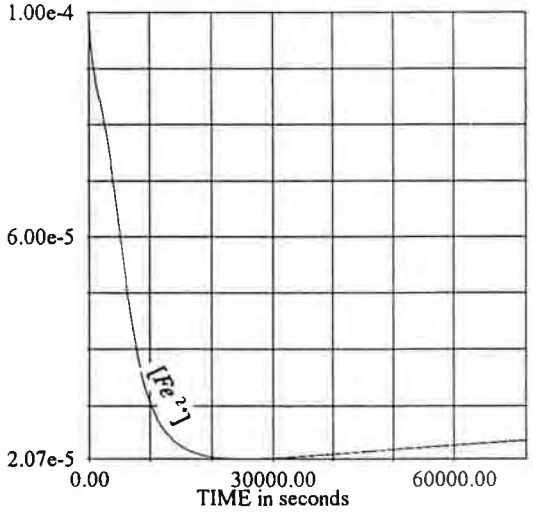

T=293K (12)

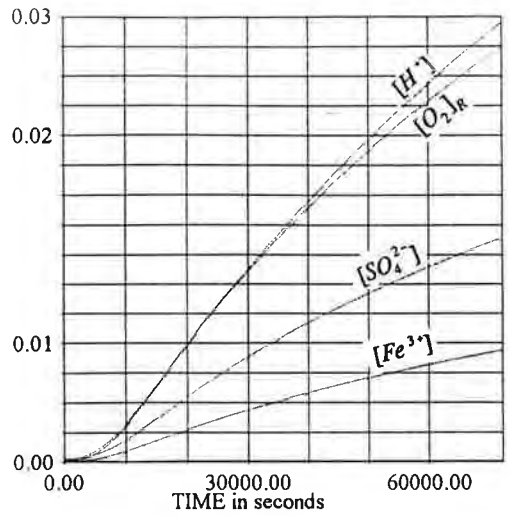

(21)

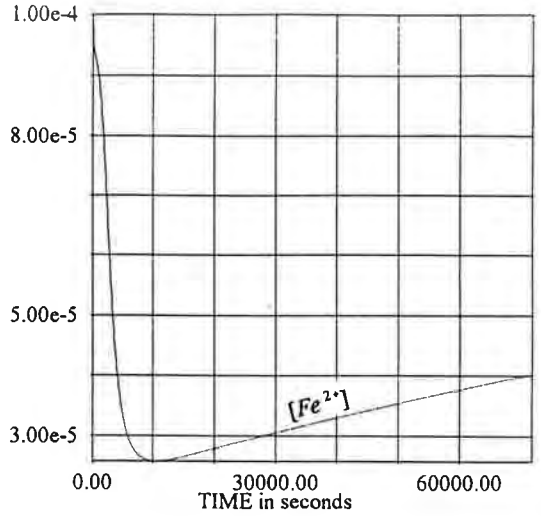

(22)

T=303K

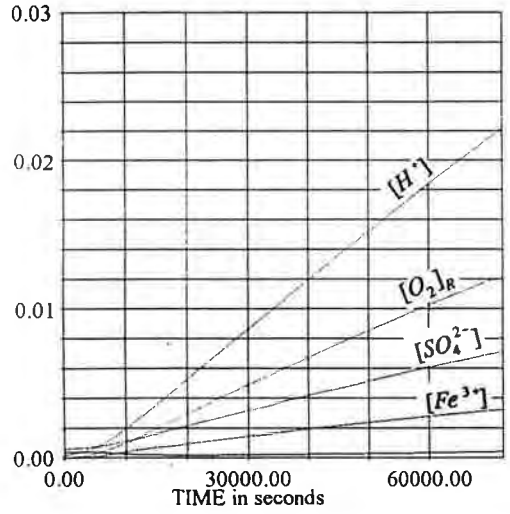

(31)

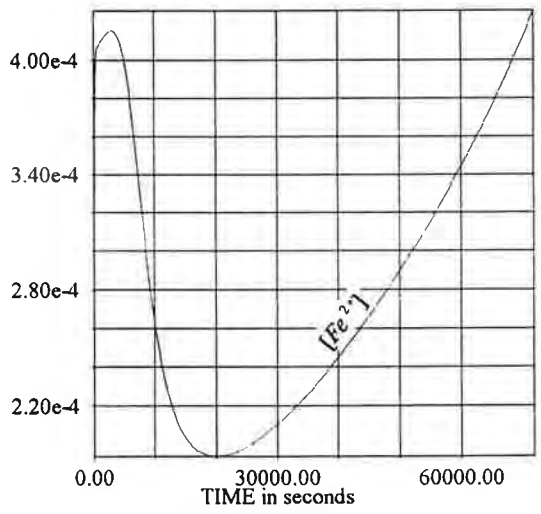

(32)

T=313K

Fig. 4.1.1. The kinetics of the bacterial processes for different temperatures; $[O_2]_{gas}=21\%$, $S/V=0.78m^2/l$, initial conditions: $pH(t=0)=3.9$, $[Fe^{2+}]=10^{-4}M$, $[SO_4^{2-}]=2x10^{-4}M$, $[Fe^{3+}]=0$. $[O_2]_R$ denotes the cumulative amount of consumed oxygen by constant in time but temperature dependent concentrations of dissolved oxygen. Horizontal axis: time in seconds; vertical axis: concentration in moles per litre. Horizontal axis: time in seconds (72 000s=20 hours); vertical axis: concentration in moles per litre.

Fig.4.1.1 also demonstrates that the concentration of ferrous iron evolves to the quasi-equilibrium value. The quasi-equilibrium concentration of ferrous iron is the smallest at T_m=303K. The initial increase of $[Fe^{2+}]$ in Fig. 4.1.1(32) is due to the fact that at pH values close to 4 the bacterial activity is small and the dominant role is played by the reaction (R1).

We also present results of the numerical simulation for high initial concentration of ferric iron, $[Fe^{3+}(t=0)]=0.01$. As we see in Fig. 4.1.2 ferric iron is initially rapidly reduced to ferrous iron and reaches a quasi-equilibrium value which then slowly evolves during the rest of the oxidation process. For the total concentration of iron ($[Fe^{2+}]+[Fe^{3+}]$), the ratio $[Fe^{2+}]/[Fe^{3+}]$ is defined by temperature, pH and S/V. In all our computer simulations we have used the same values S/V=0.78m^2/l as in the experiments by Suzuki et al. [SuL] and Lizama and Suzuki [LiS4]. Further extrapolation to other values of S/V should be performed in a physical model. A physical model should account for site-specific values of S/V which depend on several factors, including geochemical properties of waste rock and water transport.

Information on the oxygen consumption rates is important for a future physical waste rock model and an underwater disposal model which should properly describe oxygen depletion leading to lower concentration of oxygen.

The process of bacterial oxidation is much faster than the pyrite oxidation in the absence of bacteria. The key element is the bacterial oxidation of ferrous iron which provides ferric iron for the fast process of pyrite oxidation. Comparing figures 3.1.7 and 4.1.1 we conclude that at T=303K and cell concentrations on the order of 1g/l the bacterial oxidation of pyrite is about thousand times faster than the abiotic oxidation. This effect results from accelerated rates of the individual reactions of pyrite oxidation by dissolved oxygen, oxygenation of ferrous iron to ferric iron and oxidation of pyrite by ferric iron.

IV.2. Bacterial oxidation of pyrite at low concentrations of dissolved oxygen

During the process of pyrite oxidation the oxygen depletion rates are sufficiently high to cause a substantial decrease in the concentration of oxygen dissolved in the water. In waste rock piles the concentration of dissolved oxygen decreases until oxygen consumption rates become sufficiently low to be balanced by oxygen transport through porous piles. Depending on the temperature gradients established, the transport of oxygen takes place by diffusion and convection with convection rates increasing with the temperature gradient. (Often convective rolls develop in an outer layer near the pile boundaries as the result of flow instability [Ge], [Gep)]. There are field observations indicating that the coupling between chemical process and physical processes of mass and energy transport may lead to complex spatio-temporal patterns and a possible chaotic behaviour for the reaction rates controlled by the supply of oxygen and thermal energy transport. These aspects should be addressed by a physical reaction-transport model. One possible way of reducing acid rock drainage is to apply covers limiting the access of oxygen and the flow of water. Results presented here may be useful for analyzing the efficiency of covers.

We have analyzed the effect of lower oxygen concentration on the bacterial oxidation of pyrite. As an example we discuss the results obtained for 5% oxygen content in the gas phase, i.e. 4-5 times lower concentrations of dissolved oxygen than in Section 4.1. Reactions (B1) and the feedback loop (B2)-(B3) respond in a different way to lower oxygen concentrations. The rate of reaction (B1) depends on the concentration of dissolved oxygen but does not depend on the concentrations of ferrous and ferric iron. According to the kinetic equation (BD.1) the rate of direct pyrite oxidation by dissolved oxygen decreases two times when the oxygen concentration decreases four times. The kinetic equations for indirect oxidation involve the oxidation of ferrous iron with the rate proportional to the first power of oxygen concentration. It might seem, that lowering oxygen concentration four times should result in oxidation rate four times slower . This does not happen, however. The effect of reduced oxygen concentration for the reaction (B2) is much weaker than linear. The kinetic equations for the oxidation of ferrous iron also contain factors proportional to the concentration of ferrous iron. By comparing plots obtained for $[Fe^{2+}]$ in Figs. 4.1.1 and

4.2.1 we see that the decrease in oxygen concentration is accompanied by almost the same relative increase in the concentration of ferrous iron. As the result the rate of the reaction (B2) remains almost the same as for higher oxygen concentrations. By comparing plots in figures 4.1.1(22) and 4.2.1(22) we conclude that by decreasing the concentration of dissolved oxygen from 238μM to 49μM, the rate of pyrite oxidation decreases by only 30%. This indicates that the reactions (B2) and (B3) provide a negative feedback mechanism maintaining a high rate of pyrite oxidation when the oxygen concentration decreases.

In the reaction (B2) one hydronium ion is consumed per one ferrous iron oxygenated to ferric iron. One may consider the phenomenon of forming a reservoir of ferrous iron and maintaining high rate of the reaction (B2) as a chemistatic mechanism which allows the bacteria to maintain their activity for a longer time before the acidity increases and kills or deactivates the bacteria. This bacterial "self-defence against the acidic death" has a negative effect on acidic drainage. The ferric iron stored in high concentrations has a detrimental effect due to the fast anoxic process of pyrite oxidation which may continue for a long time after the bacteria become inactive (see plots in Figs. 4.2.1(21) and 4.2.1(32).

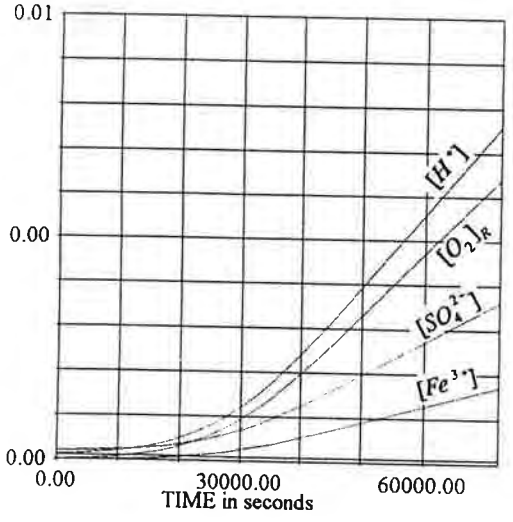

(11)

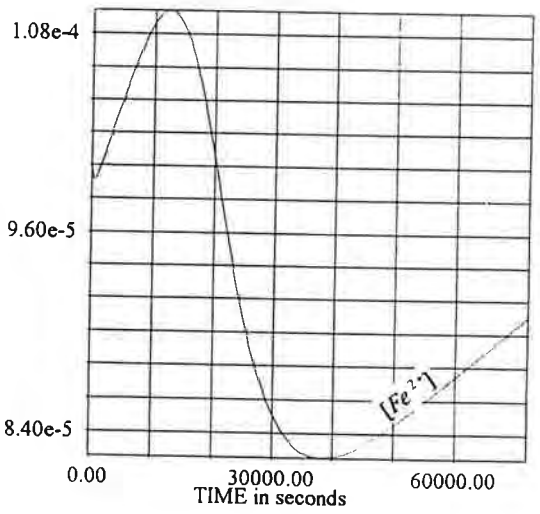

(12)

T=293K

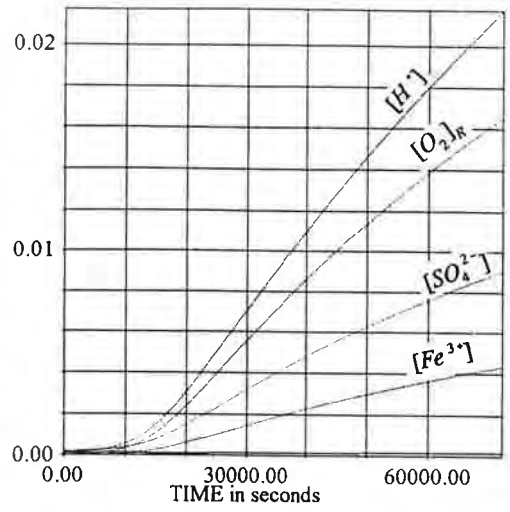

(21)

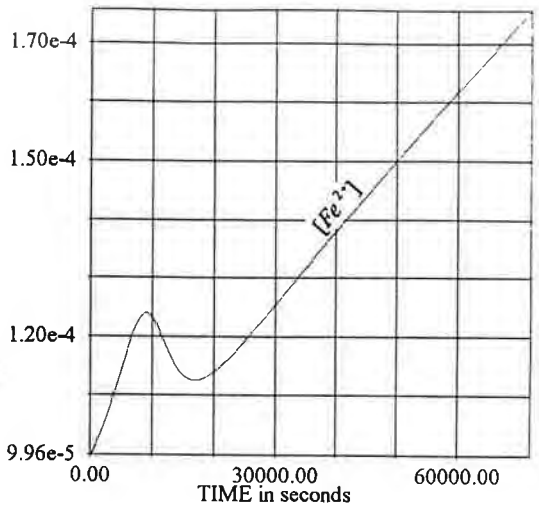

(22)

T=303K

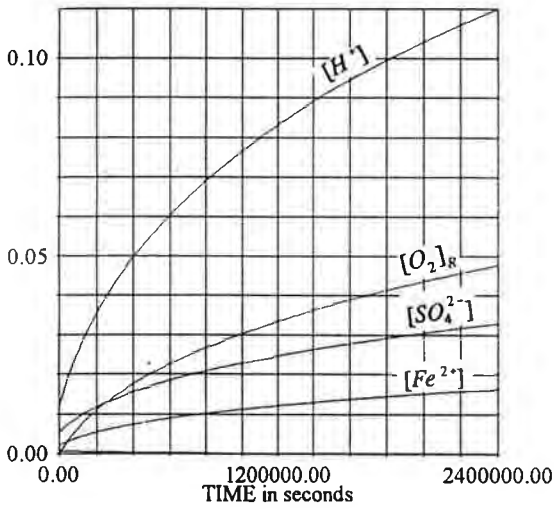

(31)

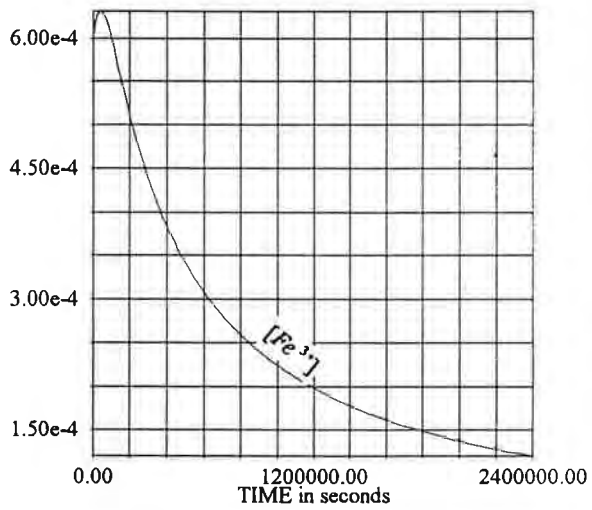

(32)

T=313K

Fig. 4.2.1. The kinetics of the bacterial processes for different temperatures; $[O_2]_{gas}=5\%$, $S/V=0.78m^2/l$, initial conditions: $pH(t=0)=3.9$, $[Fe^{2+}]=10^{-4}M$, $[SO_4^{2-}]=2x10^{-4}M$, $[Fe^{3+}]=0$. $[O_2]_R$ denotes the cumulative amount of consumed oxygen by constant in time but temperature dependent concentrations of dissolved oxygen, $[O_2]$. Horizontal axis: time in seconds; vertical axis: concentration in moles per litre. Horizontal axis: time in seconds; vertical axis: concentration in moles per litre.(2 400 000s=9 months).

The key to the understanding of the chemistatic bacterial action is provided by the stability properties of the set of eqs. (BD). In one of our future publications we will use analytical mathematical tools for a rigorous stability analysis of the set of kinetic equations (BD). The stability properties of the set of kinetic equations are responsible for a spontaneous evolution of the biogeochemical system to a quasi-equilibrium state characterized by the ratio, $[Fe^{2+}]/[Fe^{3+}]$ between the concentration of ferrous and ferric iron, which strongly depends on the oxygen concentration. Again, we interpret this property as the presence of quasi-equilibrium concentrations of ferric and ferrous iron because for a given initial total iron concentration, the system evolves very fast to the state characterized by the ratio $[Fe^{2+}]/[Fe^{3+}]$ which is independent of its initial value. Proper understanding of nonequlibrium thermodynamics of physical, chemical and biological processes involved is very important for formulating reasonable predictive waste rock and underwater disposal models. The total rates of pyrite oxidation are controlled by mass and energy transport which are relatively slow in comparison with chemical rates. It is known that various physical reaction-transport models involving very different chemical reactions often give very similar results for the distribution of oxygen and temperature. The comparison between model results and field data for temperature and oxygen distribution inside a waste rock pile cannot be used as a decisive criterion for the validity of a mathematical model. The environmental impact is related to the acidity and concentrations of dissolved heavy metals and sulphate which may be quite different under very similar physical conditions and depend strongly on the detailed features of the chemical reactions involved.

The fact that the chemical reactions alone do not lead to a chaotic behaviour is a nice feature which should facilitate the analysis of a realistic physical model. On the other hand, the strong dependence of the ratio between ferrous and ferric iron on temperature, oxygen concentration and geochemical properties of waste rock, requires some advanced numerical techniques to be used in a mathematical analysis of a future physical waste rock model. The expected rapid spatial variation in the rates of the chemical reactions involved, requires adaptive numerical methods for solving a set of coupled partial differential (reaction-transport) equations (see [SyT] and literature therein).

V. FURTHER EXPERIMENTS

The results of this study should be confronted with field data and calibrated before any practical recommendations are formulated.

By constructing the kinetic model we have used quantitative experimental data from at least two different sources. In some cases, however, we were forced to make assumptions which should be tested in further experiments. We list some problems which, in our view, merit further experimental and modelling work which should lead to a reliable physical waste rock model and a model for underwater disposal.

1. The kinetics of the neutralization process requires further work. The total amounts of sulphate and ferric hydroxide formed as a result of pyrite oxidation depend strongly on pH and temperature values. pH values are controlled by the amount and dissolution rates of the neutralizing minerals, and affect also the stoichiometry of the neutralization process. These aspects should be analyzed together with the problem of stoichiometric incompatibility (discussed in Section II.2). Results may be significant for predicting the amount of sludge generated and for designing the site-specific neutralization processes which would minimize the amount of sludge. Temperature is very important for the efficiency of neutralization because it affects both the rates of chemical reactions and exsolution of carbon dioxide from the water.

2. Different elementary reactions respond in a different way to various methods used to minimize ARD. To reduce acid rock drainage at existing sites in the most effective way it is important to know the relative contributions from the elementary processes involved. Oxygen in water molecules and molecular oxygen dissolved in water have a different isotope composition. Isotope techniques can be used to analyze the isotope composition of sulphate and should allow the determination of the relative contributions from the elementary abiotic and bacterial processes.

3. The nature of the chemical reactions indicates that pe and Eh values may be almost as important as pH for the bacterial activity. Further experiments measuring bacterial activity as a function of Eh may provide information useful in designing methods of reducing ARD.

4. The oxidation-reduction potential, Eh affects the stability of passive films formed by precipitated ferric hydroxide [Yo]. Passive films of ferric hydroxide dissolve at negative Eh values. For this reason Eh should be measured inside waste rock piles during field tests.

5. There are no systematic experimental data on the dependence of the rates of bacterial reactions (B1) and (B2) on the oxygen concentration. Our model predicts that as the result of bacterial activity, the rate of pyrite oxidation may be still fast at low oxygen concentrations.

6. There are no systematic experimental data which would determine the order of reaction (B3) with respect to the concentration of ferric iron. We have obtained a reasonable agreement with experimental data by using the same reaction order, 0.6 as for the reaction (R3). The same agreement should be reached with future experimental data for other initial concentrations of ferric iron.

7. The assumption about the same form of coefficients $B([H^+])$ and $B(T)$ which describe pH and temperature dependence of the bacterial activity in reactions (B1), (B2) and (B3) remains to be tested.

8. It seems quite possible that Thiobacillus ferrooxidans may attack pyrite coated by the ferric hydroxide. This process may lead to locally low pH values at which ferric hydroxide dissolves and the ferric iron contributes to the accelerated pyrite oxidation.

9. Surface reactions (B1) and (B3) may show a similar competitive inhibition as the reaction (B2). Experimental analysis of anaerobic bacterial oxidation of pyrite by different concentrations of bacteria and different values S/V should provide useful results for estimating the efficiency of covers limiting water flow. Such laboratory analysis should be performed for the whole range of bacterial concentrations observed in the field studies. After a formula for competitive inhibition of reaction (B3) is derived, it can be used for an analysis of the total oxygen consumption measured for different bacterial concentrations.

10. Parameters T_m and $[H^+]_m$ should be determined for bacterial cultures at different sites.

11. Hydraulic connectivity of the water film surrounding different mineral particles affects

the neutralization process. During dry periods the water film surrounding different mineral particles may become disjointed. It is known that pyrite coated with ferric hydroxide is hydrophobic. On the other hand, bacteria have a natural tendency to accumulate on pyrite. The bacterial ability to retain water during dry periods should be analyzed. This may lead to the local acid production despite the presence of neutralizing minerals.

12. Because of the ubiquitous nature of bacteria, traditional methods of acid/base accounting should be reevaluated. If pH values become initially low in some regions, the bacterial oxidation may lead to a very fast acid production. Under such circumstances the efficiency of neutralization process is governed not by the stoichiometric relations but by the dissolution rates and the kinetics of neutralization reactions.

13. The kinetic model analyzed in this study is based on small-scale experimental data for pure pyrite. Our results should be compared with medium-scale results obtained for pyritic rocks. A set of standard tests should be designed to measure independently the acidic potential and the neutralization potential for rocks at different sites.

14. The usefulness of any predictive model depends on the availability of entry data. A standard data base should be designed and created together with a set of inexpensive experimental procedures which would provide data for a predictive physical model which can be also used as a monitoring tool and provide clues on the most effective ways of minimizing acidic drainage. A great deal of work has been already done in this direction. Several static and kinetic geochemical tests for determining ARD potential have been designed [Al], [BrC], [CoR1], [CoR2], [LaR], [CaG], [FnG], [LawR], [McC], [Go], [SoS], [Res], [DuB], [ScG], [SnL], [Sul]. However, comparison and correlation of test generated data with field data has been minimal (refs. [FeM] and [Da] are notable exceptions). One of the key problems is the ability to scale the results obtained for small quantities of rock to generate quantitative predictions for a much greater mass of rock in the field. The small-scale geochemical tests should be conducted together with physical tests which should measure thermal energy released and simulate water and oxygen transport. This is very important because the mass and energy transport controls the rates of chemical reactions involved in the processes of acid generation and acid neutralization. While the existing tests (humidity cell test, for example

[Res]) often simulate the water transport, they do not simulate the nonhomogeneous distribution of oxygen and do not provide information on oxygen transport at the rates different for various parts of waste rock piles. A possible solution to this problem is the derivation of simple scaling relations for the rates of chemical and physical processes. Such scaling relations can be used to translate the existing laboratory data into large-scale estimates on acid-producing potential (AP) and acid neutralizing potential (NP) for waste rock piles. The scaling relations often allow to make large-scale and long-term predictions for the behaviour of chemically active minerals, which is impossible to simulate during laboratory experiments. Typically, a very large mass of chemically active minerals evolves to one of several possible spatially nonhomogeneous states which are characterized by different rates of chemical reactions and different temperatures controlled by the mass and energy transport. The size of the system and other physical and chemical parameters, like particle size, macroscopic pile porosity, thermal conductivity ambient atmospheric conditions and chemical rates determine various possible types of the thermodynamic behaviour of chemically active systems [Ar], [ScD], [Ot1], [Ot2]. Often very small changes in the physical and chemical (often controllable) parameters lead to a dramatic change in oxygen transport rates and temperature distribution which control chemical and bacterial processes. Simple scaling relations should be both a good step towards a predictive waste rock model and a useful practical tool for estimates based on the existing test results. The scaling relations should also help in designing geochemical tests which would provide suitable data for a predictive large-scale model.

15. A carefully designed sampling procedure is very important for the successful use of predictive models. The minimum number of samples collected from each site should increase with mass of rock, the number of different rock types and variability of other significant physico-chemical characteristics. Elemental composition, mineralogy, sulphide content, solubility and reactivity of carbonate compounds and general weathering characteristics should be analyzed for the samples. Morphologic characteristics of pyrite are important. The surface area (and chemical reactivity) of framboidal pyrite is greater than that of euhedral and subhedral pyrite [WhJ]. Determination of the range of variability of individual characteristics is important for reliable estimates.

REFERENCES

[Al] R. Albright
in Proceedings of Acid Mine Drainage Workshop; Environment Canada and Transport Canada, Halifax, NS, p. 146, 1987.

[An] Graham F. Andrews
"*The Selective Adsorption of Thiobacilli to Dislocation Sites on Pyrite Surfaces*"
Biotechnology and Bioengineering **31**, 378 (1988).

[AnM] G. F. Andrews and J. Maczuga
"*Bacterial coal desulfurization*"
Biotechnology and Bioengineering Symposium No. **12**, 337 (1982).

[ApK] R.J. Applegate and M. Kraatz
"*Rehabilitation of Rum Jungle Mine*"
Proc. MEND Conf, Montreal 1991.

[Ar] R. Aris
A Mathematical Theory of Reacting and Diffusing Systems
Wiley 1981.

[AsR] A.N. Astanina and A.P. Rudenko
Russ. J. Phys. Chem. 45, 191 (1971).

[BaZ] G.I. Barenblatt and Y.B. Zeldovich
A. Rev. Fluid Mech. **4**, 285 (1972)

[BaO] J.E. Bailey and D.F. Ollis
"*Biochemical engineering fundamentals*"
McGraw-Hill, New York 1986.

[BaP] L. K. Bailey and E. Peters
"*Decomposition of pyrite in acids by pressure leaching and anodization: the case for an electrochemical mechanism*".
Can. Metall. Quart. **15**, 333 (1976).

[Be] T. Beer
Applied Environmetrics Hydrological Tables
Applied Environmetrics, Victoria, Australia, 1991.

[BeK] B.B. Benson and D. Krouse, Jr.,
"The concentration and isotopic fractionation of gases dissolved in fresh water in equilibrium with the atmosphere, I Oxygen"
Limnol. Oceanog., **25**, 662 (1980).

[BeP] J.W. Bennet and G. Pantelis
"*Construction of a waste rock dump to minimise acid mine drainage a case study*"
Proc. MEND Conf., Montreal 1991.

[BeR] J. W. Bennett and A.I.M. Ritchie
"*Measurements of the transport of oxygen into two rehabilitated waste rock dumps*"
Proc. MEND Conf., Montreal 1991.

[BoB] F.C. Boogerd, C. van den Beemd, T. Stoelwinder, P.Bos and J.G. Kuenen
"*Relative contributions of biological and chemical reactions to the overall rate of pyrite oxidation at temperatures between 30°C and 70°C* "
Biotechnology and Bioengineering **38**, 109 (1991).

[BoL] Jacques Boulegue, Charles J. Lord III and Thomas M. Church
"*Sulfur speciation and associated trace metals (Fe, Cu) in the pore waters of Great Marsh, Delaware*"
Geochimica et Cosmochimica Acta **46**, 453 (1982).

[Br] C.L. Brierley
"*Bacterial Leaching*"
CRC Critical Reviews in Microbiology **6**, 207 (1979).

[BrC] British Columbia Acid Mine Drainage Task Force
"Acid Rock Drainage Technical Guide"
BC AMD Task Force Report, 1989.

[CaG] F.T. Carruccio, G. Geidel and M. Pelletier
J. Energy (Amer. Soc. Civil Engineers) **107**, (1981).

[CaW] M.C. Campbell, D.Wadden, A. Marchbank, R.G.L. McCready and G.Ferroni
"*In-place leaching of uranium at Denison Mines Ltd.*"
Proc. IAEA Meeting, Vienna 1985.

[CdO] J. Chadam and P. Ortoleva
Earth Science Reviews **29**, 175 (1990).

[Ch] F. Chaiken, private communication (1992).

[ChB] K. Ye Cheng and P.L. Bishop
J. Air&Waste Manage. Assoc. **42**, 164 (1992).

[Co] W.R. Cowan
Hazardous Mat. Mgmt., **3**, 12 (1991)

[CoR1] Coastech Research
"Investigation of Prediction Techniques for Acid Mine Drainage"
MEND Project, West Vancouver, BC, Canada, 1989.

[CoR2] Coastech Research
"Acid Rock Drainage Prediction Manual: A manual of Chemical Evaluation Procedures for the prediction of Acid Generation from Mine Wastes"
Mend Project, North Vancouver, BC, Cnada 1990.

[CrT] G. Cragnolio and O.H. Tuovinen
"*The role of sulphate-reducing and sulfur-oxidizing bacteria in the localized corrosion of iron-base alloys - a review*"
International Biodeterioration **20**, 9 (1984)

[Da] S. Day
"Long term kinetic acid generation studies: Cinola project"
B.C. AMD Task Force, 1993.

[DaR1] G.B. Davis and A.I.M. Ritchie
"*A model of oxidation in pyritic mine wastes: part 1: equations and approximate solutions*"
Appl. Math. Modelling **10**, 314 (1986).

[DaR2] G.B. Davis and A.I.M. Ritchie
"*A model of oxidation in pyritic mine wastes: part: comparison of numerical and approximate solutions*"
Appl. Math. Modelling **10**, 323 (1986).

[DaR3] G.B. Davis and A.I.M. Ritchie
"*A model of oxidation in pyritic mine wastes: part 3: importance of particle size distribution*"
Appl. Math. Modelling **11**, 417 (1987)

[DaS] W.Davison and G.Seed
Geochimica et Cosmochimica Acta 47, 67 (1983).

[DuB] D.W. Duncan and A. Bruynsteyn
"*Determination of the Acid Production Potential of Waste Materials*"

Metallurgical Society of AIME Annual Meeting, New Orleans (1979).

[DuD] J.G. Dunn, G.C. De and P.G. Fernandez
"*The effect of experimental variables on the multiple peaking phenomenon observed during the oxidation of pyrite*"
Thermochimica Acta, **135**, 267 (1988).

[Eh] H.L. Ehrlich
Geomicrobiology
Dekker, New York, 1981.

[ErH] P.M. Erickson, R.W. Hammack and R.L.P. Kleinman
"Prediction of acid drainage potential in advance of mining"
in Control of Acid Mine Drainage, USBM IC 9027.

[Es] H. Ese
"Acidic mine drainage from the Killingdal Mine Norway"
Proc. MEND Conf., Montreal 1991.

[EvK] R.O. van Everdingen and H.R. Krouse
"Isotope composition of sulphates generated by bacterial and abiological oxidation"
Nature **315**, 395 (1985).

[Fe] K.D. Ferguson
"Static and Kinetic Methods to Predict Acid Mine Drainage"
Env. Canada, 1985.

[FeE] K.D. Ferguson and P.M. Erickson
"Approaching the AMD Problem-from Prediction and early Detection"
In. Proc. Int. Conf. on Control of Environmental Problems from Metal Mines, 1988, Roros, Norway.

[FeE1] K.D. Ferguson and P.M. Erickson
"Will It Generate Acid? An Overview of Methods to Predict Acid Mine Drainage"

[FeMe] K.D. Ferguson and P.E. Mehling
"Acid Mine Drainage in B.C. The Problem and Search for Solutions"
Environment Canada, 1986.

[FeM] K.D. Ferguson and K.A. Morin
"The prediction of Acid Rock Drainage - Lesson from the Database"

Environment Canada Report, 1992.

[FiN] R. J. Field, R.M. Noyes
J. Chem. Phys. **60**, 1877, (1974).

[FnG] R.B. Finkelman, D.E. Giffin
Reclamation and Revegetation Research **5**, 521 (1986).

[FrC] R.A. Freeze and J.A. Cherry
Groundwater
Prentice -Hall of Canada, 1979

[Ga] D.M. Galbraith
"The mount Washington acid mine drainage reclamation project"
Proc. MEND Conf., Montreal 1991.

[Ge] P. Gelinas and R. Guay
"Acid Mine Drainage Generation from a Waste Rock Dump and Evaluation of Dry Covers Using Natural Minerals: La Mine Doyon Case Study"
MEND Report (1990)

[Ge] P. Gelinas
private communication (1993)

[Go] B. Godin
private communication (1992)

[Gol] M.B. Goldhaber
"Experimental study of metastable sulpfur oxyanion formation during pyrite oxidation"
Am. J. Sci. 283, 193 (1983).

[GrW] H.C. Granger and C.G. Warren
"Unstable Sulfur Compounds and the Origin of Roll-type Uranium Deposits"
Economic Geology **64**, 160, (1969)

[Gu] R. Guay
private communication (1993)

[Ha] Sophie Bierens de Haan
"A review of the rate of pyrite oxidation in aqueous systems at low temperature"
Earth-Science Reviews **31**, 1, (1991).

[HiP] J.B. Hiskey and M.D. Pritzker
"Electrochemical behavior of pyrite in sulfuric acid solution containing silver ions"
J. Appl. Electrochem. **18**, 484 (1988).

[HoS] George R. Holdren, Jr. and Patricia M. Speyer
"Reaction rate - surface area relationships during the early stages of weathering - I. Initial observations"
Geochimica et Cosmochimica Acta **49**, 675 (1985).

[HwS] C.C. Hwang, R. C. Streeter, R.K. Young and Y.T. Shah
"Kinetics of the ozonation of pyrite in aqueous suspension"
Fuel **66**, 1574 (1987).

[In] W.J. Ingledew
"Ferrous iron oxidation by Thiobacillus ferrooxidans"
Biotechnology and Bioengineering Symp. No. **16**,23 (1986).

[Jo] B.B. Jorgensen
"A theoretical model of the stable sulfur isotope distribution in marine sediments"
Geochimica et Cosmochimica Acta **43**, 363 (1979).

[Ka] G.I. Karavaiko
"Microbiological processes for the leaching of metals from ores"
United Nations Environmental Program, 1985.

[KaB] H.C. Kasan and A.A.W Baecker
"An assessment of toxic metal biosorption by activated sludge from the treatment of coal-gasification effluent of a petrochemical plant"
Water Research **23**, 795 (1989).

[KeW1] G.H. Kelsall and R.A. Williams
"Electrochemical behavior of ferrosilicides (Fe_xSi) in Neutral Alkaline Aqueous Electrolites. I. Thermodynamics of Fe-Si-H_2O systems at 298 K"
J. Electrochem. Soc. **138**, 941 (1991).

[KeW2] G.H. Kelsall and R.A. Williams
"Electrochemical behavior of ferrosilicides (Fe_xSi) in Neutral and Alkaline Aqueous Electrolites. II. Fe_xSi Electrochemical kinetics and Corrosion behavior"
J. Electrochem. Soc. **138**, 941 (1991).

[KeW3] G.H. Kelsall and R.A. Williams

"Electrochemical behaviour of ferrosilicides (Fe_xSi) in Neutral and Alkaline Aqueous Electrolites. III. The nature of passive films on Fe_xSi Electrodes"
J. Electrochem. Soc. **138**, 941 (1991).

[KoB] A. Kok, N. Bolt and J.H.N. Jergersma
KEMA Sci.&Tech. Reports **7**, 63 (1989)

[KrG] H.R. Krouse, W.D. Gould, R.G.L. McCready and S.Rajan
"^{18}O incorporation into sulphate during the bacterial oxidation of sulphide minerals and the potential for oxygen isotope exchange between O_2, , H_2O and sulphur intermediates"
Earth and Planetary Sci. Lett. **107**, 90 (1991).

[KuM] C.F. Kulpa, Jr., N. Mjoli and M.T. Roskey
"Comparison of iron and sulfur oxidation in Thiobacillus ferrooxidans: inhibition of iron oxidation by growth on sulfur"
Biotechnology and Bioengineering Symp. No. **16** (1986).

[Kw] Y.T.J. Kwong
"Acid generation in waste rock as exemplified by the Mount Washington minesite, B.C., Canada"
Proc. MEND Conf., Montreal 1991.

[LaB] E.J. Laishley, R.D. Bryant, B.W. Kobryn and J.B. Hyne
"Microcrystalline structure and surface area of elemental sulphur as factors influencing its oxidation by Thiobacillus Oilbirds"
Can. J. Microbial. **32**, 237 (1986).

[LaN] S.B. Lalvani, B.A. DeNeve and A. Weston
"Prevention of pyrite dissolution in acidic media"
Corrosion **47**, 55 (1991).

[LaS] S.B. Lalvani and M. Shami
"Passivation of pyrite oxidation with metal cations"
J. Mat. Sci. **22**, 3503 (1987).

[Las] Antonio C. Lasaga
"Chemical Kinetics of Water-Rock Interactions"
Journal of Geophysical Research **89**, 4009, (1984).

[LawR] R.W. Lawrence, G.M. Ritcey, G.W. Poling, P.B. Marchant
"Strategies for the Prediction of Acid Mine Drainage"
Proceedings of the 13th Mine Reclamation Symposium, Ministry of Energy,

Mines and Petroleum Resources; Victoria, 1989.

[LeK] H. Lees, S.C. Kwok and I. Suzuki
"The thermodynamics of iron oxidation by the ferrobacilli"
Can. J. Microbiology **15**, 43 (1969).

[LeW] J.H. Levy and T. J. White
"The reaction of pyrite with water vapour"
Fuel **67**, 1336 (1988)

[LiN] X.-P. Li, N.A. Vante and H. Tributsch
"Involvement of coordination chemistry during electron transfer in the stabilization of the pyrite (FeS_2) photoanode"
J. Electroanal. Chem. **242**, 255 (1988)

[LiS1] H.M. Lizama and I. Suzuki
"Bacterial leaching of a sulfide ore by Thiobacillus ferrooxidans and Thiobacillus thiooxidans: I. Shake Flask Studies"
Biotechnology and Bioengineering **32**, 110 (1988).

[LiS2] H. M. Lizama and I. Suzuki
"*Bacterial leaching of a sulfide ore by Thiobacillus ferrooxidans and Thiobacillus thiooxidans Part II: Column leaching studies*"
Hydrometallurgy **22**, 301 (1989).

[LiS3] H.M. Lizama and I. Suzuki
"Synergistic competitive inhibition of ferrous iron oxidation by Thiobacillus ferrooxidans by increasing concentrations of ferric iron and cells"
Appl. Env. Microbiology **55**, 2588 (1989).

[LiS4] H.M. Lizama and I. Suzuki
"Rate equations and kinetic parameters of the reactions involved in pyrite oxidation by Thiobacillus ferrooxidans"
Appl. Env. Microbiology **55**, 2918 (1989).

[LiS5] H. M. Lizama and I. Suzuki
"Kinetics of sulfur and pyrite oxidation by Thiobacillus thiooxidans. Competitive inhibition by increasing concentrations of cells"
Can. J. Microbiology **37**, 182 (1991).

[LiS6] H.M. Lizama and I. Suzuki
"Interaction of chalcopyrite and sphalerite with pyrite during leaching by Thiobacillus ferrooxidans and Thiobacillus thiooxidans".

Can. J. Microbiology **37**, 304 (1991).

[LoC] C. J. Lord III and Thomas M. Church
"The geochemistry of salt marshes: sedimentary ion diffusion, sulfate reduction, and pyritization"
Geochimica et Cosmochimica Acta **47**, 1381 (1983).

[Low] Richard T. Lowson
"Aqueous Oxidation of Pyrite by Molecular oxygen"
Chemical Reviews **82**, 461 (1982).

[LuC] D.G. Lundgren and M. Silver
"Ore leaching by bacteria"
Ann. Rev. Microbiol. **34**, 263 (1980).

[LuV] D.G. Lundgren, M.Valkova-Valchanova and R.Reed
"Chemical reactions important in bioleaching and biaccumulation"
Biotechnology and Bioengineering Symp. No.**16** (1986).

[Lu] George W. Luther III
"Pyrite oxidation and reduction: Molecular orbital theory considerations"
Geochimica et Cosmochimica Acta **51**, 3193 (1987).

[LuF] G.W. Luther III, T.G. Ferdelman, J.E. Kostka, E.J. Tsamakis and T.M. Church
"Temporal and spatial variability of reduced sulpfur species and porewater parameters in salt marsh sediments"
Biogeochemistry **14**, 57 (1991).

[LuK] G.W. Luther III, J.E Kostka, T.M. Church, B. Sulzberger and W. Stumm
"Seasonal iron cycling in the salt-marsh sedimentary environment: the importance of ligand complexes with Fe(II) and Fe(III) minerals and pyrite, respectively"
Marine Chemistry **40**, 81 (1992).

[MaR1] C.T. Mathews and R.G. Robins
Australas. Ins. Mining Metall. **242**, 47 (1972).

[MaR2] C.T. Mathews and R.G. Robins
Aust. Chem. Eng. **15**, 19 (1975).

[MaR3] C.T. Mathews and R.G. Robins
Aust. Chem. Eng. **13**, 129 (1972).

[McC] R. McCandless
private communication, 1993.

[McK] Michael A. McKibben and Hubert L. Barnes
"Oxidation of pyrite in low temperature acidic solutions: Rate laws and surface textures"
Geochimica et Cosmochimica Acta **50**, 1509-20 (1986).

[MiS] F.J. Millero, S. Sotolongo and M. Izaguirre
"The oxidation kinetics of Fe(II) in Seawater"
Geochimica et Cosmochimica Acta **51**, 793-801 (1987).

[MoC] K.A. Morin and J.A. Cherry
"Trace Amounts of Siderite Near a Uranium-Tailing Impoundment, Elliot Lake, Ontario, Canada, and Its implication in Controlling Contaminant Migration in a Sand Aquifer"
Chemical Geology, **56**, 117 (1986).

[MoJ] K. A. Morin, E. Gerencher, C.E. Jones, D. Konasewich and J.R. Harries
"Critical literature review of acid drainage from waste-rock"
Nrthwest Geochem, 1990.

[MoM] John W. Morse, Frank J. Millero, Jeffrey C. Cornwell and D. Rickard
"The chemistry of the Hydrogen Sulfide and Iron Sulfide Systems in Natural Waters"
Earth-Science Review **24**, 1 (1987).

[MsH] Carl O. Moses, Alan T. Herlihy, Janet. S. Herman and Aaron L. Molls
"Ion-chromatographic analysis of mixtures of ferrous and ferric iron"
Talanta **35**, 15 (1988).

[MsH] Carl O. Moses and Janet S. Herman
"Homogeneous Oxidation Kinetics of Aqueous Ferrous Iron at Circumneutral pH"
Journal of Solution Chemistry **18**, 705 (1989).

[MsH] Carl O. Moses and Janet S. Herman
"Pyrite oxidation at circumneutral pH"
Geochimica et Cosmochimica Acta **55**, 471 (1991).

[MsN] Carl O. Moses, D.Kirk Nordstrom, Janet S. Herman and Aaron L. Mills
"Aqueous pyrite oxidation by dissolved oxygen and by ferric iron"
Geochimica et Cosmochimica Acta **51**, 1561 (1987).

[Ni] R.V. Nicholson, private communication (1993).

[NiG] Ronald V. Nicholson, Robert W. Gillham and Eric J. Reardon
"Pyrite oxidation in carbonate-buffered solution:. 1. Experimental kinetics"
Geochimica et Cosmochimica Acta **52**, 1077 (1988)

[NiG] Ronald V. Nicholson, Robert W. Gillham and Eric J. Reardon
"Pyrite oxidation in carbonate-buffered solution:. 2. Rate control by oxide coatings"
Geochimica et Cosmochimica Acta" **54**, 395 (1990)

[NiP] G. Nicolis and I. Prigogine
Self-Organization in Nonequilibrium Systems
Wiley, 1977.

[NiS] R.V. Nicholson and J.M. Scharer
"Laboratory Studies of Pyrrhotite Oxidation Kinetics"
preprint

[No] D.K. Nordstrom
"Aqueous pyrite oxidation and the consequent formation of secondary iron minerals"
in Acid sulfate wearhering: pedogeochemistry and relationship to manipulation of soil materials, Soil Science Soc. Amer. Press, Madison, 1982.

[No] Nordstrom D.K. , E.A. Jenne and J.W. Ball
"Redox equilibria of iron in acid mine waters",
ACS Symposium Series **93**, 51-59 (1979).

[Ol] G.J. Olson
Biohydrometallurgy, p. 73 CANMET 1989.

[Ot1] M. Otwinowski
"A thermodynamic model for the spontaneous heating and combustion of coal. I:Elementary exothermic processes"
Fuel, submitted; also Alberta Energy Report, Edmonton 1991.

[Ot2] M. Otwinowski
"A thermodynamic model for the spontaneous heating and combustion of coal. II: Reaction-diffusion model"
Fuel, submitted; also Alberta Energy Report, Edmonton 1991.

[Ot3] M. Otwinowski
Static and Dynamic Patterns in Equilibrium and Nonequilibrium Systems
in Nonlinear Structures in Physical Systems, Chaos Pattern formation and Waves ,Springer, 1990

[OtL1] M. Otwinowski, W.G. Laidlaw and R. Paul
"Structural instability of the Brusselator model with reversible chemical reactions"
Can. J. Phys. **68**, 743 (1990)

[OtL2] M. Otwinowski, W.G. Laidlaw and R. Paul
"Explicit solutions to a class of nonlinear diffusion equations"
Phys. Lett. **124**, 149 (1988).

[Otp] M. Otwinowski
in preparation.

[OtP] M. Otwinowski and R. Paul
"A thermodynamic theory of axon permeability"
Biophysical Journal **29**, 126 (1989)

[PaR] G. Pantelis and A.I.M. Ritchie
"Macroscopic transport mechanisms as a rate-limiting factor in dump leaching of pyrite ores"
Appl. Math. Modelling **15**, 136 (1991)

[PrL] I. Prigogine and R. Lefevre
J. Chem. Phys. **48**, 1695 (1968).

[PrT] William A. Pryor and Umberto Tonnellato
"Nucleophilic Displacements at Sulfur. III. The Exchange of Oxygen-18 between Sodium Thiosulfate-^{18}O and Water"
Journal of the American Chemical Society **89**, 3379 (1967).

[Pr] J. Pronk
private communication (1993)

[RaF] S.R. Rao and J.A. Finch
"Galvanic interaction studies on sulphide minerals"
Can. Metall. Quart. **27**, 252 (1988).

[Res] Rescan Env. Services Ltd.
"Kutcho Creek project. Acid generation testwork"

Report, 1990, Vancouver,Canada.

[ReB] Brian J. Reedy, James K. Beattie and Richard T. Lowson
"A vibrational spectroscopic ^{18}O tracer study of pyrite oxidation"
Geochimica et Cosmochimica Acta **55**, 1609 (1991).

[Sa] V. Sanmugasunderam
"Bacterially assisted column leaching"
Biotechnology and Bioengineering Symp. **16**, 73 (1986).

[SaG] A.F. Saprygin and L.S. Gusar
Zh. Prikl. Khim. **45**, 345 (1971)

[ScG] J.M. Scharer, V. Garga, R. Smith and B.E. Halbert
"Use od Steady-State Models for Assesing Acid Generation in Pyritic Mine Tailings"
in Proceedings of the 2nd International Conference on Abatement, Montreal, p. 211, Tome 2, 1991.

[ScD] A. Schmal, J.H. Duyzer and J.W. van Heuven
Fuel **64**, 1969 (1985)

[Se] Senes Consultants
"Description of RATAP.BMT3 Component Modules"
Report, 1991.

[SiS] P.C. Singer and W. Stumm
"Acidic Mine Drainage: The Rate Determining Step"
Science **167**, 1121 (1970).

[SnL] G.A. Singleton and L.M. Lavkulich
Soil Science **42**, 984 (1978).

[SoS] A.A. Sobek, W.A. Schuller, J.R. Freeman and R.M. Smith
US EPA Report; EPA 600/2-78-054, 1978

[SpB] P.A. Spencer, J.R. Budden and R. Sneyd
Biohydrometallurgy, p.231, CANMET 1989.

[St] W. Stumm ed.,
"Aquatic Chemical Kinetics. Reaction Rates of Processes in Natural Waters", Wiley, 1991.

[StL1] W. Stumm and G.F. Lee

Schwei. Z. Hydrol. **22**, 295 (1960).

[StL2] W. Stumm and G.F. Lee
Ind. Eng. Chem. **53**, 143 (1961).

[StM] W. Stumm and J.J. Morgan,
"Aquatic Chemistry. An introduction Emphasizing Chemical Equilibria in Natural Waters", Wiley,1986.

[Sul] P.J. Sullivan and A.A. Sobek
Minerals and the Environment **4**, 9 (1982)

[SuR] A. O. Summers P. Roy and M.S. Davidson
"Current techniques for the genetic manipulation of bacteria and their application to the study of sulfur-based autotrophy in Thiobacillus"
Biotechnology and Bioengineering Symp. No. **16**, 268 (1986).

[Su] I. Suzuki, private comminication (1993)

[SuL] I. Suzuki, H.M. Lizama and P.D Tackaberry
"Competitive inhibition of ferrous iron oxidation by thiobacillus ferrooxidans by increasing concentrations of cells"
Appl. Env. Microbiology **55**, 1117 (1989).

[SuT] I. Suzuki, T.L. Takeuchi, T.D. Yuthasastrakosol and J.K. Oh
"Ferrous iron and sulfur oxidation and ferric iron reduction activities of Thiobacillus ferrooxidans are affected by growth on ferrous iron, sulfur, or a sulfide ore"
Appl. Env. Microbiology **56**, 1620 (1990).

[SyT] Synergetic Technology
"A Thermodynamic Reaction Transport Model for Acidic Drainage from Waste Rock Piles"
project proposal (1993)

[TaG] H. Tamura, K. Goto and M.J. Nagayama
Inorg. Nucl. Chem. **38**, 113 (1976).

[TaW1] B.E. Taylor, M.C. Wheeler and D.K Nordstrom
"Isotope composition of sulphate in acid mine drainage as measure of bacterial oxidation"
Nature **308**, 538 (1984).

[TaW2] B.E. Taylor and M.C. Wheeler and D.K. Nordstrom
"Stable isotope geochemistry of acid mine drainage: Experimental oxidation of pyrite"
Geochimica et Cosmochimica Acta **48**, 2669 (1984)

[To] A.E. Torma
"Biohydrometallurgy as an emerging technology"
Biotechnology and Bioengineering Symp. No. **16**, 49 (1986).

[Ty] J.J. Tyson
in *Oscillations and Travelling Waves* ,
Wiley, 1985.

[UhH] W. Uhl, H.-J. Hone, M.Beyer and J.Klein
"Continuous microbial desufurization of coal-application of a multistage slurry reactor and analysis of the interactions of microbial and chemical kinetics"
Biotechnology and Bioengineering **34**, 1341 (1989)

[VSK] D.R. Van Stempvoort and H.R. Krouse
"Controls of $\delta^{18}O$ in Sulfate: A Review of Experimental Data and Application to Specific Environments"
preprint (1993).

[VaP] J.A. Vastano, J.E. Pearson, W. Horshemke and H.L. Swinney
J. Chem. Phys. **88**, 6175 (1988)

[WaK] E. I. Wallick, H.R. Krouse and A. Shakur
"Environmental isotopes: principles and applications in ground water geochemical studies in Alberta, Canada"
in First Can. Conf. on Hydrology, 1984.

[We] Bernhard Wehrli
"Redox reactions of metal ions at mineral surfaces"
in Aquatic Chemical Kinetics W. Stumm ed.,Willey, 1990.

[WhJ] W.W. White III and T.H. Jeffers
"Chemical predictive modelling of acid mine drainage from metallic sulfide-bearing waste rock"
U.S. Department of Interior, Bureau of Mines, 1992.

[WiU] P.L. Wichlacz and R. F. Unz
"Fixed film biokinetics of ferrous iron oxidation"
Biotechnology and Bioengineering Symp. No. **11** (1981).

[WiR] C.L. Wiersma and J.D Rimstidt
"Rates of reaction of pyrite and marcasite with ferric iron at pH 2"
Geochimica et Cosmochimica Acta **48**, 85 (1984)

[YaW] E.K. Yanful, K.G. Wheeland, C. Luc and N. Kuyucak
"Overview of Noranda Research on Prevention and Control of Acid Mine Drainage"
Environmental Workshop 1991, Australian Mining Industry Council

[Yo] R.M. Yoon
private communication (1993)

[YuR] S.B. Yunker and J.M. Radovich
"Enhanced Growth of Thiobacillus ferrooxidans in an Electrolytic Bioreactor"
Biotechnology and Bioengineering Symp. No. **15** (1985).

[ZiM] Z.D. Zivkovic, N. Molosavljevic and J. Sestak
"Kinetics and Mechanism of Pyrite Oxidation"
Thermochimica Acta **157**, 215 (1990).